

The effect of casting and curing temperatures on the properties of concrete

Mohammed Sharfuddin Ahmed

Civil Engineering

June 1996

Abstract

This study was conducted to investigate the effect of casting and curing temperatures on the properties of plain and blended cement concretes. To achieve the objective of this research more than 1200 concrete specimens were cast. The effect of casting and curing temperature on the compressive strength, pulse velocity, and absorption were evaluated up to a period of 168 days. Furthermore, these tests were supplemented with pore size distribution, X-ray diffraction, and differential thermal and thermogravimetric analysis.

The long-term properties of plain cement concrete specimens were not affected for casting temperatures of up to 50°C, provided they are cured at 20°C. The long-term properties of blast furnace slag cement concrete specimens cast at 20 and 35°C and cured at 20, 35, and 50°C were also not affected. Moreover, these concretes can be cast at higher temperatures of 50 and 65°C, provided they are cured at 20°C. The long-term properties were not affected in the silica fume cement concrete specimens cast and cured at 20°C only. The long-term properties of fly ash cement concrete specimens cast at temperatures of up to 50°C were not affected provided they are cured at 20°C.

The Effect of Casting and Curing Temperatures on the Properties of Concrete

by

Mohammed Sharfuddin Ahmed

A Thesis Presented to the

FACULTY OF THE COLLEGE OF GRADUATE STUDIES

KING FAHD UNIVERSITY OF PETROLEUM & MINERALS

DHAHRAN, SAUDI ARABIA

In Partial Fulfillment of the
Requirements for the Degree of

MASTER OF SCIENCE

In

CIVIL ENGINEERING

June, 1996

INFORMATION TO USERS

This manuscript has been reproduced from the microfilm master. UMI films the text directly from the original or copy submitted. Thus, some thesis and dissertation copies are in typewriter face, while others may be from any type of computer printer.

The quality of this reproduction is dependent upon the quality of the copy submitted. Broken or indistinct print, colored or poor quality illustrations and photographs, print bleedthrough, substandard margins, and improper alignment can adversely affect reproduction.

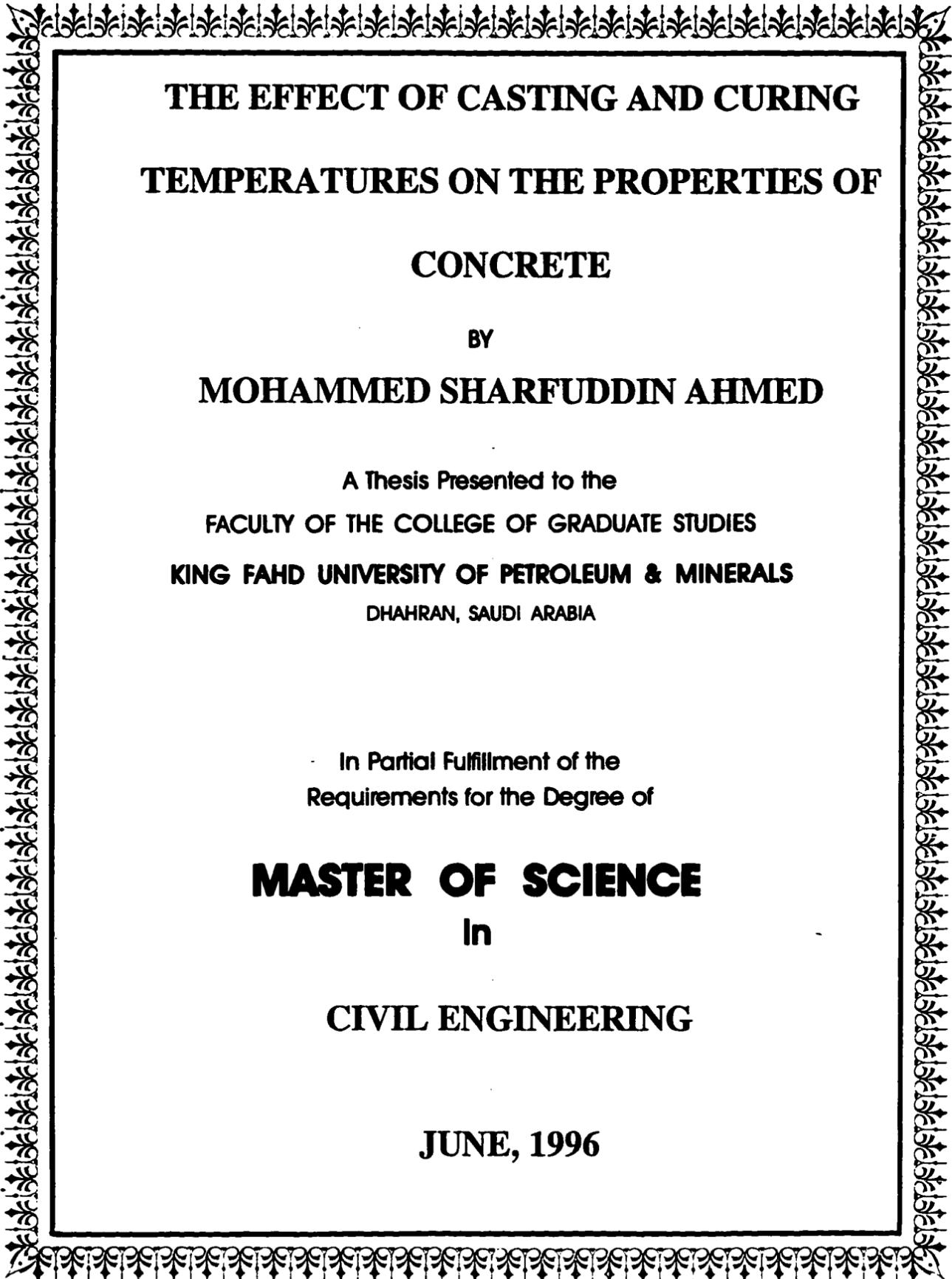
In the unlikely event that the author did not send UMI a complete manuscript and there are missing pages, these will be noted. Also, if unauthorized copyright material had to be removed, a note will indicate the deletion.

Oversize materials (e.g., maps, drawings, charts) are reproduced by sectioning the original, beginning at the upper left-hand corner and continuing from left to right in equal sections with small overlaps. Each original is also photographed in one exposure and is included in reduced form at the back of the book.

Photographs included in the original manuscript have been reproduced xerographically in this copy. Higher quality 6" x 9" black and white photographic prints are available for any photographs or illustrations appearing in this copy for an additional charge. Contact UMI directly to order.

UMI

**A Bell & Howell Information Company
300 North Zeeb Road, Ann Arbor MI 48106-1346 USA
313/761-4700 800/521-0600**



**THE EFFECT OF CASTING AND CURING
TEMPERATURES ON THE PROPERTIES OF
CONCRETE**

**BY
MOHAMMED SHARFUDDIN AHMED**

**A Thesis Presented to the
FACULTY OF THE COLLEGE OF GRADUATE STUDIES
KING FAHD UNIVERSITY OF PETROLEUM & MINERALS
DHAHRAN, SAUDI ARABIA**

**In Partial Fulfillment of the
Requirements for the Degree of**

**MASTER OF SCIENCE
In
CIVIL ENGINEERING**

JUNE, 1996

UMI Number: 1384116

UMI Microform 1384116
Copyright 1997, by UMI Company. All rights reserved.

**This microform edition is protected against unauthorized
copying under Title 17, United States Code.**

UMI
300 North Zeeb Road
Ann Arbor, MI 48103

**King Fahd University of Petroleum and Minerals
Dhahran 31261, Saudi Arabia**

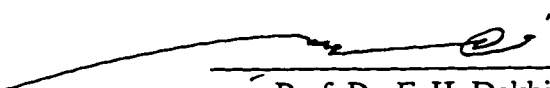
COLLEGE OF GRADUATE STUDIES


This thesis, written by

MOHAMMED SHARFUDDIN AHMED

under the direction of his Thesis Advisor and approved by his Thesis Committee, has been presented to and accepted by the Dean of the College of Graduate Studies, in partial fulfillment of the requirements for the degree of MASTER OF SCIENCE IN CIVIL ENGINEERING.

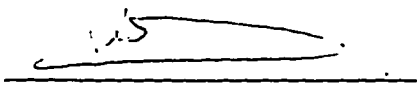
Thesis Committee

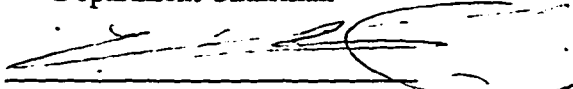

Prof. Dr. F. H. Dakhil
Thesis Advisor


Dr. M. Maslehuddin
Co-Advisor


Dr. A. S. Al-Gahtani
Member


Dr. A. Al-Musallum
Member


Dr. Al-Farabi Sharif
Department Chairman


Dr. Ala H. Al-Rabeh
Dean, College of Graduate Studies

Date: 10/8/96



بِسْمِ اللَّهِ الرَّحْمَنِ الرَّحِيمِ

In the Name of Allah, the Most Beneficent and Merciful

IN THE NAME OF ALLAH, THE MOST BENEFICENT AND MERCIFUL

- Read! In the Name of your Lord, who has created all that exists [Surah Al-Alaq: Verse 1]
- My Lord! Increase me in knowledge [Surah Taha: Verse 114]
- O you who believe! Stand out firmly for justice, as witnesses to Allah, even though it be against yourselves, or your parents, or your kin, be he rich or poor. [Surah Al-Nisa: Verse 135]
- And that you be dutiful to your parents. If one of them or both of them attain old age in your life say not to them a word of disrespect, nor shout at them but address them in terms of honor. [Surah Bani Israel: Verse 23-24]
- And Certainly, we shall test with you some thing of fear hunger, loss of wealth, lives and fruits, but give glad tidings to the patient who when afflicted with calamity, Say: "Truly! To Allah we belong and truly, to Him we shall return [Surah Al-Baqarah: Verse 155-156]
- Nay, you prefer the life of this world; Although the Hereafter is better and more lasting. [Surah Al-AAala Verse 16-17]

THIS THESIS
IS
DEDICATED TO MY PARENTS

ACKNOWLEDGMENTS

Firstly, I thank “Allah” for bestowing sound health and knowledge. I wish to thank my thesis Advisor Dr. F. H. Dakhil, whose guidance, supervision, instructions, and constructive criticism made this work possible. I also thank my thesis Co-Adviser Dr. M. Maslehuddin for his support, encouragement, and help which was infallible during this course of research, which made the work both enjoyable and rewarding. Thanks are also due to Dr. A. S Al-Gahtani for his comments and suggestions during the entire research. Acknowledgments are also attributed to Dr. A. Al-Musallam for his instant help at difficult times and also with his suggestions.

Thanks are due to the Civil Engineering Department KFUPM, which under the patronage of Dr. Al-Farabi Sharif, who provided financial support in the form of assistantship.

I also thank present and past graduate students of the department, Br. Md. Ibrahim, Br. Safder Khan, Br. Mujeebullah Khan, deceased Ashrafuddin, and also to all my friends who directly or indirectly helped me in this research. I am grateful to research Engineer Mr. M. Mukarram Khan for his help in the initial stages of this research. Special thanks are due to Lab supervisor Ibrahim Asi, and Lab technicians Br. Omar and Br. Hassan for their assistance and co-operation.

Finally, by the virtue of blessings and encouragement of my parents, brothers, and sister made this work possible.

TABLE OF CONTENTS

Title	Page
LIST OF TABLES.....	vii
LIST OF FIGURES.....	viii
THESIS ABSTRACT.....	xii
 CHAPTER 1 INTRODUCTION.....	 1
1.1 CONCRETE DETERIORATION IN THE ARABIAN GULF.....	1
1.2 NEED FOR THIS RESEARCH.....	4
1.3 RESEARCH OBJECTIVES.....	5
1.4 RESEARCH PROGRAM.....	5
 CHAPTER 2 LITERATURE SURVEY.....	 8
2.1 EFFECT OF HOT WEATHER ON THE PROPERTIES OF CONCRETE.....	8
2.2 EFFECT OF HOT WEATHER CONDITIONS ON THE PROPERTIES OF FRESH CONCRETE.....	 9
2.2.1 Shrinkage.....	9
2.2.2 Slump Loss.....	11
2.2.3 Setting Time.....	12
2.3 EFFECT OF HOT WEATHER CONDITIONS ON THE PROPERTIES OF HARDENED CONCRETE.....	 12
2.3.1 Strength.....	12
2.3.2 Cracking.....	24
2.4 POZZOLANS IN CONCRETE.....	24
 CHAPTER 3 METHODOLOGY OF RESEARCH.....	 36
3.1 MATERIALS.....	36
3.1.1 Aggregate.....	37
3.1.2 Admixture.....	37
3.2 SPECIMEN PREPARATION.....	37
3.3 CURING.....	38
3.4 TEST TECHNIQUES.....	38
3.4.1 Compressive Strength.....	38
3.4.2 Pulse Velocity.....	38
3.4.3 Absorption.....	39
3.4.4 Pore Size Distribution.....	40
3.4.5 Differential Thermal Analysis.....	41
3.4.6 X-ray Diffraction.....	42
 CHAPTER 4 RESULTS.....	 47
4.1 EFFECT OF CASTING AND CURING TEMPERATURES ON COMPRESSIVE STRENGTH IN PLAIN AND BLENDED CEMENT CONCRETE SPECIMENS.....	 47
4.2 EFFECT OF CASTING AND CURING TEMPERATURES ON PULSE VELOCITY.....	 70
4.3 EFFECT OF CASTING AND CURING TEMPERATURES ON WATER ABSORPTION.....	 92
4.4 EFFECT OF CASTING TEMPERATURE ON THE PORE SIZE DISTRIBUTION IN PLAIN AND BLENDED CEMENTS.....	 114
4.5 EFFECT OF CASTING TEMPERATURE ON CALCIUM HYDROXIDE CONTENT IN PLAIN AND BLENDED CEMENTS.....	 124

4.6	EFFECT OF CASTING TEMPERATURE ON THE MINERALOGICAL COMPOSITION IN PLAIN AND BLENDED CEMENTS.....	139
4.6.1	Effect of Casting Temperature on the Transition Zone.....	140
CHAPTER 5	DISCUSSION OF RESULTS.....	156
5.1	PROPERTIES OF PLAIN AND BLENDED CEMENT CONCRETES CAST AT 20 °C AND CURED AT 20, 35, AND 50 °C.....	156
5.1.1	Compressive Strength.....	156
5.1.2	Pulse Velocity.....	158
5.1.3	Water Absorption.....	159
5.2	PROPERTIES OF PLAIN AND BLENDED CEMENT CONCRETES CAST AT 35 °C AND CURED AT 20, 35, AND 50 °C.....	161
5.2.1	Compressive Strength.....	161
5.2.2	Pulse Velocity.....	163
5.2.3	Water Absorption.....	164
5.3	PROPERTIES OF PLAIN AND BLENDED CEMENT CONCRETES CAST AT 50 °C AND CURED AT 20, 50, AND 65 °C.....	165
5.3.1	Compressive Strength.....	165
5.3.2	Pulse Velocity.....	166
5.3.3	Water Absorption.....	167
5.4	PROPERTIES OF PLAIN AND BLENDED CEMENT CONCRETES CAST AT 65 °C AND CURED AT 20 AND 65 °C.....	167
5.4.1	Compressive Strength.....	167
5.4.2	Pulse Velocity.....	168
5.4.3	Water Absorption.....	168
5.5	SUMMARY.....	169

LIST OF TABLES

Table		Page
Table 1.1	Specimens Cast and Tested to Evaluate the Effect of Varying Casting and Curing Temperatures on the Properties of Concrete.....	6
Table 3.1	Chemical Composition of Type I Cement and Pozzolanic Materials	44
Table 4.1	Pore Size Distribution in the Plain and Blended Cement Mortar Specimens.	123
Table 4.2	Calcium Hydroxide Content in the Plain and Blended Cement Mortar Specimens.....	138
Table 4.3	Approximate Weight Fraction of Mineralogical Phases Present in the Cement Mortars by X-ray Diffraction Method.....	154
Table 4.4	Orientation of the Transition Zone.....	155
Table 5.1	Effect of Casting and Curing Temperatures on the Long-Term Properties of Plain Cement Concrete.....	171
Table 5.2	Effect of Casting and Curing Temperatures on the Long-Term Properties of Blast Furnace Slag Cement Concrete.....	172
Table 5.3	Effect of Casting and Curing Temperatures on the Long-Term Properties of Silica Fume Cement Concrete.....	173
Table 5.4	Effect of Casting and Curing Temperatures on the Long-Term Properties of Fly Ash Cement Concrete.....	174

LIST OF FIGURES

Figure		Page
Fig. 1.1	Experimental Variables to Evaluate the Effect of Varying Casting and Curing Temperatures on the Properties of Concrete.....	7
Fig. 3.1	Coarse Aggregate Grading.....	45
Fig. 3.2	Effect of Temperature on Absorption of Water in the Coarse Aggregates.....	46
Fig. 4.1	Compressive Strength Development in the Plain Cement Concrete Specimens Cast at 20 °C and Cured at various Temperatures.....	54
Fig. 4.2	Compressive Strength Development in the Blast Furnace Slag Cement Concrete Specimens Cast at 20 °C and Cured at various Temperatures.....	55
Fig. 4.3	Compressive Strength Development in the Silica Fume Cement Concrete Specimens Cast at 20 °C and Cured at various Temperature.....	56
Fig. 4.4	Compressive Strength Development in the Fly Ash Cement Concrete Specimens Cast at 20 °C and Cured at various Temperatures.....	57
Fig. 4.5	Compressive Strength Development in the Plain Cement Concrete Specimens Cast at 35 °C and Cured at various Temperatures.....	58
Fig. 4.6	Compressive Strength Development in the Blast Furnace Slag Cement Concrete Specimens Cast at 35 °C and Cured at various Temperatures.....	59
Fig. 4.7	Compressive Strength Development in the Silica Fume Cement Concrete Specimens Cast at 35 °C and Cured at various Temperatures.....	60
Fig. 4.8	Compressive Strength Development in the Fly Ash Cement Concrete Specimens Cast at 35 °C and Cured at various Temperatures.....	61
Fig. 4.9	Compressive Strength Development in the Plain Cement Concrete Specimens Cast at 50 °C and Cured at various Temperatures.....	62
Fig. 4.10	Compressive Strength Development in the Blast Furnace Slag Cement Concrete Specimens Cast at 50 °C and Cured at various Temperatures.....	63
Fig. 4.11	Compressive Strength Development in the Silica Fume Cement Concrete Specimens Cast at 50 °C and Cured at various Temperatures.....	64
Fig. 4.12	Compressive Strength Development in the Fly Ash Cement Concrete Specimens Cast at 50 °C and Cured at various Temperatures.....	65
Fig. 4.13	Compressive Strength Development in the Plain Cement Concrete Specimens Cast at 65 °C and Cured at various Temperatures.....	66
Fig. 4.14	Compressive Strength Development in the Blast Furnace Slag Cement Concrete Specimens Cast at 65 °C, and Cured at various Temperatures.....	67
Fig. 4.15	Compressive Strength Development in the Silica Fume Cement Concrete Specimens Cast at 65 °C and Cured at various Temperatures.....	68
Fig. 4.16	Compressive Strength Development in the Fly Ash Cement Concrete Specimens Cast at 65 °C and Cured at various Temperatures.....	69

Fig. 4.17	Pulse Velocity in the Plain Cement Concrete Specimens Cast at 20 °C and Cured at various Temperatures.....	76
Fig. 4.18	Pulse Velocity in the Blast Furnace Slag Cement Concrete Specimens Cast at 20 °C and Cured at various Temperatures.....	77
Fig. 4.19	Pulse Velocity in the Silica Fume Cement Concrete Specimens Cast at 20 °C and Cured at various Temperatures.....	78
Fig. 4.20	Pulse Velocity in the Fly Ash Cement Concrete Specimens Cast at 20 °C and Cured at various Temperatures.....	79
Fig. 4.21	Pulse Velocity in the Plain Cement Concrete Specimens Cast at 35 °C and Cured at various Temperatures.....	80
Fig. 4.22	Pulse Velocity in the Blast Furnace Slag Cement Concrete Specimens Cast at 35 °C and Cured at various Temperatures.....	81
Fig. 4.23	Pulse Velocity in the Silica Fume Cement Concrete Specimens Cast at 35 °C and Cured at various Temperatures.....	82
Fig. 4.24	Pulse Velocity in the Fly Ash Cement Concrete Specimens Cast at 35 °C and Cured at various Temperatures.....	83
Fig. 4.25	Pulse Velocity in the Plain Cement Concrete Specimens Cast at 50 °C and Cured at various Temperatures.....	84
Fig. 4.26	Pulse Velocity in the Blast Furnace Slag Cement Concrete Specimens Cast at 50 °C and Cured at various Temperatures.....	85
Fig. 4.27	Pulse Velocity in the Silica Fume Cement Concrete Specimens Cast at 50 °C and Cured at various Temperatures.....	86
Fig. 4.28	Pulse Velocity in the Fly Ash Cement Concrete Specimens Cast at 50 °C and Cured at various Temperatures.....	87
Fig. 4.29	Pulse Velocity in the Plain Cement Concrete Specimens Cast at 65 °C and at Cured various Temperatures.....	88
Fig. 4.30	Pulse Velocity in the Blast Furnace Slag Cement Concrete Specimens Cast at 65 °C and Cured at various Temperatures	89
Fig. 4.31	Pulse Velocity in the Silica Fume Cement Concrete Specimens Cast at 65 °C and Cured at various Temperatures.....	90
Fig. 4.31	Pulse Velocity in the Fly Ash Cement Concrete Specimens Cast at 65 °C and Cured at various Temperatures.....	91
Fig. 4.33	Absorption in the Plain Cement Concrete Specimens Cast at 20 °C and Cured at various Temperatures.....	98
Fig. 4.34	Absorption in the Blast Furnace Slag Cement Concrete Specimens Cast at 20 °C and Cured at various Temperatures.....	99
Fig. 4.35	Absorption in the Silica Fume Cement Concrete Specimens Cast at 20 °C and Cured at various Temperatures.....	100
Fig. 4.36	Absorption in the Fly Ash Cement Concrete Specimens Cast at 20 °C and Cured at various Temperatures.....	101
Fig. 4.37	Absorption in the Plain Cement Concrete Specimens Cast at 35 °C and Cured at various Temperatures.....	102

Fig. 4.38	Absorption in the Blast furnace Slag Cement Concrete Specimens Cast at 35 °C and Cured at various Temperatures.....	103
Fig. 4.39	Absorption in the Silica Fume Cement Concrete Specimens Cast at 35 °C and Cured at various Temperatures.....	104
Fig. 4.40	Absorption in the Fly Ash Cement Concrete Specimens Cast at 35 °C and Cured at various Temperatures.....	105
Fig. 4.41	Absorption in the Plain Cement Concrete Specimens Cast at 50 °C and Cured at various Temperatures.....	106
Fig. 4.42	Absorption in the Blast Furnace Slag Cement Concrete Specimens Cast at 50 °C and Cured at various Temperatures.....	107
Fig. 4.43	Absorption in the Silica Fume Cement Concrete Specimens Cast at 50 °C and Cured at various Temperatures.....	108
Fig. 4.44	Absorption in the Fly Ash Cement Concrete Specimens Cast at 50 °C and Cured at various Temperatures.....	109
Fig. 4.45	Absorption in the Plain Cement Concrete Specimens Cast at 65 °C and Cured at various Temperatures.....	110
Fig. 4.46	Absorption in the Blast Furnace Slag Cement Concrete Specimens Cast at 65 °C and Cured at various Temperatures.....	111
Fig. 4.47	Absorption in the Silica Fume Cement Concrete Specimens Cast at 65 °C and Cured at various Temperatures.....	112
Fig. 4.48	Absorption in the Fly Ash Cement Concrete Specimens Cast at 65 °C and Cured at various Temperatures.....	113
Fig. 4.49	Pore Size Distribution in the Plain Cement Mortar Specimens Cast at various Temperatures and Cured at 20 °C.....	119
Fig. 4.50	Pore Size Distribution in the Blast Furnace Slag Cement Mortar Specimens Cast at various Temperatures and Cured at 20 °C.....	120
Fig. 4.51	Pore Size Distribution in the Silica Fume Cement Mortar Specimens Cast at various Temperatures and Cured at 20 °C.....	121
Fig. 4.52	Pore Size Distribution in the Fly Ash Cement Mortar Specimens Cast at various Temperatures and Cured at 20 °C	122
Fig. 4.53	Effect of Casting Temperature on the Ca(OH)_2 Content in the Plain Cement Mortar Specimens Cast and Cured at 20 °C.....	126
Fig. 4.54	Effect of Casting Temperature on the Ca(OH)_2 Content in the Plain Cement Mortar Specimens Cast at 35 °C and Cured at 20 °C.....	127
Fig. 4.55	Effect of Casting Temperature on the Ca(OH)_2 Content in the Plain Cement Mortar Specimens Cast at 50 °C and Cured at 20 °C.....	128
Fig. 4.56	Effect of Casting Temperature on the Ca(OH)_2 Content in the Blast Furnace Slag Cement Mortar Specimens Cast and Cured at 20 °C.....	129
Fig. 4.57	Effect of Casting Temperature on the Ca(OH)_2 Content in the Blast Furnace Slag Cement Mortar Specimens Cast at 35 °C and Cured at 20 °C.....	130
Fig. 4.58	Effect of Casting Temperature on the Ca(OH)_2 Content in the Blast Furnace Slag Cement Mortar Specimens Cast at 50 °C and Cured at 20 °C.....	131

Fig. 4.59	Effect of Casting Temperature on the Ca(OH)_2 Content in the Silica Fume Cement Mortar Specimens Cast and Cured at 20 °C.....	132
Fig. 4.60	Effect of Casting Temperature on the Ca(OH)_2 Content in the Silica Fume Cement Mortar Specimen Cast at 35 °C and Cured at 20 °C.....	133
Fig. 4.61	Effect of Casting Temperature on the Ca(OH)_2 Content in the Silica Fume Cement Mortar Specimens Cast at 50 °C and Cured at 20 °C.....	134
Fig. 4.62	Effect of Casting Temperature on the Ca(OH)_2 Content in the Fly Ash Cement Mortar Specimens Cast and Cured at 20 °C.....	135
Fig. 4.63	Effect of Casting Temperature on the Ca(OH)_2 Content in the Fly Ash Cement Mortar Specimens Cast at 35 °C and Cured at 20 °C.....	136
Fig. 4.64	Effect of Casting Temperature on the Ca(OH)_2 Content in the Fly Ash Cement Mortar Specimens Cast at 50 °C and Cured at 20 °C.....	137
Fig. 4.65	Effect of Casting Temperature on the X-ray Diffraction in the Plain Cement Mortar Specimens Cast and Cured at 20 °C.....	142
Fig. 4.66	Effect of Casting Temperature on X-ray Diffraction in the Plain Cement Mortar Specimens Cast at 35°C and Cured at 20 °C.....	143
Fig. 4.67	Effect of Casting Temperature on X-ray Diffraction in the Plain Cement Mortar Specimens Cast at 50 °C and Cured at 20 °C.....	144
Fig. 4.68	Effect of Casting Temperature on X-ray Diffraction in the Blast Furnace Slag Cement Mortar Specimens Cast and Cured at 20 °C.....	145
Fig. 4.69	Effect of Casting Temperature on X-ray Diffraction in the Blast Furnace Slag Cement Mortar Specimens Cast at 35 °C and Cured at 20 °C.....	146
Fig. 4.70	Effect of Casting Temperature on X-ray Diffraction in the Blast Furnace Slag Cement Mortar Specimens Cast at 50 °C and Cured at 20 °C.....	147
Fig. 4.71	Effect of Casting Temperature on X-ray Diffraction in the Silica Fume Cement Mortar Specimens Cast and Cured at 20 °C.....	148
Fig. 4.72	Effect of Casting Temperature on X-ray Diffraction in the Silica Fume Cement Mortar Specimens Cast at 35 °C and Cured at 20 °C.....	149
Fig. 4.73	Effect of Casting Temperature on X-ray Diffraction in the Silica Fume Cement Mortar Specimens Cast at 50 °C and Cured at 20 °C.....	150
Fig. 4.74	Effect of Casting Temperature on X-ray Diffraction in the Fly Ash Cement Mortar Specimens Cast and Cured at 20 °C.....	151
Fig. 4.75	Effect of Casting Temperature on X-ray Diffraction in the Fly Ash Cement Mortar Specimens Cast at 35 °C and Cured at 20 °C.....	152
Fig. 4.76	Effect of Casting Temperature on X-ray Diffraction in the Fly Ash Cement Mortar Specimens Cast at 50 °C and Cured at 20 °C.....	153

THESIS ABSTRACT

NAME OF THE STUDENT MOHAMMED SHARFUDDIN AHMED

**TITLE OF STUDY THE EFFECT OF CASTING AND
CURING TEMPERATURES ON THE
PROPERTIES OF CONCRETE**

MAJOR FIELD CIVIL ENGINEERING

DATE OF DEGREE JUNE 1996

This study was conducted to investigate the effect of casting and curing temperatures on the properties of plain and blended cement concretes. To achieve the objectives of this research more than 1200 concrete specimens were cast. The effect of casting and curing temperatures on the compressive strength, pulse velocity, and absorption were evaluated up to a period of 168 days. Furthermore, these tests were supplemented with pore size distribution, X-ray diffraction, and Differential thermal and thermogravimetric analysis.

The long-term properties of plain cement concrete specimens were not affected for casting temperatures of up to 50 °C, provided they are cured at 20 °C. The long-term properties of blast furnace slag cement concrete specimens cast at 20 and 35 °C and cured at 20, 35, and 50 °C were also not affected. Moreover, these concretes can be cast at higher temperatures of 50 and 65 °C, provided they are cured at 20 °C. The long-term properties were not affected in the silica fume cement concrete specimens cast and cured at 20 °C only. The long-term properties of fly ash cement concrete specimens cast at temperatures of up to 50 °C were not affected provided they are cured at 20 °C.

The proportion of coarse pores increased with an increase in the casting temperatures in all the concrete specimens. However, temperature did not affect the pore size distribution in the blast furnace slag cements. This indicates that these cements can be beneficially utilized at higher casting temperatures. The orientation of the transition zone became less preferential with increasing casting temperature. The orientation of transition zone in the fly ash cement concrete specimens cast at 50 °C was highly preferential indicating that these cements can be utilized at higher casting temperatures provided they are cured at 20 °C.

ملخص رسالة البحث

الإسم : محمد شرف الدين أحمد

العنوان : تأثير الصب وحرارة الإنضاج على خصائص الخرسانة

التخصص : هندسة مدنية (إنشاءات).

تاريخ الدرجة : يونيو ١٩٩٦ م.

تم إجراء هذه الدراسة لبحث تأثير درجة حرارة الصب وحرارة الإنضاج على خصائص الخرسانة العادية والخرسانة المحسنة بمواد أخرى. ولتحقيق هذه الدراسة فقد تم اختيار أكثر من ألف ومائتان عينة خرسانية، لمعرفة تأثير حرارة الصب وحرارة النضج على قوة الخرسانة، وسرعة النضجات، وقابلية الإمتصاص لفترات امتدت إلى ١٦٨ يوماً. بالإضافة إلى ذلك فقد تم تدعيم الدراسة والاختبارات بمعرفة توزيع أحجام المسامات وإنكسار الأشعة السينية، وكذلك التحليل الحراري.

لم تتأثر الخصائص طويلة المدى للخرسانة التي لم يضاف إليها مواد محسنة والتي تم صبها على درجات حرارة وصلت إلى ٥٠ درجة مئوية وذلك إذا تم إنضاجها على درجة حرارة ٢٠ درجة مئوية. وكذلك بالنسبة للخصائص طويلة المدى للخرسانة التي تم إضافة خبث الحديد إليها فإن خصائصها لم تتأثر بدرجات الصب على حرارة ٢٠ درجة مئوية و ٣٥ درجة مئوية حيث تم إنضاجها على درجة حرارة ٢٠ درجة مئوية ٣٥ درجة مئوية و ٥٠ درجة مئوية. بالإضافة لذلك فيمكن صب هذه الخرسانة على درجات حرارة تصل إلى ٥٠ درجة مئوية و ٦٥ درجة مئوية وذلك إذا تم إنضاجها على درجة حرارة ٢٠ درجة مئوية. أما الخصائص طويلة المدى للخرسانة التي إستخدم فيها رذاذ السيليكا فإنها لا تتأثر إذا تم صبها وإنضاجها على درجة ٢٠ درجة مئوية فقط. أما بالنسبة للخصائص طويلة المدى للخرسانة التي إستخدم فيها الرماد المتطاير فإنها لا تتأثر حتى درجات صب ٥٠ درجة مئوية وذلك إذا تم إنضاجها على ٢٠ درجة مئوية.

وقد لوحظ في جميع العينات الخرسانية زيادة نسبة المسامات الكبيرة نتيجة لزيادة درجات حرارة الصب. بالرغم من ذلك فإن درجة حرارة الصب لم تؤثر على توزيع أحجام المسامات في عينات خبث الحديد الخرسانية. ويوضح هذا إمكانية إستخدام هذه الخرسانة عند درجات صب مرتفعة. أما إتجاه منطقة التحول فقد أصبحت أقل وضوحاً مع إرتفاع درجة الصب. وبالنسبة لخرسانة الرماد المتطاير المصبوبة على درجة ٥٠ درجة مئوية فقد كان إتجاه منطقة التحويل واضحاً مما يدل على إمكانية صب هذه المواد على درجات حرارة مرتفعة إذا تم إنضاجها على درجة حرارة ٢٠ درجة مئوية.

درجة ماجستير في العلوم الهندسية

جامعة الملك فهد للبترول والمعادن

الظهران، المملكة العربية السعودية

CHAPTER 1

INTRODUCTION

1.1 CONCRETE DETERIORATION IN THE ARABIAN GULF

The poor durability performance of reinforced concrete construction in the coastal areas of the Arabian Gulf is very well documented [1-3]. The major causes for such a phenomena are: (i) severe climate and geomorphic conditions, (ii) inappropriate materials specifications, and (iii) inadequate construction practices. The climate, characterized by high temperature and humidity and large fluctuations in the diurnal and seasonal temperature and humidity, adversely affects the concrete durability. The temperature can vary by as much as 20 °C during summer and the relative humidity ranges from 40 to 100% over 24 hours. These sudden and continuous variations in the temperature and humidity lead to expansion/contraction of the concrete members resulting in their cracking. This variations in temperature cause thermal stresses resulting in plastic and drying shrinkage cracks. These cracks increase the permeability and diffusion of aggressive species, such as chloride, oxygen, carbon dioxide and moisture into the concrete matrix, which accelerates the deterioration processes.

The differential expansion and contraction of the aggregate and the hardened cement paste may also set up tensile stresses far beyond the tensile capacity of

concrete resulting in its microcracking and eventual spalling of the concrete cover. Limestone, the predominantly used aggregate in the Arabian Gulf has a coefficient of thermal expansion of $1 \times 10^{-6}/^{\circ}\text{C}$, whereas the coefficient of expansion of hardened cement paste is much higher (usually between $10 \times 10^{-6}/^{\circ}\text{C}$ and $20 \times 10^{-6}/^{\circ}\text{C}$). With the fall in temperature, tensile and compressive stresses are set up in the cement paste and aggregate, respectively. With the rise in temperature, however, the stresses are not exactly reversed, but tensile stresses are set up at the aggregate-paste interface tending to cause interface bond failure and significant microcracking around the transition zone. It has been shown by Hsu [4] that a volume change of 0.3% is enough to generate tensile stresses of the order of 800 psi at the aggregate-paste interface. Slate and Matheus [5] have determined volume changes of cement paste and indicated that volume changes even larger than 0.3% may occur during setting and hardening of concrete. Further they indicated that tensile stresses of more than 250 psi are created for every 10°C fall in temperature.

The major causes of concrete deterioration in the Arabian Gulf are reinforcement corrosion, sulfate attack, salt weathering, and cracking due to plastic and drying shrinkage. However, deterioration due to reinforcement corrosion overshadows that caused by other factors. The climate in the Arabian Gulf is particularly helpful to the chemical reactions involved in reinforcement corrosion and other

disintegration processes. The mean annual temperature is generally 8 °C above a value of 18 °C that defines a hot desert. The summer air temperature frequently reaches 45-50 °C. At this ambient temperature the concrete surface temperature may reach 70 °C due to solar radiation [6]. The hot weather conditions in the Arabian Gulf may cause increased water demand, slump loss and premature setting, resulting in cold joints and insufficient compaction and enhanced tendency for plastic shrinkage cracking. Concrete cast under hot weather conditions and not sufficiently cured may show as much as 30 to 40% reduction in strength [7]. Any deficiency in curing, which may have negligible effect in the mild climatic conditions may impair the quality of concrete cover in the hot weather conditions.

The high temperature and humidity conditions in the Arabian Gulf also accelerate the chemical reactions involved in concrete deterioration. The penetration of aggressive substances such as chlorides and carbon dioxide proceeds more rapidly. Studies [8] conducted on the effect of temperature and humidity on reinforcement corrosion indicated that the rate of reinforcement corrosion is increased by high temperature and high humidity. It is also sharply increased by a rise in the temperature, in the range of 20-40 °C, especially at high humidity. Another area of concern is the effect of hot weather on the strength and microstructure of concrete. while a reduction in the strength due to hot weather

conditions is detrimental from the structural view point, a porous structure creates long-term durability problems.

1.2 NEED FOR THIS RESEARCH

ACI Committee 305 recommendations [9] provide useful guideline for concreting in the hot-weather conditions. However, the effect of casting and curing temperatures on the properties of hardened concrete have not been fully elucidated. A variation in the casting and curing temperature is bound to affect the properties of concrete. In addition, the effect of casting and curing temperatures on the properties of blended cements, made using blast furnace slag, silica fume, and fly ash needs to be evaluated. Such a study is very important as these materials are increasingly used in the Arabian Gulf for their technical advantages.

The proper understanding of the cumulative effect of casting and curing temperatures on the properties of concrete will lead to improved construction practices culminating in the production of durable concrete resulting in considerable savings in the form of repair and rehabilitation.

1.3 RESEARCH OBJECTIVES

The general objectives of this research were to evaluate the effect of casting and curing temperatures on the properties of hardened concrete. The specific objectives were:

1. to investigate the effect of casting and curing temperatures on compressive strength, pulse velocity, and water absorption in concrete,
2. to assess the effect of casting and curing temperatures on the mineralogical composition of concrete, and the orientation of transition zone, and
3. to study the pore size distribution in concrete cast and cured at varying temperatures.

1.4 RESEARCH PROGRAM

To achieve the objectives of this study, plain and blended cement concrete specimens were cast and cured at temperatures in the range of 20 to 65 °C. The effect of the casting and curing temperatures on the properties of hardened concrete was evaluated. A total number of 1176 concrete specimens were cast and tested to fulfill the objectives of this research. The details of the experimental variables are shown in Table 1.1 and Fig 1.1.

Table 1.1 : Specimens cast and tested to evaluate the effect of varying casting and curing temperatures on the properties of concrete

Mix Number	Cement	Casting Temperature (°C)	Number of Specimens
1	I	20	63
2	I	35	63
3	I	50	63
4	I	65	42
5	I+FA	20	63
6	I+FA	35	63
7	I+FA	50	63
8	I+FA	65	42
9	I+SF	20	63
10	I+SF	35	63
11	I+SF	50	63
12	I+SF	65	84
13	I+BFS	20	126
14	I+BFS	35	126
15	I+BFS	50	126
16	I+BFS	65	84

Total Number of Specimens : 1176

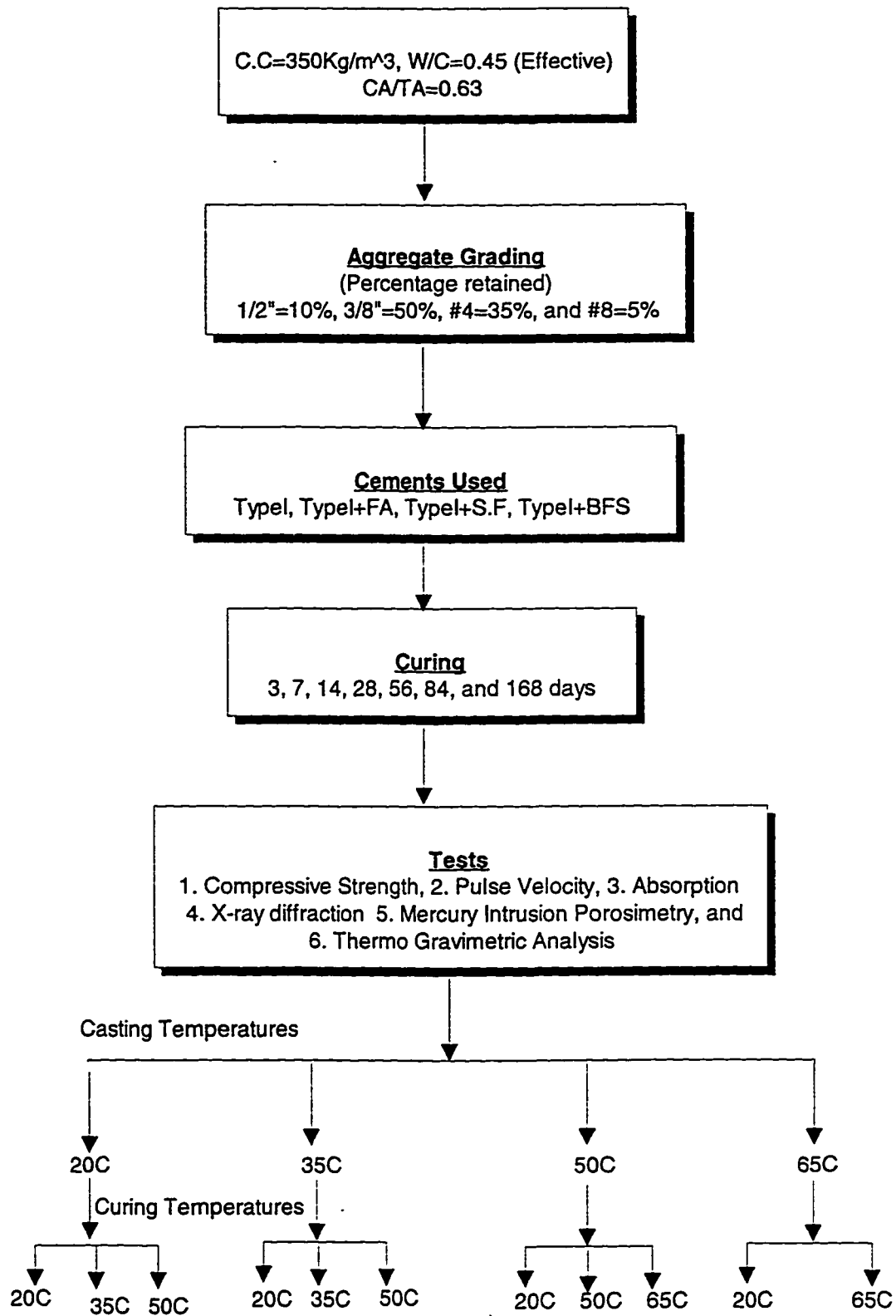


Figure 1.1: Experimental variables to evaluate the effect of casting and curing temperatures on the properties of concrete

CHAPTER 2

LITERATURE REVIEW

2.1 EFFECT OF HOT WEATHER ON THE PROPERTIES OF CONCRETE

ACI Committee 305 [9] defines hot weather as any combination of high air temperature, low relative humidity and wind velocity. Another wider definition by Shalon [10] characterizes hot climate as relatively high air temperature with both low and high relative humidity, high or low precipitation under various degrees of solar radiation and wind velocity. Irrespective of the definition, hot weather conditions pose several problems in fresh and hardened concrete. Some of the problems in fresh concrete are:

1. Increased water demand for required consistency,
2. Rapid loss of slump,
3. Accelerated set, and
4. Increased plastic and drying shrinkage cracking.

The potential problems in hardened concrete cast under hot-weather conditions are:

1. Decreased long-term strength resulting from either higher water demand or higher concrete temperature at the time of placement
2. Increased tendency for drying shrinkage from temperature differentials within the cross section of a member,

3. Decreased durability due to cracking,
4. Increased permeability, and
5. Enhanced reinforcement corrosion which is primarily due to cracking of concrete.

Some of the problems associated with hot-weather concreting are discussed in the following sections.

2.2 EFFECT OF HOT WEATHER CONDITIONS ON THE PROPERTIES OF FRESH CONCRETE

2.2.1 Shrinkage

Cracking of concrete due to plastic shrinkage is a major hazard of hot-weather concreting, particularly in the arid regions. It occurs when the shrinkage force generated by concrete exceeds the tensile strength of the fresh concrete.

Plastic shrinkage produces very fine cracks which facilitate the diffusion of the aggressive species into concrete. A major draw back with plastic shrinkage cracking is that the cracks are very difficult to repair. Plastic shrinkage cracking is dependent on the rate of bleeding and evaporation in such a way that the latter should be less than the former. Another point which should be noted is that the rate of bleeding is dependent on the concrete mix design. Therefore, Menzel's formula may not precisely predict plastic shrinkage cracking. Hence, there is a need to

evaluate the effect of environmental conditions and concrete composition on plastic shrinkage cracking. Presently research is in progress at KFUPM [11] to elucidate this phenomena.

Plastic shrinkage cracking may be relatively greater in the pozzolanic cement concretes than in the plain cement concrete. Silica fume cement concrete is more cohesive and less prone to segregation. Moreover, it shows significantly reduced bleeding, as silica fume reduces bleeding by physically blocking the pores in the fresh concrete. Therefore, the potential for plastic shrinkage cracking in this cement is significantly accelerated. Hence, care should be taken to prevent early moisture loss from freshly placed silica fume cement concrete.

The physical properties of high strength silica fume cement concretes and their sensitivity to curing procedure was evaluated and compared with reference to ordinary Portland cement concrete by Bentur and Goldman [12]. The shrinkage of the silica fume cement concretes was much lower due to the smaller weight loss on drying. The effects of poor curing procedures on the strength or skin properties were equally detrimental in the reference and silica fume cement concretes.

Novokschenov [13] recommends use of Type V Portland cement which has lower cracking tendency compared to Type I and Type III cements in hot climate.

Moreover, the author suggests the use of normal water reducers with slight retarding effect and to avoid Type III Portland cement in hot climate. Furthermore, various precautions such as precast concrete elements, low slump concrete, good consolidation, proper evaluation of superplasticizer, and curing under controlled conditions with low or high pressure steam must be considered in hot weather conditions.

2.2.2 Slump Loss

Concreting under hot weather conditions significantly affects its workability. Klieger [14] reported a decrease in slump of 2.5 cm for every 11 °C rise in temperature. Mehta [15] indicated that the quantity of water required to produce a given slump decreases with an increase in the maximum size of the aggregate, thereby lowering the w/c ratio for a specified workability.

Slump tests were conducted at various temperature and humidity conditions by Shalon and Ravina [16], both in the laboratory and in the field. The results indicated that slump was affected in concrete cast at 50 °C and 20% R.H, whereas concrete cast up to 40 °C and 70% R.H had no measurable effect on the slump. The authors further indicated that the higher the initial slump, the higher the loss, even after 20 minutes in a climatic temperature of 28-37 °C and 17-40% R.H. The problem of loss of slump is, however, more relevant to the ready-mixed concrete

(potentially difficult to discharge, handle and place), particularly when the time lapse between mixing and placing may be considerable. It is generally assumed that retarders or water reducers and retarding admixtures have a beneficial effect on the loss of slump under hot weather conditions. Contrary to the above assumption, with regard to loss of slump, experiments conducted by Ravina [17] on ready mixed concrete mixed continuously for 1 or 2 hrs at 30 °C and made with water retarding admixtures (ASTM type D) showed a higher loss of slump than concrete without any admixture.

2.2.3 Setting Time

The elevated temperature increases the rate of cement hydration and this accelerates its setting. However, the degree of acceleration depends on the composition and fineness of cement.

2.3 EFFECT OF HOT WEATHER CONDITIONS ON THE PROPERTIES OF HARDENED CONCRETE

2.3.1 Strength

The property of hardened concrete which appears to be significantly affected by hot weather conditions is compressive strength, particularly at later ages. Tsui [18] reported that in concrete cast at a temperature ranging from 19-33 °C, the 7-day compressive strength was 3/4 of that at 28 days, whereas in concrete cast at

normal temperature the 7-day compressive strength was about 2/3 of that at 28 days. Ridgley [19] found that the reduction in the compressive strength of concrete, cast at an average temperature of 30 °C and a relative humidity of 70-87%, was 85% of that cast at 23 °C. In a study conducted by Court [20] the compressive strength of concrete cured at 32 °C was 92% of that cured at 23 °C.

Experiments conducted by Shalon and Ravina [16], showed that concrete specimens cast at mid-day exhibited higher compressive strength at 3,7, and 56 days, compared to those cast in the mornings and evenings. In the same study, concrete cast at different combinations of temperatures of 20,30,40 °C and R.H of 20, 45, and 70%, a significant reduction in the compressive strength at 56 days was indicated. Concrete cast at 30 °C and a R.H of 70%, showed a reduction in strength of 8-15%, while at 45% R.H the reduction in strength was 15-25%. An increase in temperature above 30 °C brought no further reduction in the compressive strength. Hermite [21] reported that concrete cast at 40 °C required an increase of 10% W/C ratio, whereas, concrete cast at 60 °C required an increase of 20% W/C ratio, compared to concrete cast at 20 °C.

In research conducted by Shalon and Bentur [7] on portland cements with C_3A content of 3.7, 7.5, 12.5%, and exposed to temperatures of 10, 25 and 40 °C,

exhibited 400-600% increase in 1 day strength and a decrease of 10% in the later-age strength. They indicated that C_3A content of cement also influenced the strength along with the initial temperature of casting. Verbeck and Helmuth [22] reported that an increase in one day strength of concrete cured at a temperature in the range of 5-110 °C is attributable to the heat evolved by the chemical hydration process. They further indicated that elevated temperature is beneficial to early strength development. According to them, at normal temperatures, about 20% of the cement hydrates in two hours, while at 40 °C, 30 to 40% of cement hydrates in the same time. However, as the accelerated initial hydration forms a dense layer around the cement grains it retards subsequent hydration. Consequently the distribution of hydration products within the paste will be non-uniform, thereby reducing the ultimate strength.

The properties of fresh and hardened concrete containing up to 30% fly ash were examined by Ravina [23]. The specimens were cast at 20 and 40 °C. It was found that the decrease in slump was smaller and the amount of water required to maintain a constant slump increased in the fly ash cement concrete. The compressive strength of constant water content fly ash cement concrete was, however, not affected by the elevated temperature, but the strength of constant workability mix was reduced. Ray et al. [24] reported that addition of superplasticizers by 2% weight of cement, and four latexes of 5, 10, 15, and 20%

solid polymer content by weight of cement, improved the 7 and 28 days compressive strength, deformation, ultrasonic pulse velocity, toughness, and water resistance of hardened latex modified mortar after the testing period.

The effect of curing on strength development in both plain and fly ash cement concretes was investigated by Haque [25]. Cylindrical concrete specimens, 200X100 mm, were exposed to ambient condition of 23 °C at 40% R.H and 45 °C at 20% R.H. The 91 day compressive strength of plain and fly ash concrete was 67 and 50% of the continuously fog cured specimens. However, 7 days prior curing improved these values to 95 and 82% of the fully cured specimens. This shows that the initial 7 days curing is much more important for strength development and durability of fly ash cement concrete than plain cement concrete specimens.

In another study Haque and Kayyali [26] stated that the total porosity of continuously fog-cured fly ash cement concrete specimens was up to 1.7 times the porosity of the corresponding plain cement concrete specimens. However, 7 days of initial fog curing, followed by 91 days of hot exposure reduced this ratio to 1.1. Furthermore, the pore size distribution in the fly ash cement concrete specimens was also finer than that of the corresponding plain cement concrete specimens. Consequently, the strength development in the fly ash cement concrete specimens

and the beneficial effects of hot weather exposure conditions on the pore size distribution increased subsequently with adequate curing.

The properties of fresh and hardened concrete using 356 to 486 kg/m³ of Type III cement was examined by Lapinas [27]. Cylindrical concrete specimens, 100X200 mm, were cast and steam was injected during the mixing to raise the temperature of fresh concrete up to 79 °C. Compressive strength of approximately 4000 psi was obtained within 6 hours. The high mixing and initial curing temperature resulted in a loss of 20 to 30% in the 28 day strength if no additional moist curing was used. However, 5 to 15% loss in the compressive strength was noted if the specimens were moist cured following elevated temperature curing. The splitting tensile strength of hot concrete at early ages and 28 days were as good as those of standard cured concrete in relation to their compressive strength.

Zivkovic [28] evaluated the effect of temperature on the properties of plain cement concrete with 15 to 20% blast furnace slag. Six different temperatures ranging from 8-60 °C were used in casting at a relative humidity of 95 to 98% and the specimens were cured for 28 days. Results indicated that workability of fresh concrete decreased with an increase in the temperature. In order to obtain satisfactory consolidation, higher W/C was used, this lead to a higher porosity of hardened concrete. The compressive strength decreased in the concrete cast at

temperatures of more than 20 °C compared to concrete cast and cured below 20 °C. The effect of hot and dry environments on the strength of plain and pozzolanic cements, containing ground granulated blast furnace slag, was studied by Wainwright et al. [29]. The plain cement mortars were severely affected by hot-dry environments independent of the length of curing, while pozzolanic mortars exhibited better properties when subjected to one day curing.

In general, curing ensures that the mixing water is available for cement hydration. According to Powers [30] a minimum of 80% humidity is required for cement hydration. Moreover, he suggested that the permeability of the surface concrete may increase five to ten folds if concrete is insufficiently cured. High wind and temperature increases the drying of skin concrete. Therefore, the recommendations of ACI Committee 305 [9] should be adopted. The sensitivity of curing is more pronounced in cements containing high percentage of blast furnace slag, fly ash and silica fume. The protection of concrete against corrosion of steel, which is mainly due to the ingress of chloride ions is greatly decreased with an increase in the period of curing [31].

The type of curing water also influences the properties of hardened concrete. The chlorides and sulfate ions initiate the deterioration of the passivating film more rapidly if brackish water is used. Investigations conducted by Rasheeduzzafar et al.

[31] showed that the chloride concentration at 1.5 inch was 18 times more than the allowable value of 0.15% by weight of cement when brackish water was used. Page et al. [32] reported that in hardened cement paste of 0.5 w/c, the effective diffusivity of Cl^- ions increased from 45×10^{-9} to $1.15 \times 10^{-7} \text{ cm}^2/\text{sec}$, when the curing medium was changed from lime water to saturated air. Smolczyk [33] reported that in hardened cement paste of 0.6 w/c, the Cl^- permeability is halved when the curing period is increased from 7 to 28 days.

Curing is mainly responsible for pore structure, permeability, diffusion, and absorption characteristics of concrete. These properties determine the performance of concrete against penetration of liquids, gases and other ions [34]. Gowripalan et al. [35] have suggested that the most effective and ideal condition for strength development and hydration of cement is to keep concrete surface continuously moist by ponding or spraying it with water.

Concrete can be cured by covering it with an impermeable sheet such as polyethylene, using water retaining techniques, and by the application of curing membranes. The curing efficiency of solvent-borne resin, wax emulsion, solvent-borne acrylic, and acrylic emulsion curing compounds were studied by Wainwright et al. [36]. They found that concrete specimens cured with water ponding technique and those cured with curing compounds was better than un-cured

concrete specimens. The performance of 3 day water cured specimens was better than those cured with the curing compounds. Of the curing membranes used, wax emulsion was the most efficient and as effective as 3 days water ponding. The acrylic emulsion membrane was the least efficient of all the curing membranes tested. Taryal et al. [37] evaluated the effect of various curing methods on the compressive strength such as: (i) sprinkling water twice a day and covering by plastic sheets, (ii) sprinkling water twice a day and covering by jute cloth, and (iii) sprinkling water twice a day, and (iv) covering by plastic sheet only without any water. The compressive strength of concrete specimens cured using the first method was 10% more than those of the second category. The compressive strength of the second category of concrete specimens was 30% more than those of category (iii). The effective curing period for category (i) was about 14 days, while it was 28 days for category (ii) specimens.

The effect of curing period and curing delay on the properties of concrete in hot weather was studied by Al-Ani et al. [38]. They stated that the wet burlap curing method was an effective method for maintaining the moisture content and curing in hot weather. Moreover, the authors recommended a minimum curing period of three days for rich mixes, while longer curing period was necessary for concretes of lower cement content and minimum of seven days was required for lean mixes. A delay of one day curing caused significant loss in compressive strength exposed to

hot weather in all the mixes. The authors also observed that the delay and stopping of curing caused substantial dimensional changes which gave rise to shrinkage. This behavior increases the cracking tendency especially at early ages.

Bergstrom [39] studied the effect of curing temperature and age on the strength of concrete and stated that these properties can be expressed in terms of a single parameter given by the product of age and temperature as suggested by Nurse [40] and Saul [41]. The author suggested that special precautions must be taken to protect the concrete from freezing during the initial period after placing and the humidity of the ambient air must be taken into account.

The effect of curing on the strength development in high strength concrete, made using silica fume and fly ash, at low temperatures was studied by Marzouk and Hussein [42]. Tests were performed on three sets of specimens cured for 1, 14, and 28 days at room temperature. The test specimens were exposed to five temperatures varying from -10°C to 20°C for a period of three months in cold ocean water. The authors found that the gain in compressive and tensile strength with time were directly proportional to the temperature increase. The highest gain in strength with time was recorded in the specimens cured at 20°C and lowest in those cured at -10°C for all the three-sets of specimens. In the specimens cured for 1-day, the reduction in the strength was profound. However, it was

insignificant in the specimens cured initially for 14 days, and negligible in the specimens cured initially for 28 days. The maturity analysis using hyperbolic function was in reasonable agreement with all the three sets of specimens at different temperatures except in the specimens cured for 1-day and exposed to 7-days.

Soroka et al. [43] studied the effect of steam curing on the later-age strength of concrete with a cement content in the range of 150 to 400 kg/m³. Three series of tests were conducted by varying time of setting, curing period, and temperature of curing, respectively. The delay in pouring the concrete was 30 to 60 minutes, the curing period varied from two to five hours, and the curing temperature ranged from 60 to 80 °C. The results showed that steam-curing affected adversely the later-age strength of concrete. However, under short curing periods and moderate temperatures this adverse effect was primarily due to the lack of supplementary wet-curing and not due to physical factors such as increased porosity, internal cracking, and the heterogeneity of the paste. Accordingly, under these conditions supplementary seven days wet curing was found effective in eliminating the adverse effect of steam curing on concrete strength.

Kjellsen et al. [44] studied the influence of curing temperatures on the micro structure of plain portland cement paste and found that low curing temperatures

resulted in uniformly distributed hydration products and fine self-contained pores. Elevated temperatures, however, resulted in non-uniform hydration products and coarse inter-connected pores. They also found that a more open pore structure resulting from elevated curing temperature would adversely affect the resistance of concrete to the ingress of harmful species. The effect of curing at elevated temperature on the micro structure in calcium silicate and portlandite was studied by several authors [45-55]. The authors agree that the paste becomes more permeable with increasing curing temperature due to the formation of coarser calcium silicate hydrate. Bentur et al. [50] reported that an increase in the polysilicate content was indicated in the gel with increasing temperature of 4, 25, and 65 °C when C_3S with a w/c of 0.4 was used.

The effect of curing conditions on the properties of silica fume cement concrete was investigated by Cabrera and Claise [56]. In that study two concrete mixes with 20% silica fume and a water-cementitious materials ratio of 0.3 and 0.46 were compared with corresponding plain cement concrete specimens. The effect of both cold and dry curing on the concrete properties and the progress of pozzolanic reaction was measured after 90 and 165 days. The results indicated that silica fume is more sensitive to changes in temperature and period of curing compared to plain cement concrete. Even after 90 days of curing, at a temperature of 6 °C, the pozzolanic reaction was barely detectable in the silica fume cement concrete and

the benefits derived from it were not observed. Goto and Roy [54] showed that permeability of cement paste increased when it was cured at 60 °C when compared to 20 °C. However, the porosity, determined by MIP was less in the pastes cured at elevated temperature. The authors attributed this observation to an increase in the porosity to above the detection limit (7.5µm pore radii).

According to Cao and Detwiler [57] elevated curing temperature results in a coarser, more continuous pore structure for cement hydrated to a given degree of hydration. However, blast furnace slag cement paste at 30% hydration appeared to benefit from elevated curing temperature in contrast to Portland cement and silica fume cement pastes. In the same study [57] it was observed that the microstructure of pastes cured at 70 °C was more porous and less uniform than that of pastes cured at 23 °C, regardless of the composition of the cement pastes. The presence of additives, particularly silica fume, had pronounced effect in refining the pore structure and homogenizing the distribution of the hydrates. These findings were consistent with the measurements of chloride diffusion in comparable concretes.

Austin and Robins [58] indicated that wet burlap curing was the most effective and air curing was the least effective between 7 and 28 days in hot climate. Moist cured blast furnace slag cement concrete exhibited a greater increase in pulse velocity than the plain cement concrete mixes. The influence of hot weather on

plain cement concrete was only minimal at earlier ages. Wang and Black [59] evaluated the performance of curing membranes. Curing Efficiency Index (C.E.I) did co-relate well with the capability of the curing membranes in retaining moisture within it. The authors caution that such a single index is far from adequate and is liable to give misleading information.

2.3.2 Cracking

Elevated temperature casting and curing may induce micro cracks in the concrete. Studies by Patel et al. [60] reported that microstructure of concrete at elevated temperature was coarser than those cured at 20 °C. Microcracking was observed in all the concrete specimens forming a prominent network, particularly those cured at 85 °C. This was observed in eighteen year old precast concrete. The fissures within the most extensively microcracked concrete were characterized by hydrate in fill, notably ettringite interface. The ettringite occurred as a crust like layer on the surface of coarse aggregate particles. The presence of microcracks is likely to increase the mobility of moisture within the concrete which may produce density gradients leading to further microcracking. The domination of the matrix by a network of microcracks is conducive to the formation of secondary ettringite.

2.4 POZZOLANS IN CONCRETE

Pozzolans and industrial by-products, such as fly ash, silica fume and blast furnace slag, are often used to improve the concrete durability. The inclusion of

these materials in cement makes the concrete impervious and enhances its durability. Several researchers [61-63] have used a single pozzolan as a replacement of cement. However, recent research [64-65] recommends mixing of two pozzolans to cement to make more durable concrete.

In a study conducted by Ozyildirim [64] concrete with silica fume of 3 to 5% mixed with up to 47% blast furnace slag at a w/c of 0.4 and 0.45 showed lower strength than the plain and silica fume cement concretes. Strength mainly depended on the curing temperature. All the specimens cured at 6, 23, and 38 °C showed a satisfactory strength, exceeding 27.6 Mpa (4000 Psi) after 7 days, except for concrete cured at 6 °C and tested at 7 days. In another study, the authors [65] stated that sufficient strength and very low permeable concrete can be obtained when mixed with small amounts of silica fume to fly ash cement concrete with a w/c of 0.4 and 0.45, but chloride permeability reduced when the curing temperature was increased up to 38 °C. Furthermore, the authors [65] reported that concrete with lower chloride permeability was obtained at 28 days with Type III cement than similar concrete made with Type II cement.

An increase in the early and later-age strength, and low temperature rise were obtained using high volume fly ash cement concrete compared to ASTM Type I cement by Bisailon et al. [66]. The authors have suggested that high volume fly

ash concrete is an alternative to ASTM Type I and modified Type II cement for mass structures. On the other hand, performance of high volume fly ash was unsatisfactory in deicing salt-scaling test. Sybertz and weins [67] conducted tests on the effect of fly ash fineness on the hydration characteristics and strength development in the concrete. The fineness of fly ash influenced the rate of pozzolanic reaction. As a result, the strength contribution was not only affected after a longer hydration period, but also within the first 28 days. This shows that the improvement in the properties of hardened fly ash cement concrete are only achieved with fine fly ashes. At higher curing temperature, pozzolanic reaction increased. However, after 28 days, the pozzolanic reaction slowed down due to changes in the reaction mechanism.

Tests were conducted to determine the temperature rise in thin concrete sections containing fly ash by Marsh [68]. In that study, concrete of nominal grades, such as C30, C40, and C50 with fly ash replacement of 0, 30, and 40% by weight of total cement were used. Compressive strength was measured after 28 and 91 days on site stored cube specimens and also after 91 days from the cores taken from the beam specimens. The results showed that heat of hydration in the fly ash cement concretes was less than that in the ordinary portland cement concretes. The authors state that the reduced heat of hydration of fly ash cement concrete may be a disadvantage in small section in which the temperature rise is important for

strength development. However, the long-term strength development in the OPC and OPC/fly ash was similar.

The effect of blast furnace slag fineness on the engineering properties of high strength concrete was studied by Nakamura et al. [69]. Finely ground granulated blast furnace slag was used as a partial replacement of cement to obtain 28-day compressive strength of 60 to 120 Mpa. Two series of experiments were performed. In the first series, slag of 453 m²/kg fineness was used to replace 30, 50, and 70% of portland cement, and water to cementitious materials ratio of 0.35 to 0.45 were used. Blast furnace slags of 453, 786, and 1160 m²/kg fineness with a substitution of 50% was used in the second series of specimens and w/c varied from 0.3 to 0.4. The 3 and 7 day compressive strength of concretes containing slag of 453 m²/kg fineness was less than those cast using plain cement concrete. However, all mixes cast with 50 and 70% replacement of slag attained strength equal to all OPC concrete at 28 and 91 days, respectively. The compressive strength in these specimens was 50-70 Mpa and 60-80 Mpa at 28 and 91 days, respectively. The results showed that the higher fineness increased the high early strength. Slag of 1160 m²/kg fineness and 50% replacement and w/c ratio of 0.4 and 0.3, exhibited compressive strength of 35 and 50 Mpa after 3 and 7 days, respectively. With the addition of blast furnace slags of 786 and 1160 m²/kg fineness and the same percentage of replacement with a w/c ratio of 0.3 the

strength was 105-110 Mpa and 115-120 Mpa after 28 and 91 days, respectively, compared to about 90 and 97 Mpa in plain cement concrete after 28 and 91 days, respectively. In addition the researchers [69] suggested that air curing can result in substantial losses in the strength irrespective of the slag fineness and water binder ratio. The strength of 91 day air cured specimens was only about 60-70% of the 28-days water cured strength. In addition, they indicated that a minimum of 6 days of water curing is necessary for slag concrete to reach strength obtained by continuous water curing.

Meland [70] investigated carbonation in the hardened fly ash cement. Paste specimens were made using three types of cements of OPC and two fly ash cements of 10 and 25% fly ash, respectively. The paste specimens were stored in CO₂ atmosphere (3%) under a R.H. of 60%. Carbonation was evaluated by the use of phenolphthalein and thermogravimetry (TG). As expected, carbonation rate and depth depends on the fineness/degree of hydration of concrete. The results showed the importance to adopt the grinding of cement according to their content of fly ash in order to attain the same resistance against CO₂ penetration. Compared with OPC, a retardation of CO₂ penetration in an outer layer of 1-10 mm was attributed to a pozzolanic reaction of the fly ash cements.

Justness and Havdahl [71] evaluated the effect of curing temperature on the microstructure of cementitious paste in the light weight aggregate concrete. Concrete was cast with 0 to 20% silica fume and $w/(c+s)$ of 0.2 to 0.4. These specimens were cured at 20, 50, 70, or 90 °C for 7, 28, or 90 days. The results indicated that the initial curing temperature influenced the microstructure of paste even after 28 days of curing. This is due to an increase in the degree of hydration and pozzolanic activity of microsilica at this age with increase in initial curing temperature. This effect was most pronounced at low $w/(c+s)$ ratio and with the dosage of micro silica. Consequently, the free $\text{Ca}(\text{OH})_2$ content significantly decreased and the porosity reduced. As a result, light weight aggregate concrete proved to be durable and protected the rebars against corrosion.

Owens [72] reported that the use of Class F fly ash can effectively reduce the permeability of heat affected concrete, when compared to concrete cast only with Portland cement concrete. Concrete subjected to in-situ temperature cycle (ITC) of 20 °C with a w/c of 0.5 may have satisfactory level of impermeability. However, if it is subjected to ITC of 40 °C its permeability is affected as though it had a w/c of 0.59. If ITC increased to 60 °C the effect is equivalent to that of w/c of 0.69. Powers et al. [73] suggested that concrete with cement containing at least 25% fly

ash and subjected to ITC of more than 40 °C is equivalent in permeability to a OPC with a w/c of less than 0.42 at 20 °C.

The effect of curing on the compressive strength, resistance to chloride ion penetration and porosity of concretes, incorporating blast furnace slag, fly ash, and silica fume was evaluated by Ramezaninanpour and Malhotra [74]. Concrete specimens, 102X203 mm cylinders, were cast from each batch of concrete. A water-cementitious materials ratio of 0.5 was maintained invariant in all the concrete mixes, except in fly ash cement concrete, in which it was 0.35. The concrete specimens were subjected to different curing regimes, such as moist curing, curing at room temperature after demoulding, curing at room temperature after 2 days of moist curing, and curing at 38 °C and 65% R.H. Results indicated that concrete which received no curing after demoulding showed the poorest performance. The continuous moist cured concrete specimens achieved highest strength, lower porosity, and highest resistance to chloride ion penetration. The concrete specimens cured at 38 °C and 65% R.H achieved early strength gain in comparison to the moist cured specimens [74]. In addition, the compressive strength at 180 days was significantly lower and adversely affected the resistance to chloride ion penetration than moist cured specimens. The later age performance of fly ash and 10% silica fume concretes cured at 38 °C and 65% R.H was equal to or

superior than the control concrete in both strength development and resistant to chloride ion penetration.

In a research conducted by Ravina [23] on fly ash cement concrete under hot weather conditions, the compressive strength was reported to be affected by moisture condition of the specimen. The difference in the compressive strength between the dry and saturated specimen was between 20 to 30%. The author also stated that the average value of the compressive strength after 38 days in air cured specimens (air dry for 21 days) was higher than those cured under water by about 12%. Roy et al. [61], Marsh et al. [62], and Villkadsen [63] have suggested that supplementary cementing materials might improve the performance of concretes cured at elevated temperature. Campbell and Detwiler [75] have suggested that a durable concrete can be obtained both by the combination of blast furnace slag and silica fume and optimizing the mix design. In addition, these combinations were observed to be beneficial in reducing the rate of diffusion of chloride ion through concrete. Marsh et al. [62] have reported that an optimal mix design, for a particular curing condition, with the use of fly ash, will produce durable concrete.

The influence of cement composition on compressive strength of concrete cast and initially cured at elevated temperatures was investigated by Saroka and Peer [76]. Seven different brands of OPC were used in combination with a cement

content of 250-450 kg/m³ and a temperature in the range of 10 to 50 °C. The results confirm that the adverse effect of elevated temperature on compressive strength depends mainly on the cement composition. Kanda et al. [77] studied the effect of compressive strength on the silica fume cement concrete specimens cast at temperatures ranging from 20 to 75 °C, simulating site curing conditions in structural members by varying aggregate and admixtures. The results indicated that 7 days strength in the specimens cured at higher temperature was higher but strength gain from 7 to 28 days tended to be low. Moreover, the type of aggregate greatly influenced the strength properties, irrespective of admixtures. In addition, the authors stated that except limestone aggregate higher temperature curing influenced concrete strength independently of the admixture and aggregate. Vandewalle and Mortelmans [78] performed a series of tests on mortar mixes with a range of fly ash-cement ratios to study the effect of curing on the strength development of mortar. They found that the strength of mortar specimens containing fly ash has greater susceptibility to poor curing than plain cement concrete.

Wimpenny and Ellis [79] evaluated the effect of temperature on strength development in concrete elements made with blast furnace slag under low ambient temperatures. They used computer controlled temperature monitors and temperature matched curing systems (TMC) similar to the concrete subjected in the

field. Specimens, 450 X 450 X 150 mm blocks, with cementitious materials content of 300 and 400 kg/m³ of OPC and 70% BFS and a w/c of 0.4 were used. Core specimens cut from the concrete blocks and the specimens cured from the same concrete and temperature curing systems provided two estimates of in-situ strength. The use of BFS significantly influenced temperature and strength development within the simulated elements. In-situ cube strength estimates derived from the cores and TMC were in close agreement after 7 days curing. However, 28 day in-situ cube strength from the cores was lower by about 5 to 20% than the value from the TMC specimens.

Tanaka et al. [80] investigated the exothermic characteristics of blast furnace slag considering the reaction ratio of slag. They considered exothermic characteristics of portland cement and BFS individually. Results indicated that the reaction ratio of the slag in the blended cement decreased with a rise in the replacement ratio of slag. Moreover, there was an increase in the reaction ratio for an increase in the hydration temperature for the same replacement ratio. Justnes and Havdahl [71] indicated that the quantity of free Ca(OH)₂ decreased with increasing temperature. At low w/(c+s) of 0.25 and higher dosage of microsilica (16%), the Ca(OH)₂ reserve was below the detection limit. Moreover, at a moderate w/c of 0.4 and 16% silica fume the Ca(OH)₂ depleted after 7 days when the initial curing temperature was 50 °C. An increase in the microsilica content to

20% lead to a depletion of Ca(OH)_2 after 90 days of curing at 20 °C for all w/(c+s) ratios. Eventhough the Ca(OH)_2 reserve depleted, the pH in the pore solution was about 12.4 in all the pastes. This was attributed to the reaction of alkalis with microsilica forming alkali silicates. Since C-S-H gel is alkaline and it may incorporate free hydroxyl ions as a consequence of high c/s ratio.

In a study conducted by Detwiler et al. [81] the effect of elevated temperature on cement paste with 5% SF or 30% BFS, by mass, were compared with control pastes made from 100% portland cement. A water/solid material ratio (w/s) of 0.5 was used in all the pastes. No chemical admixtures were used in this study. After curing to the desired degrees of hydration (30% and 70%) the specimens were immersed in iso-propanol to dehydrate. They were cut using a low-speed diamond saw and impregnated with epoxy before grinding and polishing. The samples were coated with carbon before examination. A magnification of 500X was selected and 20 fields were examined for each specimen. A voltage of 15 KV and working distance of 15 nm were used for this work. Results indicated that an increase in the curing temperature from 23 °C to 70 °C resulted in a substantial increase in the diffusivity of chloride ions through the concrete. For any curing temperature, the substitution of either 5% silica fume or 30% slag for an equal mass of cement significantly reduced the rate of chloride ion diffusion through the concrete. The dosages of 5% silica fume and 30% slag were about equally effective in reducing

the rate of diffusion in the concrete cured at 70 °C. Researchers [81] have shown that the BFS reacts mainly after 30 % hydration of the paste. The voids left by the reacted slag particles resulted in a very porous phase. However, these pores are not likely to contribute to the permeability of the paste because they are isolated. In the specimens hydrated at 23 °C, the Ca(OH)_2 was uniformly distributed in the silica fume cement paste, while in the slag cement it was in an elongated crystalline form. Elevated temperature curing resulted in smaller, more numerous deposits of Ca(OH)_2 . Hadley grains were a distinct feature of the microstructure of all the pastes at 70% hydration. The morphology largely reflects the temperature and extent of hydration. Inner hydration products which were formed through the diffusion mechanism were observed mainly in the mature pastes cured at 70 °C.

In a study conducted by Patel et al. [60] samples cast at temperatures of up to 46 °C showed a similar microstructure to that seen at 20 °C with only a limited coarsening of the fabric at 42 °C and 46 °C. Several researchers agree that surface area from water BET isotherms of the gel decreases with increasing curing temperature in both hydrated C_3S and cement. However, this might be a consequence of both closed porosity or more voluminous material with less porosity.

CHAPTER 3

METHODOLOGY OF RESEARCH

The primary objective of this research was to evaluate the effect of casting and curing temperatures on the properties of hardened plain and blended cement concretes. Three blended cements, made with blast furnace slag (BFS), fly ash (FA), and silica fume (SF), were used in this investigation. The quantity of BFS, FA, and SF, in the blended cements was 70, 20, and 10%, respectively. ASTM C 150 Type I cement was used in both the plain and blended cement concrete mixes. Table 3.1 shows the chemical composition of Type I cement and the pozzolanic materials used in this study.

3.1 MATERIALS

The concrete mixes were proportioned on a weight basis. The following parameters were kept constant in all the mixes.

1. Cement content : 350 kg /m³
2. Cement : ASTM C150 Type I
3. Coarse / Fine aggregate : 1.7
4. Effective water to cementitious materials Ratio : 0.45

3.1.1 Aggregate

Crushed limestone from Abu Hadriya was used in all the concrete mixes. It was washed to remove dust and other fines. The maximum size of the coarse aggregate was 19 mm and its grading corresponded to ASTM C33 (#7 size). Figure 3.1 shows the aggregate grading. Specific gravity and absorption of the coarse aggregate were determined in accordance with ASTM C127 and C128, respectively. In addition, the absorption of coarse aggregate exposed to various temperatures, as shown in Figure 3.2, was also determined to adjust the amount of water in each concrete mix. Dune sand with a fineness modulus of 1.3, absorption 0.57%, and specific gravity 2.57 was used as fine aggregate.

3.1.2 Admixture

A high range water reducing admixture, conplast CP 430, was used to obtain the desired workability. The admixture was added to water and mixed thoroughly to ensure uniform distribution before adding to the concrete constituents.

3.2 SPECIMEN PREPARATION

The concrete constituents were mixed in an electrically operated revolving drum type concrete mixer. The ingredients were initially mixed in dry condition and then water was added. The constituents were mixed for three minutes, from the time of adding water. Additional mixing time of two minutes was provided in the case of silica fume cement concrete mixes. The required quantities of the materials were

weighed and stored at the desired temperature for at least 48 hours before casting. Cylindrical specimens, measuring 75 mm diameter by 150 mm height, were cast. The molds were filled in two layers and vibrated until the consolidation of concrete, indicated by the formation of a thin sheen of mortar on the surface.

3.3 CURING

The specimens were demoulded after 24 hours of casting and were transferred to the curing tanks containing saturated calcium hydroxide solution and maintained at temperatures of 20, 35, 50, and 65 °C until the time of testing.

3.4 TEST TECHNIQUES

3.4.1 Compressive Strength

After the designated period of curing, concrete specimens were retrieved from the curing medium, capped with a sulfur-based capping compound and tested in compression according to ASTM C 39. Three specimens representing similar mix proportions and casting and curing conditions were tested after 3, 7, 14, 28, 56, 84, and 168 days of curing.

3.4.2 Pulse velocity

The pulse velocity in concrete was measured using Pulse Velocity Ultrasonic Non-destructive Digital Indicating Tester (PUNDIT), in which the time of travel of an ultrasonic pulse through a concrete specimen is determined. The pulse

generator circuit consists of an electronic circuitry for generating pulses and a transducer for transforming these electronic pulses into mechanical energy having vibration frequency in the range of 15 to 50 kHz. Contact between the transducers and the concrete specimen is made using a lubricating substance such as grease [82]. Before measuring the time of travel in concrete specimen, the PUNDIT is calibrated using a metallic bar of known transit time. Two transducers were placed on the opposite surface of the concrete specimen and the time of travel of the ultrasonic pulse between the transducers and receivers was measured. The length of each specimen was measured and the pulse velocity was determined by dividing the path length by the transit time.

3.4.3 Absorption

Three specimens representing similar mix composition and curing conditions were removed from the curing environment and submerged in water for 48 hours. After this time, the specimens were dried at 110 °C in an oven for a period of 24 hours and then cooled in a desicator for another 24 hours and weighed (W_1). They were then immersed in water for 48 hours and surface dried before weighting (W_2). Absorption was calculated using the following relation

$$\text{Absorption (\%)} = (W_2 - W_1) / (W_1) * 100$$

where W_1 : Weight of the dry specimen.

W_2 : Weight of the saturated surface dry specimen.

3.4.4 Pore Size Distribution

The effect of casting and curing temperatures on the pore size distribution was evaluated using mercury intrusion porosimetry (MIP). In the mercury intrusion porosimetry, mercury, a non-wetting liquid is forced into the pores of the material at a high pressure. Pore size and volume quantification is accomplished by submerging the specimen under a confined quantity of mercury and then increasing its pressure hydraulically. As the applied pressure is increased the radius of the pores which can be filled with mercury decreases and consequently the total amount of mercury intruded increases. The data obtained give the pore volume distribution directly and with the aid of pore physical model, the pore size distribution can be ascertained.

In this study, the pore size distribution of the selected specimens was evaluated using Carlo Erba Model 2000 high pressure intrusion porosimeter. This is an automatic instrument for the determination of the pore size and pore volume distribution in the range of 3.7 to 7500 nm radius. The operating pressure ranges from 0.1 to 200 Mpa. According to the Washburn equation of capillary suction or depression, the radius of a cylindrical pore which will be reached by a pressure p is given by:

$$r_1 = 2 r \cos \theta / P$$

where r is the surface tension, θ is the contact angle. r and θ are constant, for a certain material, r_1 is inversely proportional to p . In this study, a value of r equal to 480 dynes and θ equal to 141.3° was used. Then $r_1 \text{ (nm)} = 750/p \text{ Mpa}$. Representative specimens, approximately 1 gram, were used for pore size distribution. The pressure in the pressure vessel of the porosimeter was increased from 0.1 to 200 Mpa slowly. This slow increase of pressure prevents the mercury from heating up during the test. The measurement of the pressure and the introduced volume of mercury were recorded and used to draw the pore volume against the pore radius.

3.4.5 Differential Thermal Analysis

The chemical changes in the composition of cement, due to varying casting and curing temperatures, were evaluated using differential thermal/thermo gravimetric (DTA/TG) technique. In this method the temperature difference between the test substance and a reference material is measured as a function of temperature, while the substance and the reference material are subjected to a controlled temperature heating. A number of phenomena, such as decomposition, and phase change may take place in a material when heated at a constant rate. Thermogravimetry measures the change in the mass of a substance as a function of temperature.

Characteristic of decomposition phenomena is the appearance of an endothermic peak in a DTA curve with a corresponding weight loss. Phase change from

crystalline to amorphous is indicated by the presence of an exothermic peak without any weight loss. A simultaneous thermal analyzer (STA-429) manufactured by Netzsch, Germany was used for differential thermal analysis. It performs DTA/TG simultaneously. About 200 milligram of the powdered specimen was tested with Al_2O_3 as a reference material. The temperature was raised at a uniform rate of $10\text{ }^\circ\text{C}/\text{min.}$, from room temperature to $1000\text{ }^\circ\text{C}$. In the thermograms, the weight loss and temperature are plotted simultaneously.

3.4.6 X-ray Diffraction

This technique was used to evaluate the mineralogical changes in the cement brought about by the varying casting and curing temperatures. X-ray diffraction is a powerful technique for analyzing the crystal structure of a compound. It is a qualitative method of analysis primarily used for determining the weight fractions of crystalline phases down to about 1%. X-ray diffraction apparatus has a wavelengths of 1 \AA , similar to the spacing of atomic planes in a crystalline material. Each crystal has inherent planes of atoms that are separated by a specific distance pertaining only to that crystal. These distances are characteristic of the crystalline materials. As soon as these distances are determined by the X-ray diffraction, the crystalline material can be identified easily.

Bragg's law, as given below is considered the basis for identification of crystals.

$$n\lambda = 2d \sin \theta$$

where:

n = order of diffraction (1,2,3,....etc.)

λ = Wave length of X-ray

d = Spacing between atomic planes, Å

θ = Diffraction angle of X-ray, degrees

Some selected cement paste specimens were ground using an agate mortar and pestle and analyzed on a Phillips PW 1700 automated diffractometer with a monochromator and spinner. Diffraction patterns were generated on vertical goniometer attached to a broad focus X-ray tube with copper target operating at 45 kV and 30 mA. The analysis is computer assisted so that the inter planar spacing values can be corrected for the instrument error function by analyzing a silicon standard and subsequent quantitative analysis. A homogeneous sample was packed into a sample holder and scanned from $4-80^\circ$ 2θ at a speed of $0.01^\circ 2\theta/\text{sec}$. In powdered form, many grains come into orientation and the quality of the diffraction pattern is greatly improved. The phase identification process involves calculating the most likely match score for a given phase based on peak intensity and peak position when compared to a database of standard phases. The weight fraction is calculated by comparing the intensity of the most intense peaks of that phase with standards. The X-ray diffractograms were also used to calculate the orientation of the transition zone.

Table 3.1: Chemical composition of Type I cement and pozzolanic materials

Constituents (Wt. %)	Ordinary Portland Cement	Blast Furnace Slag	Silica Fume	Fly Ash Class F
CaO	64.19	43.7	0.5	0.48
SiO ₂	22.59	35.4	92.5	47.15
Al ₂ O ₃	4.61	7.8	0.4	45.12
Fe ₂ O ₃	2.71	0.52	0.4	1.38
SO ₃	2.22	1.13	0.5	0.2
Na ₂ O	---	0.39	1.1	0.08
K ₂ O	---	0.11	0.4	0.05
Alkalinity	0.27	0.46	---	---
C ₃ S	50.95	---	---	---
C ₂ S	26.33	---	---	---
C ₃ A	7.63	---	---	---
C ₄ AF	8.25	---	---	---

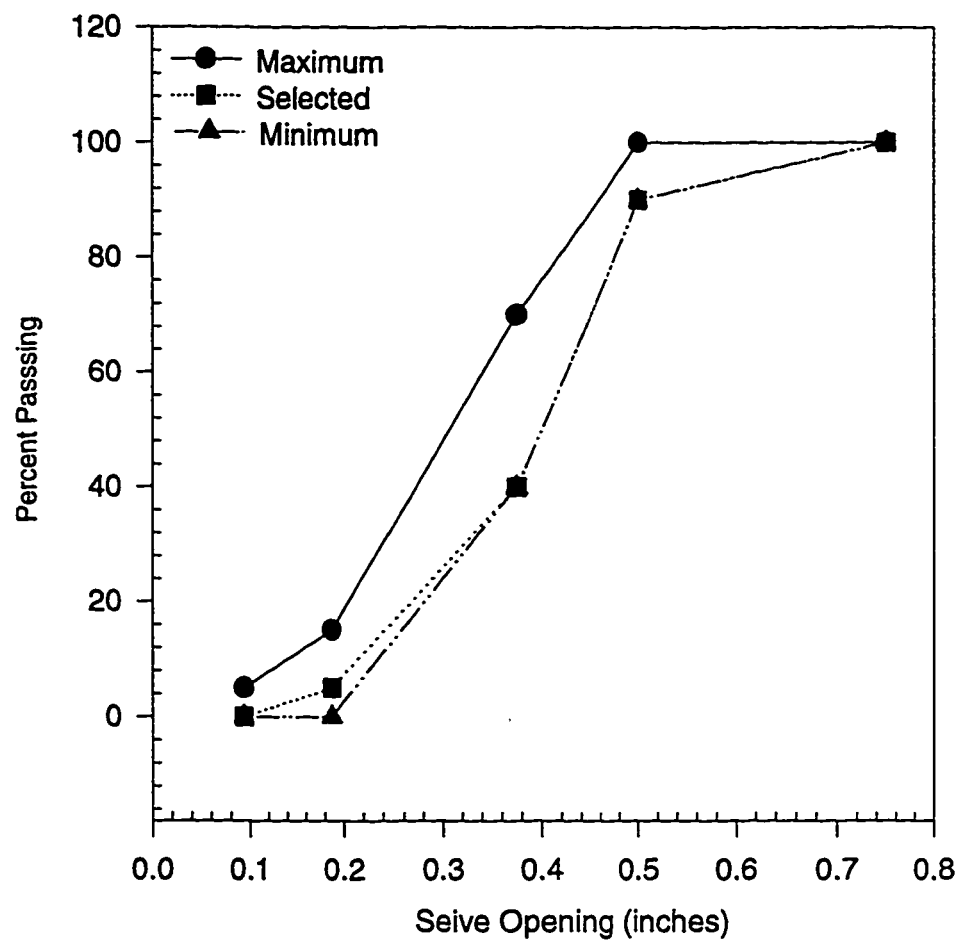


Fig. 3.1: Coarse aggregate grading

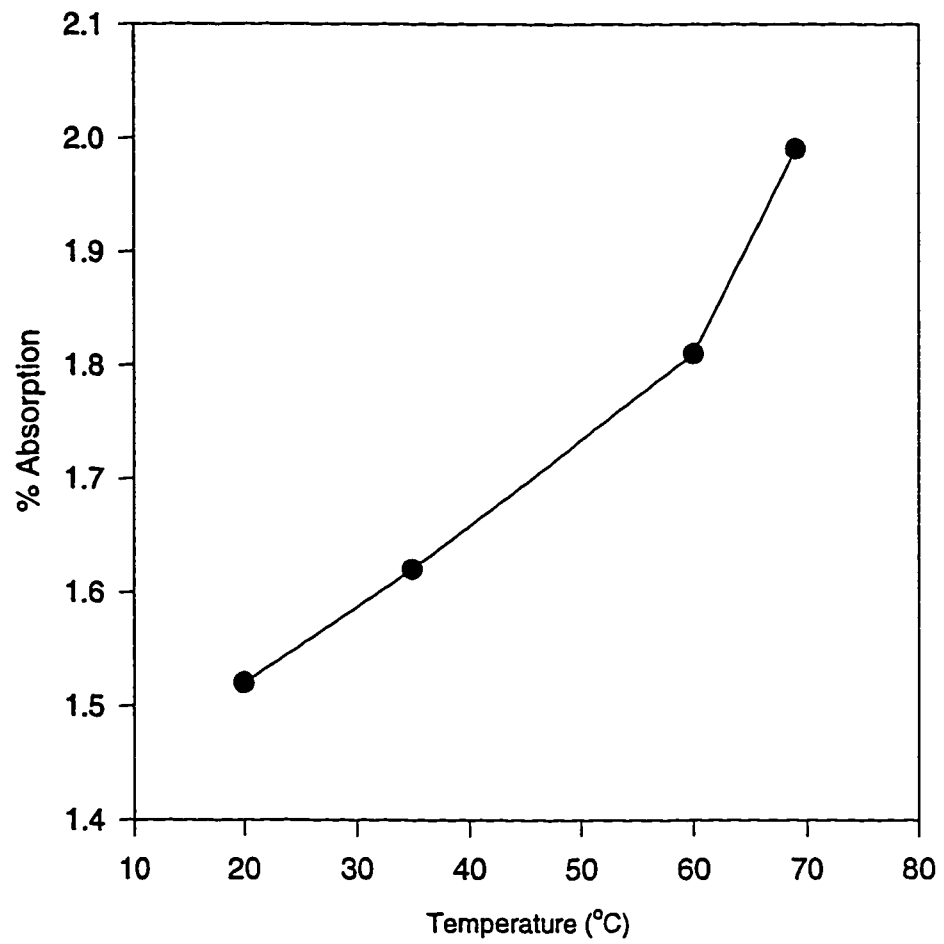


Fig. 3.2 : Effect of temperature on absorption of water in the coarse aggregates

CHAPTER 4

RESULTS

4.1 EFFECT OF CASTING AND CURING TEMPERATURES ON COMPRESSIVE STRENGTH IN PLAIN AND BLENDED CEMENT CONCRETE SPECIMENS

The compressive strength development in the plain cement concrete specimens cast at 20 °C and cured at various temperatures is shown in Figure 4.1. These values increased with age, irrespective of the curing temperature. After 7 days of curing, the compressive strength in the specimens cured at 50 °C was more than those cured at 20 and 35 °C . After 168 days of curing, the compressive strength in the specimens cured at 50, 20, and 35 °C was 44.7, 42.2, and 40.7 Mpa, respectively.

Figure 4.2 shows the compressive strength development in the blast furnace slag cement concrete specimens cast at 20 °C, and cured at various temperatures. An increase in the compressive strength with age was noted in all the specimens, irrespective of the curing temperature. However, the specimens cured at 20 °C exhibited lower compressive strength, after 168 days of curing, compared to those cured at 35 and 50 °C. After 168 days of curing, the compressive strength in the specimens cured at 20, 35, and 50 °C was 33.3, 34.9, and 34 Mpa, respectively.

Figure 4.3 shows the compressive strength development in the silica fume cement concrete specimens cast at 20 °C and cured at various temperatures. Maximum compressive strength was noted in the specimens cured at 50 °C compared to those cured at other temperatures. The compressive strength in the specimens cured at 20 °C increased almost linearly with the curing period. An exponential increase in the compressive strength was observed in the specimens cured at 35 °C with the period of curing. After 168 days of curing, the compressive strength in the specimens cured at 20, 35, and 50 °C was 41.2, 43.5, and 46.3 Mpa, respectively.

Figure 4.4 shows the compressive strength development in the fly ash cement concrete specimens cast at 20 °C and cured at various temperatures. An increase in strength with the period of curing was also observed in these specimens. However, a decrease in the compressive strength was noted in the specimens cured at 35 and 50 °C after 84 days of curing. The compressive strength in the specimens cured at 20, 35, and 50 °C was 34.2, 33.3, and 30.8 Mpa, respectively, after 168 days of curing.

The compressive strength development in the plain cement concrete specimens cast at 35 °C and cured at 20, 35, and 50 °C is shown in Figure 4.5. A rapid

increase in the compressive strength was noted in all the specimens, particularly in the early ages. However, a decrease in the compressive strength was observed in the specimens cured at 50 °C after an exposure period of 84 days. After 168 days of curing, the compressive strength in the specimens cured at 20, 35, and 50 °C was 46.4, 46.4, and 43.9 Mpa, respectively.

Figure 4.6 shows the compressive strength development in the blast furnace slag cement concrete specimens cast at 35 °C and cured at various temperatures. An increase in the strength with the period of curing was indicated in all the specimens. The strength gain in the specimens cured at 35 °C was more than that in the specimens cured at 20 and 50 °C. After 168 days, the compressive strength of the concrete specimens cured at 20, 35, and 50 °C was 28.5, 36, and 28.5 Mpa, respectively.

Figure 4.7 shows the effect of curing at various temperatures on the compressive strength development in the silica fume cement concrete specimens cast at 35 °C. The strength gain in the specimens cured at 20 °C was initially very low with a value of 22.8 Mpa, after 3 days. However, it increased gradually to 32.3 and 34.4 Mpa, after 84 and 168 days of curing, respectively. An increase in the compressive strength with the period of curing was also indicated in the specimens cured at 35

and 50 °C. After 168 days of curing, the compressive strength in these specimens was less than those cured at 20 °C. The data in Figure 4.7 also indicate that the rate of strength gain in the specimens cured at 50 °C was initially high, up to 14 days. However, after 56 days of curing the compressive strength in these specimens was less than those cured at 35 and 20 °C. This indicates that elevated temperature casting and curing is not beneficial for the silica fume cement concrete specimens. After 168 days of curing, the compressive strength in the specimens cured at 35 and 50 °C was 33.1 and 30.5 Mpa, respectively.

Figure 4.8 shows the compressive strength development in the fly ash cement concrete specimens cast at 35 °C and cured at various temperatures. The compressive strength in all the specimens continued to increase with age. However, a reduction in the strength was noted in the specimens cured at 50 °C, after 84 days of curing. An insignificant change in compressive strength was noted in the specimens cured at 20 and 35 °C. After 168 days of curing, the compressive strength of concrete specimens cured at 20, 35, and 50 °C was 26.7, 27.4, and 24.12 Mpa, respectively.

Figure 4.9 shows the compressive strength development in the plain cement concrete specimens cast at 50 °C and cured at various temperatures. The increase

in the compressive strength in the specimens cured at 20 °C was insignificant after a curing period of 14 days. However, the strength gain was almost linear in the specimens cured at 50 °C. After 168 days of curing, the compressive strength in the specimens cured at 20 and 50 °C was 42 and 45.4 Mpa, respectively. The compressive strength of specimens cured at 65 °C was very high initially, but decreased gradually with age. The compressive strength of these specimens was 43.2 Mpa, after 168 days.

Figure 4.10 shows the compressive strength development in the blast furnace slag cement concrete specimens cast at 50 °C and cured at various temperatures. An increase in the compressive strength was indicated in all the specimens. However, the increase in the compressive strength was more pronounced in the specimens cured at 65 °C. The compressive strength in the specimens cured at 20, 50, and 65 °C was 35.7, 35.5, and 37.8 Mpa, respectively, after 168 days of curing.

Figure 4.11 shows the effect of curing temperature on the strength development in the silica fume cement concrete specimens cast at 50 °C. The compressive strength increased with age in all the specimens up to about 84 days. However, these values decreased with further curing. After 168 days, the compressive strength in the specimens cured at 20, 50, and 65 °C was 34.6, 31.5, and 33.9 Mpa,

respectively. Figure 4.12 shows the compressive strength development in the fly ash cement concrete specimens cast at 50 °C and cured at various temperatures. An increase in the compressive strength was noticed in all the specimens. The compressive strength in the specimens cured at 20 °C was 19.5 and 29 Mpa, after 3 and 168 days of exposure, respectively. The compressive strength of specimens cured at 50 °C was initially low. However, it increased to a value of 25.7 Mpa, after 168 days of curing. Nevertheless, it was less than the specimens cured at 20 and 65 °C.

Figure 4.13 shows the compressive strength development in the plain cement concrete specimens cast at 65 °C and cured at various temperatures. The compressive strength of the specimens cured at 20 °C was initially less than those cured at 65 °C. However, it increased gradually and exceeded the strength of the latter group after 56 days. The compressive strength of the concrete specimens cured at 65 °C was very high right from 3 days, being 33 Mpa. However, the increase in strength with age was insignificant. The compressive strength of the concrete specimens cured at 20 and 65 °C was 39.4 and 38.2 Mpa, respectively, after 168 days of curing. The compressive strength development in the blast furnace slag cement concrete specimens cast at 65 °C and cured at various temperatures is shown in Figure 4.14. An increase in the compressive strength

with age was noted in the specimens cured at both 20 and 65 °C. After 168 days of curing, the compressive strength of concrete specimens cured at 20 and 65 °C was 31.8 and 34.2 Mpa, respectively.

Figure 4.15 shows the effect of curing temperature on the compressive strength development in the silica fume cement concrete specimens. The compressive strength in the specimens cured at 20 °C was significantly less in the initial period of 3 days, being 19.4 Mpa. Subsequently, it increased significantly with the age of curing, to a value of 42.2 Mpa, after 168 days of curing. The concrete specimens which were cured at 65 °C exhibited higher initial compressive strength of 28.23 Mpa, after 3 days of curing, which increased to 42.8 Mpa after 84 days. However, after 168 days of curing this value dropped to 39.6 Mpa.

Figure 4.16 shows the compressive strength development in the fly ash cement concrete specimens cast at 65 °C and cured at 20 and 65 °C. An increase in the compressive strength with age was observed in the specimens cured at both these temperatures. The compressive strength of the concrete specimens cured at 20 °C increased with the period of curing, while a decrease was noted in the specimens cured at 65 °C, after 84 days. After 168 days of curing, the compressive strength in the specimens cured at 20 and 65 °C was 36.4 and 32.58 Mpa, respectively.

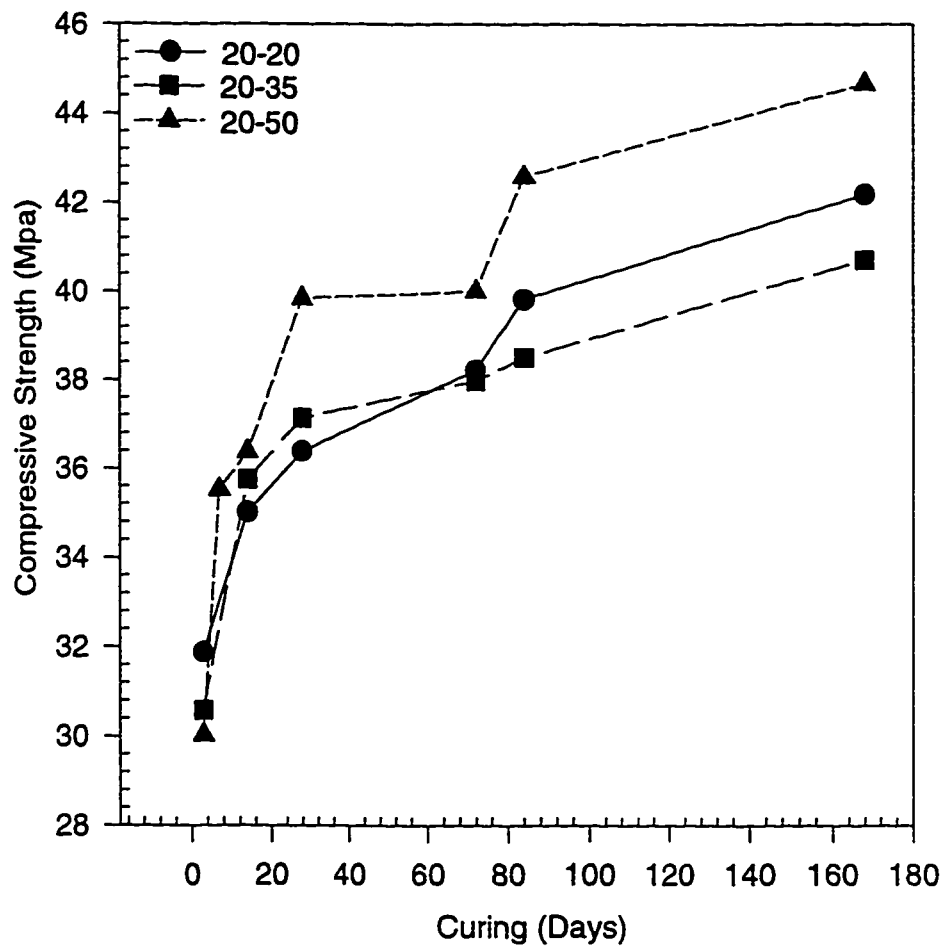


Fig.4.1: Compressive Strength Development in the Plain Cement Concrete Specimens Cast at 20 °C and Cured at various Temperatures

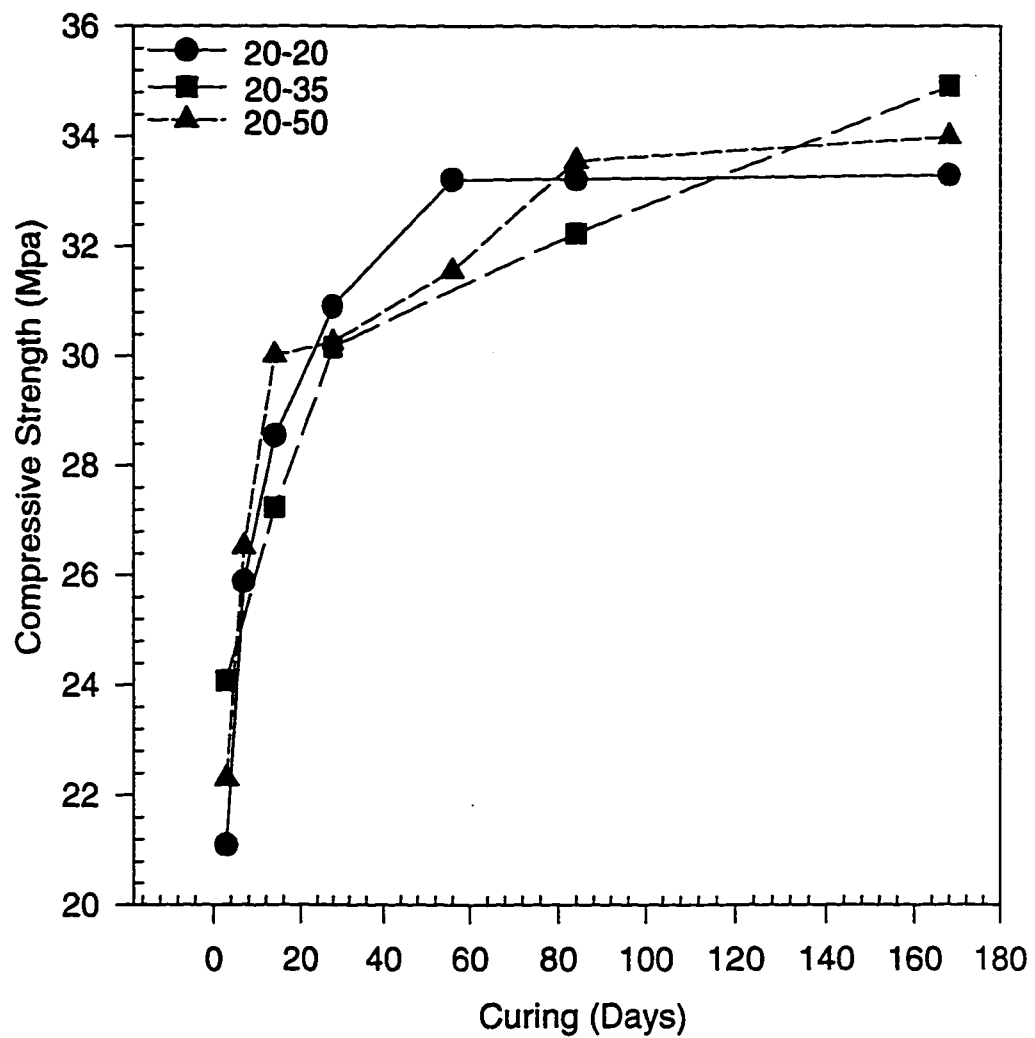


Fig. 4.2: Compressive Strength Development in the Blast Furnace Slag Cement Concrete Specimens Cast at 20 °C and Cured at various Temperatures

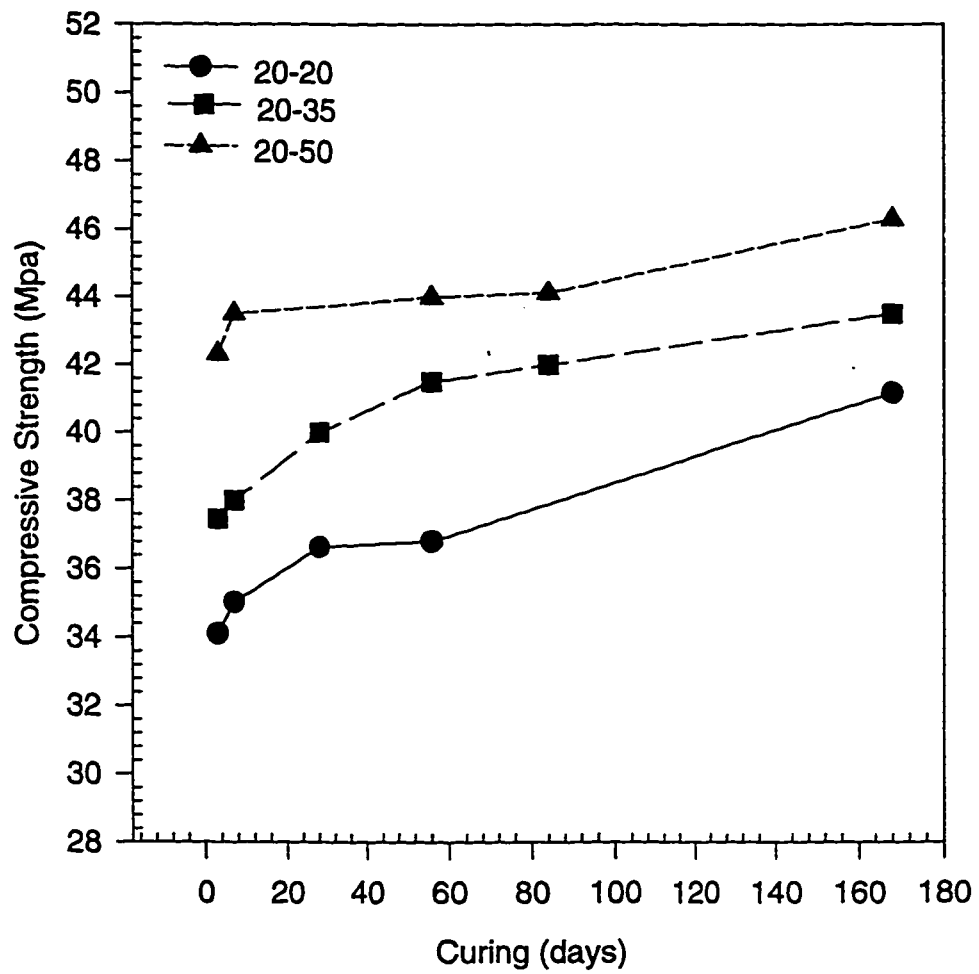


Fig. 4.3 : Compressive Strength Development in the Silica Fume Cement Concrete Specimens Cast at 20 °C and Cured at various Temperatures

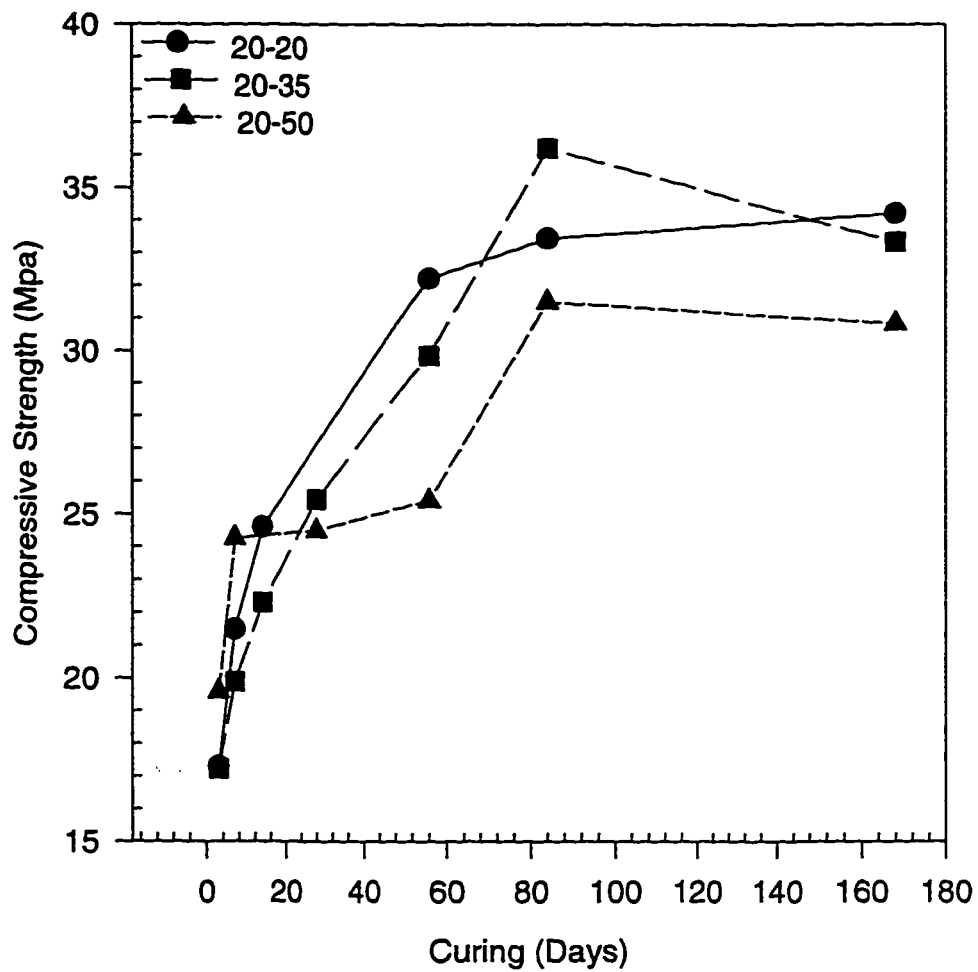


Fig. 4.4: Compressive Strength Development in the Fly Ash Cement Concrete Specimens Cast at 20 °C and Cured at various Temperatures

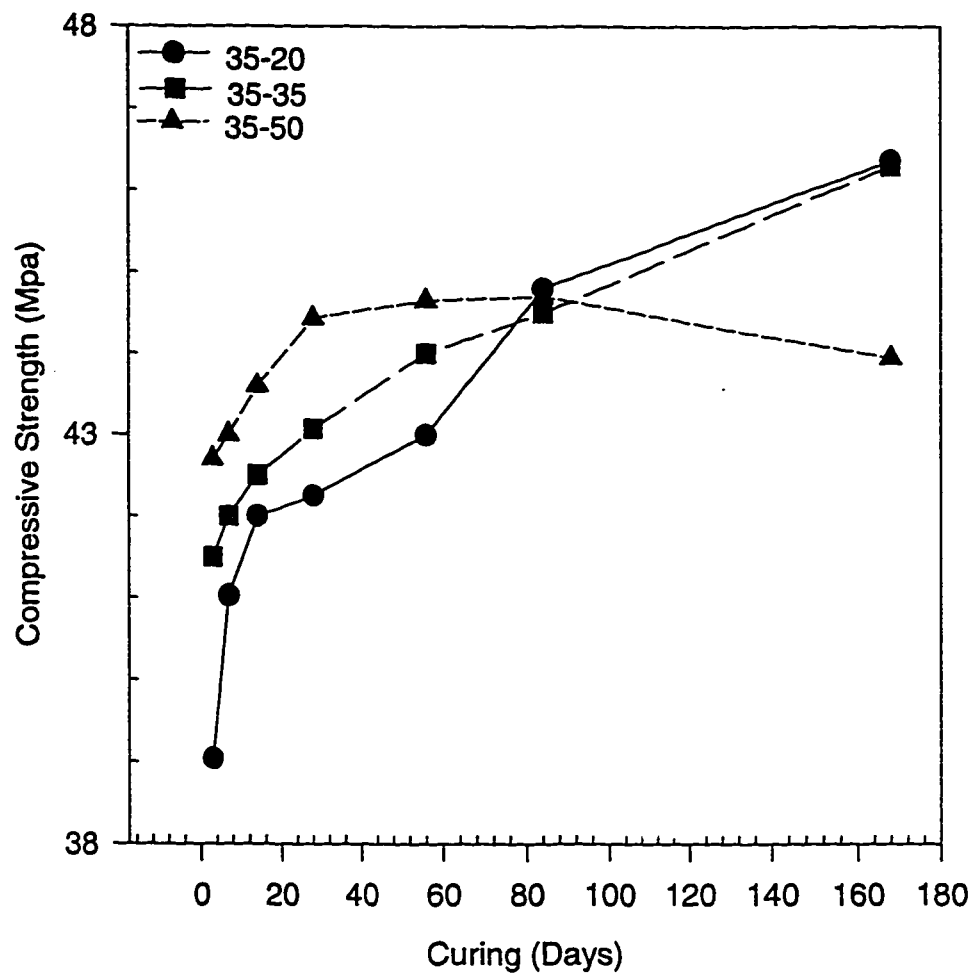


Fig. 4.5: Compressive Strength Development in the Plain Cement Concrete Specimens Cast at 35 °C and Cured at various Temperatures

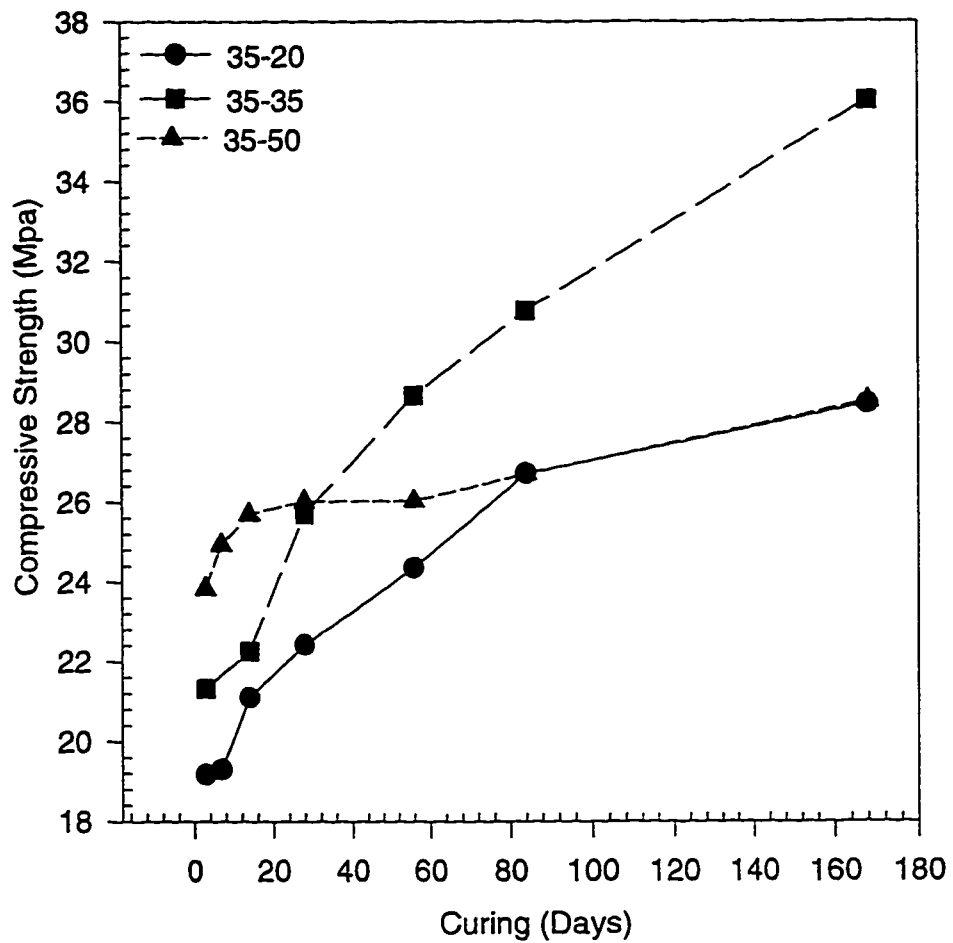


Fig. 4.6: Compressive Strength Development in the Blast Furnace Slag Cement Concrete Specimens Cast at 35 °C and Cured at various Temperatures

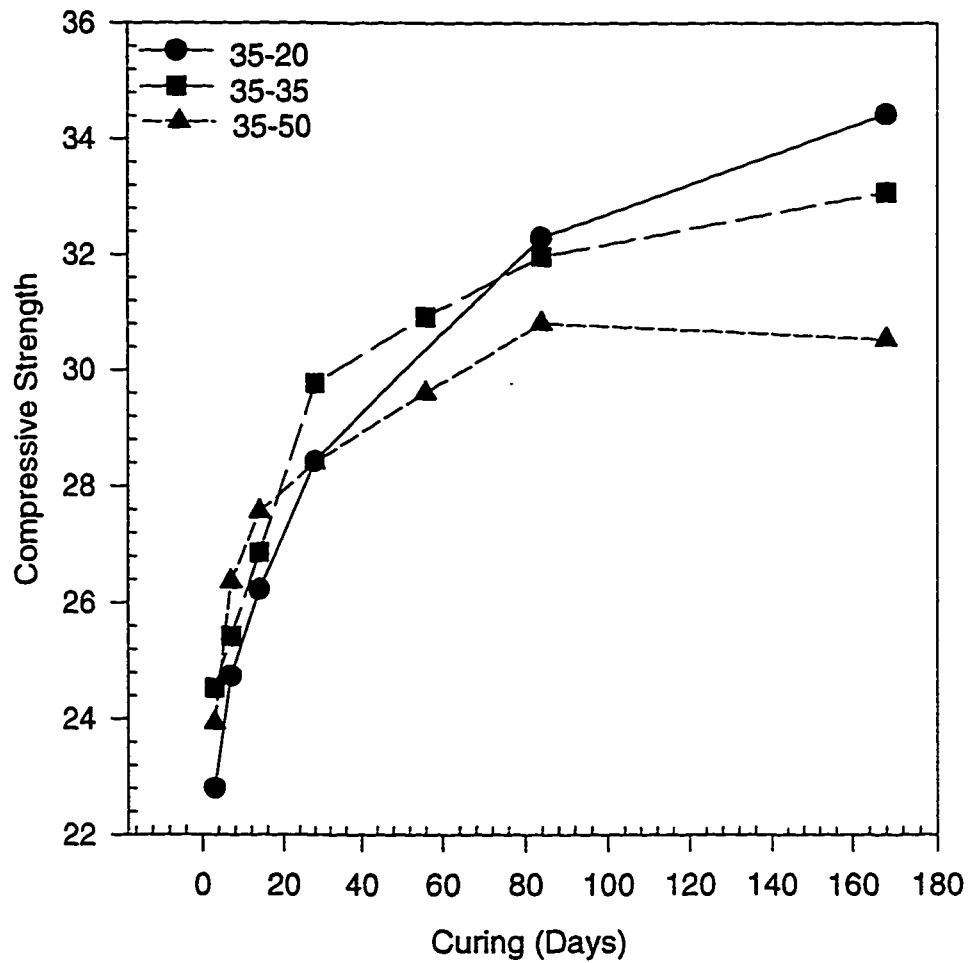


Fig. 4.7: Compressive Strength Development in the Silica Fume Cement Concrete Specimens Cast at 35 °C and Cured at various Temperatures

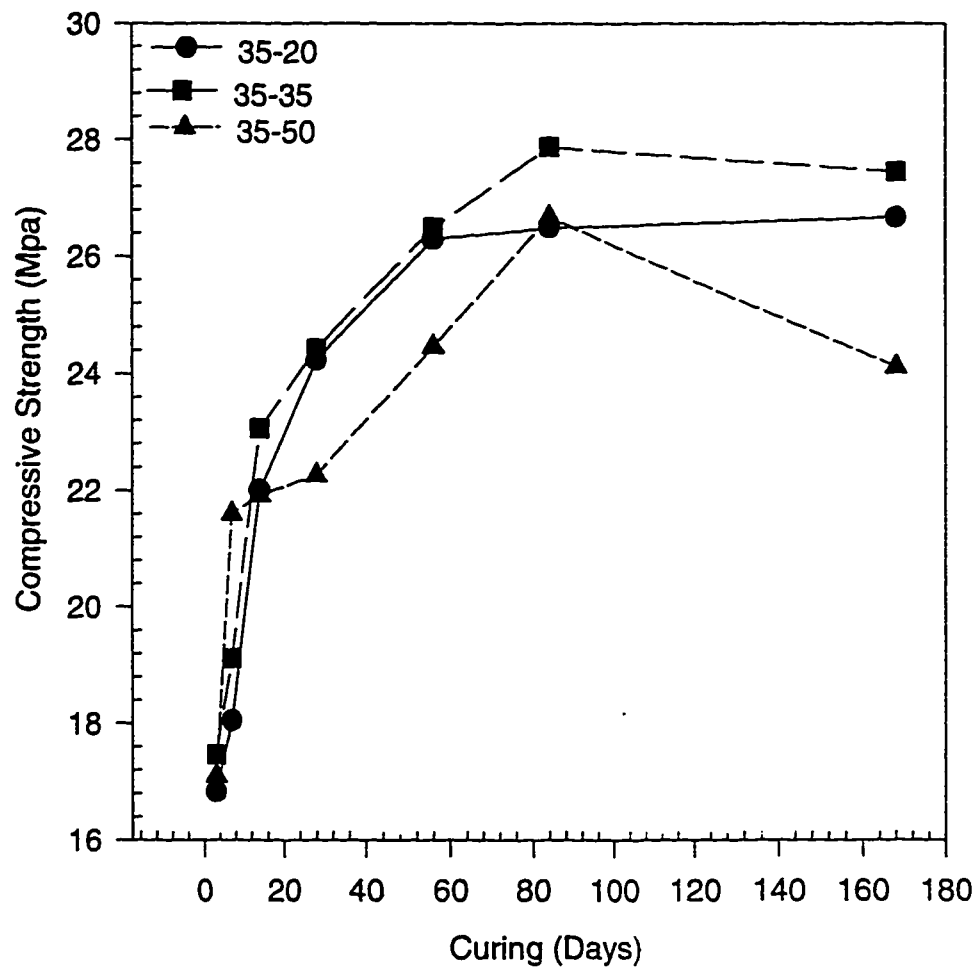


Fig. 4.8: Compressive Strength Development in the Fly Ash Cement Concrete Specimens Cast at 35 °C and Cured at various Temperatures

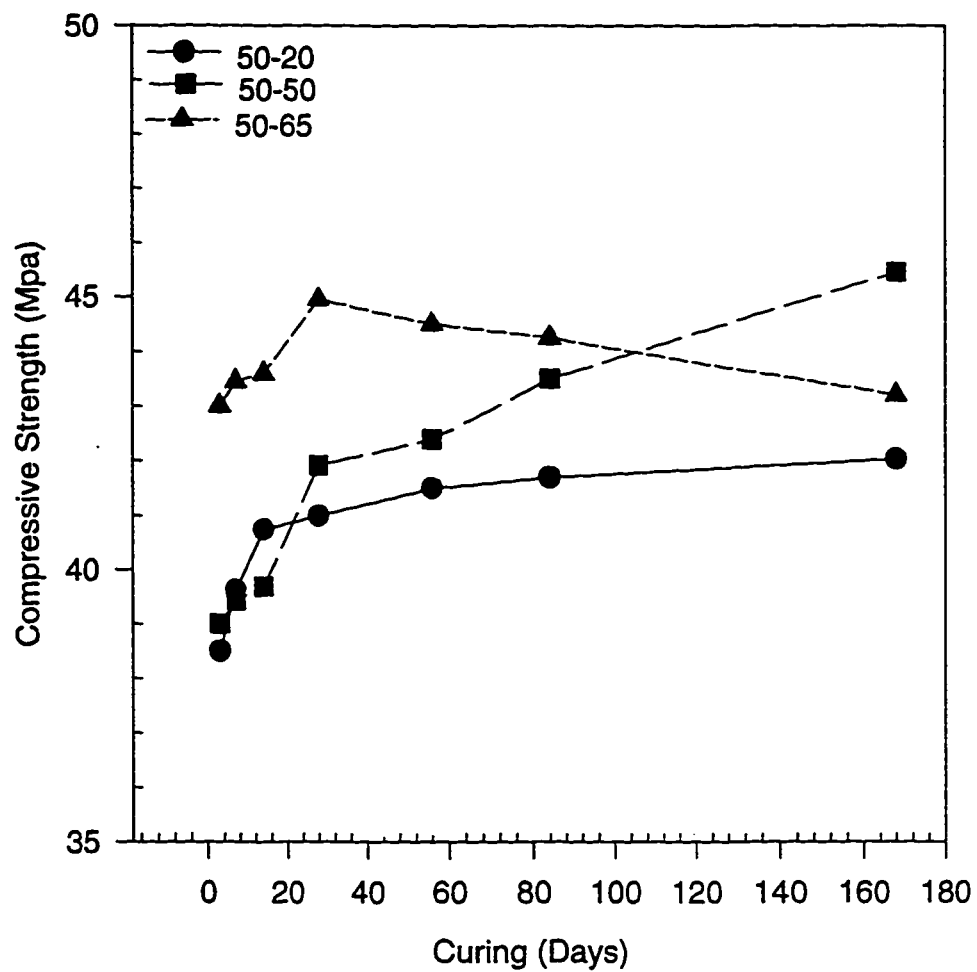


Fig.4.9: Compressive Strength Development in the Plain Cement Concrete Specimens Cast at 50 °C and Cured at various Temperatures

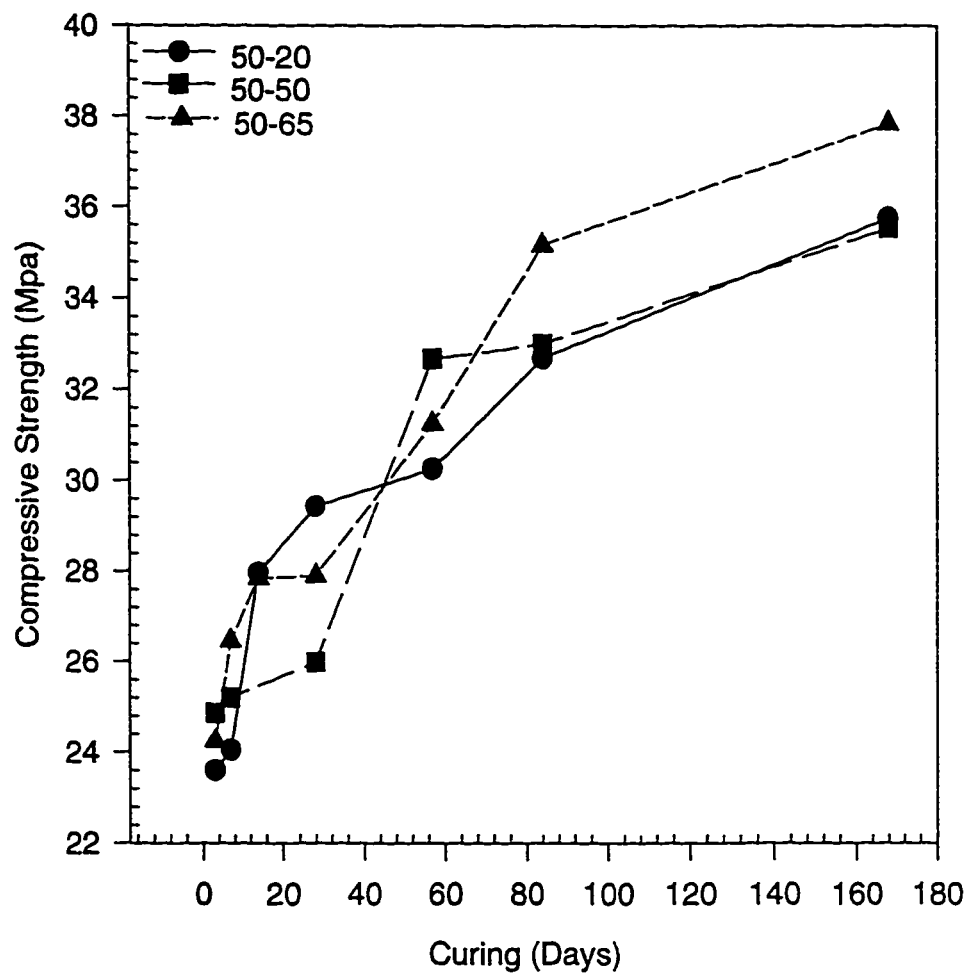


Fig.4.10: Compressive Strength Development in the Blast Furnace Slag Cement Concrete Specimens Cast at 50 °C and Cured at various Temperatures

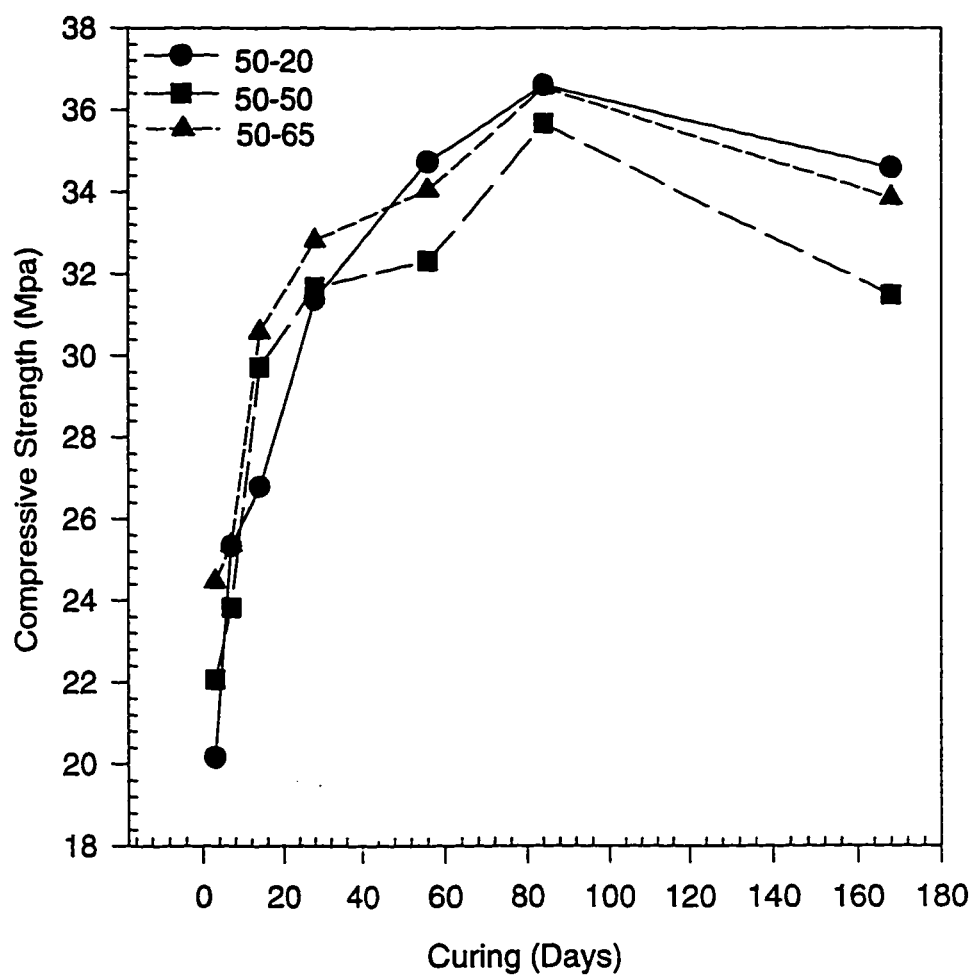


Fig.4.11: Compressive Strength Development in the Silica Fume Cement Concrete Specimens Cast at 50 °C and Cured at various Temperatures

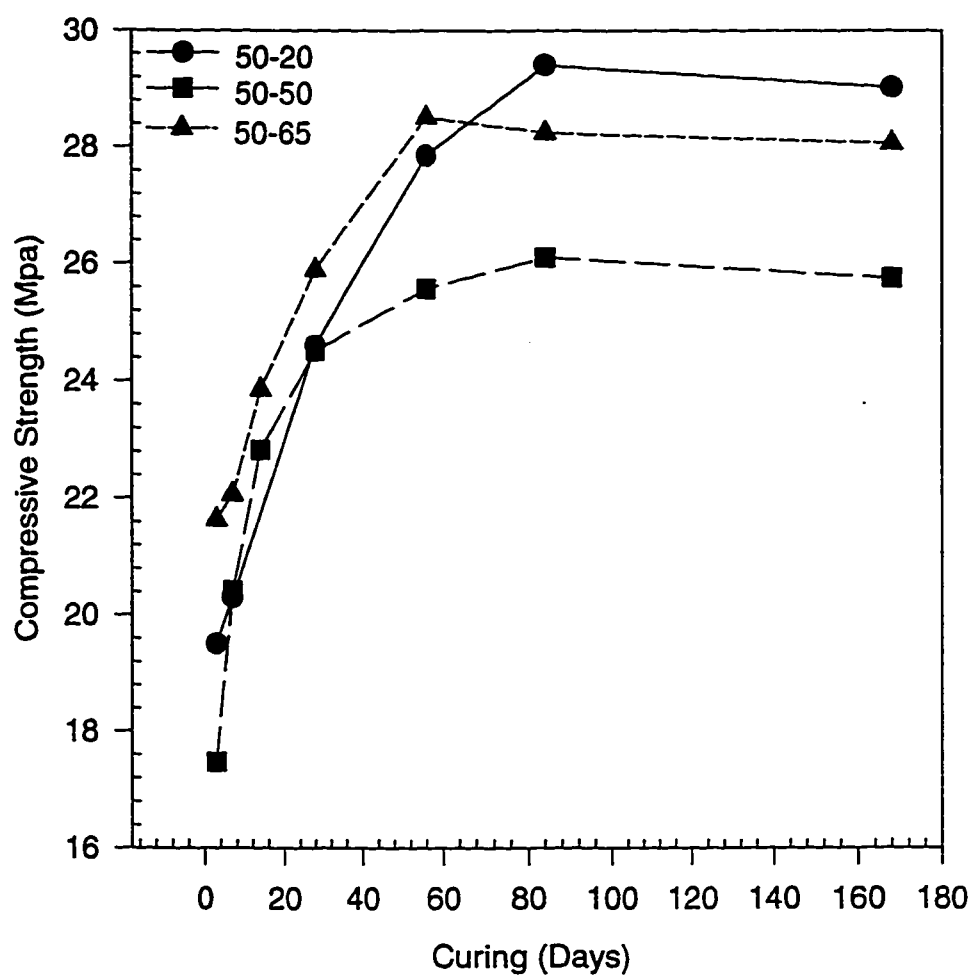


Fig. 4.12: Compressive Strength Development in the Fly Ash Cement Concrete Specimens Cast at 50 °C and Cured at various Temperatures

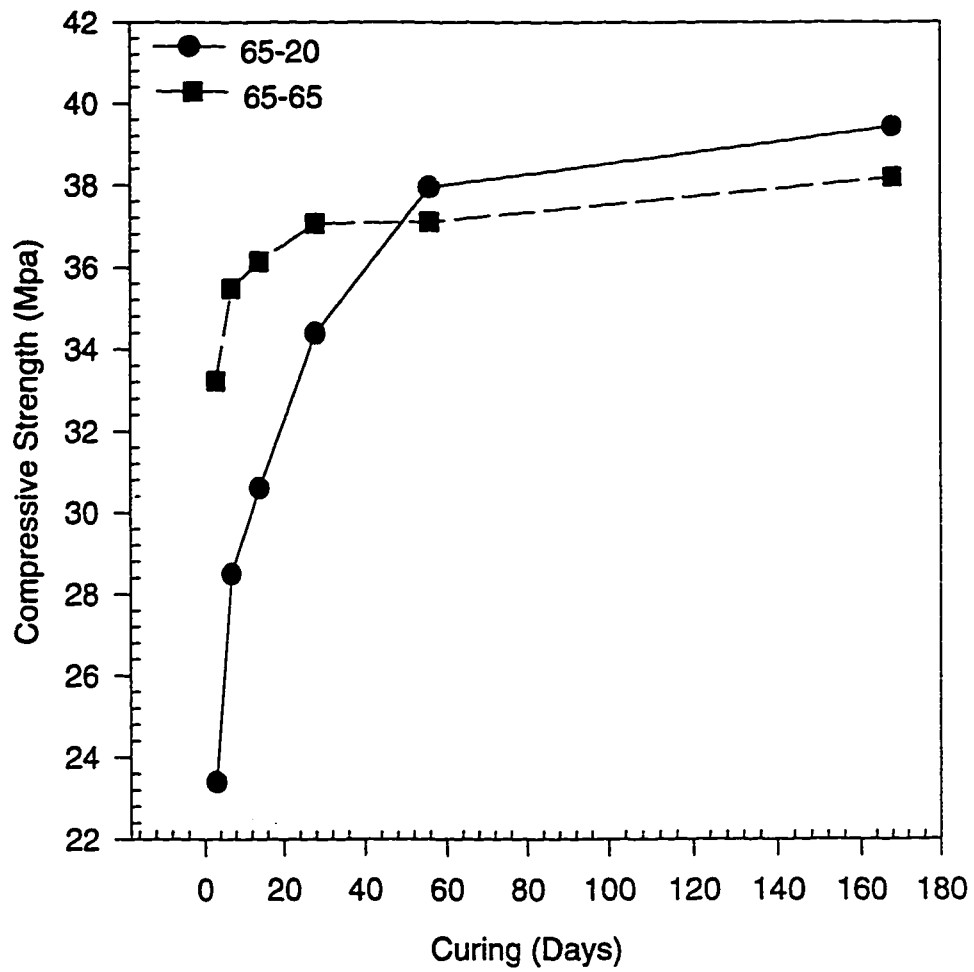


Fig. 4.13: Compressive Strength Development in the Plain Cement Concrete Specimens Cast at 65 °C and Cured at various Temperatures

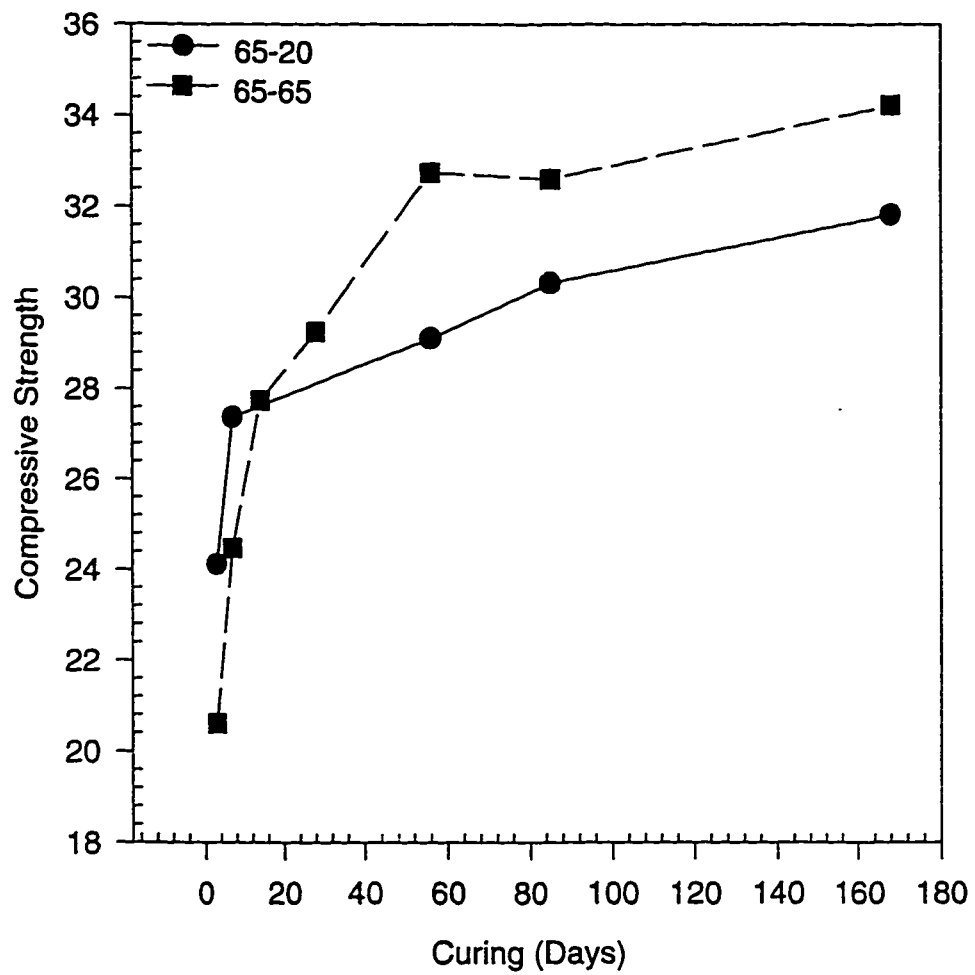


Fig. 4.14: Compressive Strength Development in the Blast Furnace Slag Cement Concrete Specimens Cast at 65 °C and Cured at various Temperatures

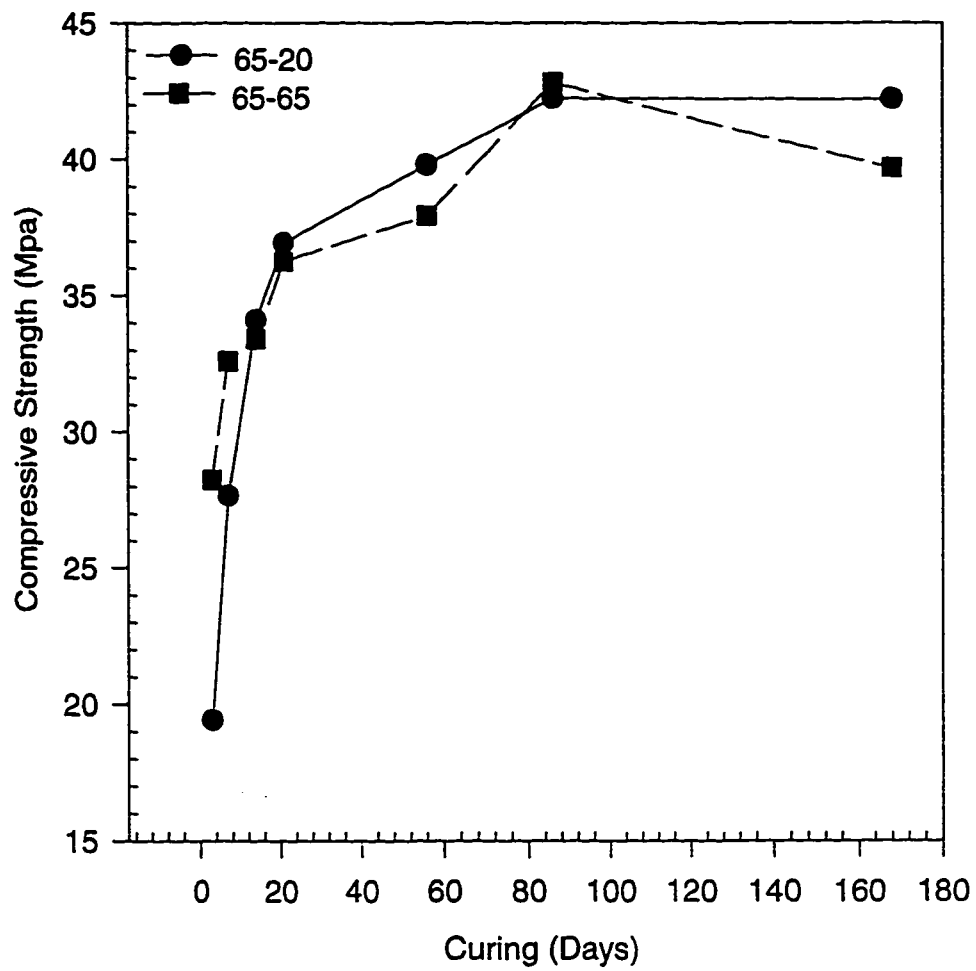


Fig. 4.15: Compressive Strength Development in the Silica Fume Cement Concrete Specimens Cast at 65 °C and Cured at various Temperatures

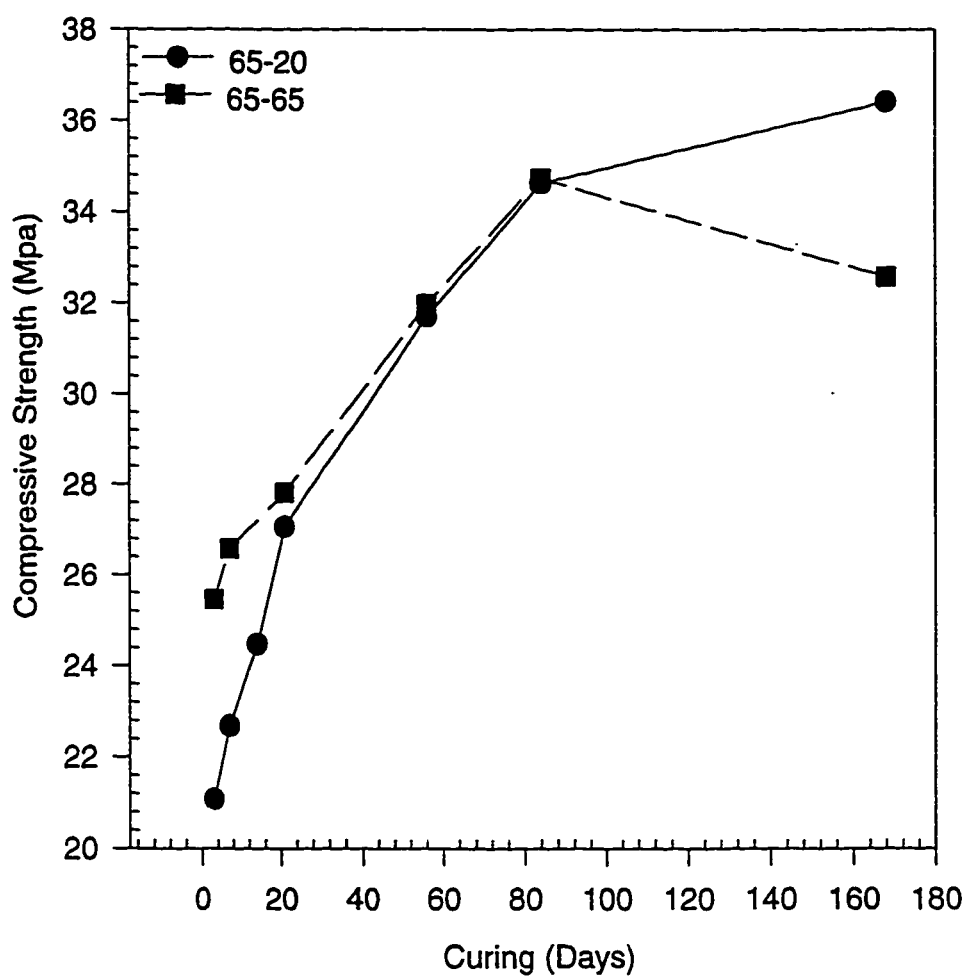


Fig.4.16: Compressive Strength Development in the Fly Ash Cement Concrete Specimens Cast at 65 °C and Cured at various Temperatures

4.2 EFFECT OF CASTING AND CURING TEMPERATURES ON PULSE VELOCITY

Figure 4.17 shows the variation of pulse velocity with curing in the plain cement concrete specimens cast at 20 °C and cured at various temperatures. An increase in the pulse velocity with age was observed in all the specimens. After 168 days of curing, the pulse velocity in the concrete specimens cured at 20, 35, and 50 °C was 4800, 4792, and 4718 m/s, respectively.

Figure 4.18 shows the effect of curing at various temperatures on the pulse velocity in the blast furnace slag cement concrete specimens cast at 20 °C. After 84 days of curing, the pulse velocity decreased in all the specimens except in those cured at 20 °C in which an increase was observed. The specimens cured at 20 and 35 °C exhibited similar values of pulse velocity until a period of 28 days. Subsequently, after 168 days of curing the pulse velocity in these specimens was 4650 and 4402 m/s, respectively. The pulse velocity in the specimens cured at 50 °C was less than those cured at 20 and 35 °C.

Figure 4.19 shows the pulse velocity in the silica fume cement concrete specimens cast at 20 °C and cured at various temperatures. An increase in the pulse velocity was observed in all the specimens up to 84 days. However, after this

curing period, the pulse velocity decreased, except in the specimens cured at 20 °C, in which an increase was noticed. The pulse velocity in the specimens cured at 20, 35, and 50 °C was 4819, 4630, and 4517 m/s, respectively, after 168 days of curing.

Figure 4.20 shows the pulse velocity in the fly ash cement concrete specimens cast at 20 °C and cured at various temperatures. The pulse velocity in the specimens cured at 20 °C increased with the period of curing. However, a decrease was observed in the specimens cured at 35 °C after 84 days of curing, while in the specimens cured at 50 °C the compressive strength decreased after 56 days of curing. The pulse velocity in the concrete specimens cured at 20, 35, and 50 °C was 4667, 4547, and 4541 m/s, respectively, after a curing period of 168 days.

Figure 4.21 shows the pulse velocity in the plain cement concrete specimens cast at 35 °C and cured at various temperatures. The pulse velocity in all the specimens increased up to 84 days. After 168 days of curing, the pulse velocity in the specimens cured at 20 °C was more or less similar to the value after 84 days. However, in the specimens cured at 35 and 50 °C the pulse velocity decreased with further curing, after 84 days. The pulse velocity in the specimens cured at 20, 35, and 50 °C was 4842, 4703, and 4665 m/s, respectively, after 168 days of curing.

Figure 4.22 shows the effect of curing at various temperatures on the pulse velocity in the blast furnace slag cement concrete specimens cast at 35 °C. An exponential increase in the pulse velocity was observed in the specimens cured at 20 °C. After 168 days of curing, the pulse velocity in these specimens was 4650 m/s. The pulse velocity in the specimens cured at 35 and 50 °C, decreased after a curing period of 28 days. The pulse velocity in these specimens after 168 days of curing was 4476 and 4448 m/s, respectively.

Figure 4.23 shows the pulse velocity in the silica fume cement concrete specimens cast at 35 °C and cured at various temperatures. The pulse velocity in the specimens cured at 20 and 35 °C increased up to 84 days of curing. After this time, the pulse velocity in these specimens decreased with the period of curing. However, the decrease in the pulse velocity of the specimens cured at 50 °C was noted only after 56 days of curing. The pulse velocity in the specimens cured at 20, 35, and 50 °C was 4519, 4513, and 4464 m/s, respectively, after 168 days of curing. Figure 4.24 shows the pulse velocity in the fly ash cement concrete specimens cast at 35 °C and cured at various temperatures. The pulse velocity in all the specimens increased with age. However, in the specimens cured at 50 °C a reduction in the pulse velocity was indicated after 84 days of curing. The pulse

velocity in the specimens cured at 20, 35, and 50 °C was 4635, 4605, and 4475 m/s, respectively.

Figure 4.25 shows the effect of curing on the pulse velocity in the plain cement concrete specimens cast at 50 °C and cured at various temperatures. A maximum initial increase in the pulse velocity was noticed in the specimens cured at 50 °C up to a curing period of 56 days, after which a reduction was observed. The pulse velocity in the specimens cured at 20 °C initially exhibited lower values. However, it was maximum in these specimens after 168 days of curing. The pulse velocity in the specimens cured at 20, 50, and, 65 °C was 4822, 4714, and 4630 m/s, after an exposure period of 168 days.

Figure 4.26 shows the pulse velocity in the blast furnace slag cement concrete specimens cast at 50 °C and cured at various temperatures. The pulse velocity in the specimens cured at 20 °C decreased with age until a curing period of 56 days, after which an increase was observed. The pulse velocity in the specimens cured at 50 and 65 °C increased up to 14 days of curing, beyond which a decrease was noted. The pulse velocity in the specimens cured at 20, 50, and 65 °C was 4538, 4391, and 4356 m/s, respectively, after 168 days of curing.

Figure 4.27 shows the effect of curing on pulse velocity in the silica fume cement concrete specimens cast at 50 °C and cured at various temperatures. Irrespective of the curing temperature the pulse velocity decreased in all the concrete specimens after about 28 to 56 days of curing. The pulse velocity in the specimens cured at 20, 50, and 65 °C was 4591, 4553, and 4533 m/s, respectively, after 168 days of curing.

Figure 4.28 shows the pulse velocity in the fly ash cement concrete specimens cast at 50 °C and cured at various temperatures. The pulse velocity in the specimens cured at 20 °C increased with the period of curing. Maximum pulse velocity, after 168 days of curing, was noted in these specimens compared to those cured at 50 and 65 °C. The pulse velocity in the specimens cured at 50 °C initially increased up to 56 days of exposure. After this time, a decrease was noticed. The pulse velocity in the specimens cured at 20, 50, and 65 °C was 4737, 4520, and 4530 m/s, after 168 days of curing.

Figure 4.29 shows the pulse velocity in the plain cement concrete specimens cast at 65 °C and cured at 20 and 65 °C. The pulse velocity in the specimens cured at 20 and 65 °C increased up to a curing period of 56 days, after which a reduction was observed. The pulse velocity in these specimens after 168 days of curing was

4687 and 4550 m/s, respectively. Figure 4.30 shows the effect of curing on the pulse velocity in the blast furnace slag cement concrete specimens cast at 65 °C and cured at 20 and 65 °C. The pulse velocity in the specimens cured at 20 °C decreased with age, until a curing period of 56 days after which an increase was observed. After 168 days of curing, the pulse velocity in the specimens cured at 20 and 65 °C was 4396 and 4299 m/s, respectively.

Figure 4.31 shows the pulse velocity in the silica fume cement concrete specimens cast at 65 °C and cured at 20 and 65 °C. The pulse velocity in the specimens cured at 20 °C increased gradually up to a curing period of 56 days, after which a decrease was noticed. The pulse velocity in the specimens cured at 65 °C increased with the period of curing. After 168 days of curing, the pulse velocity in the concrete specimens cured at 20 and 65 °C was 4526 and 4440 m/s, respectively. Figure 4.32 shows the pulse velocity in the fly ash cement concrete specimens cast at 65 °C and cured at 20 and 65 °C. Maximum pulse velocity was noted in the specimens cured at 20 °C compared to those cured at 65 °C. The pulse velocity in the specimens cured at 65 °C decreased gradually up to 28 days, However, after which no significant change was noticed. The pulse velocity in the specimens cured at 20 and 65 °C after 168 days of curing was 4568 and 4408 m/s, respectively.

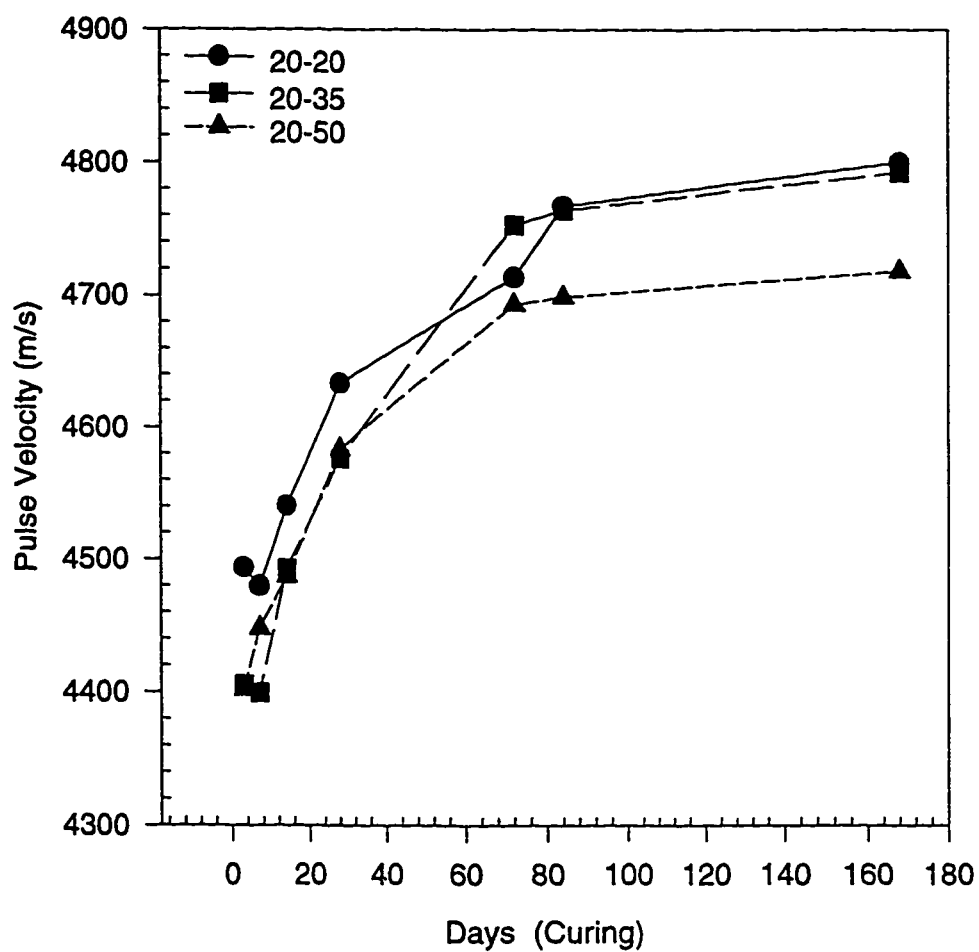


Fig. 4.17: Pulse Velocity in the Plain Cement Concrete Specimens Cast at 20 °C and Cured at various Temperatures

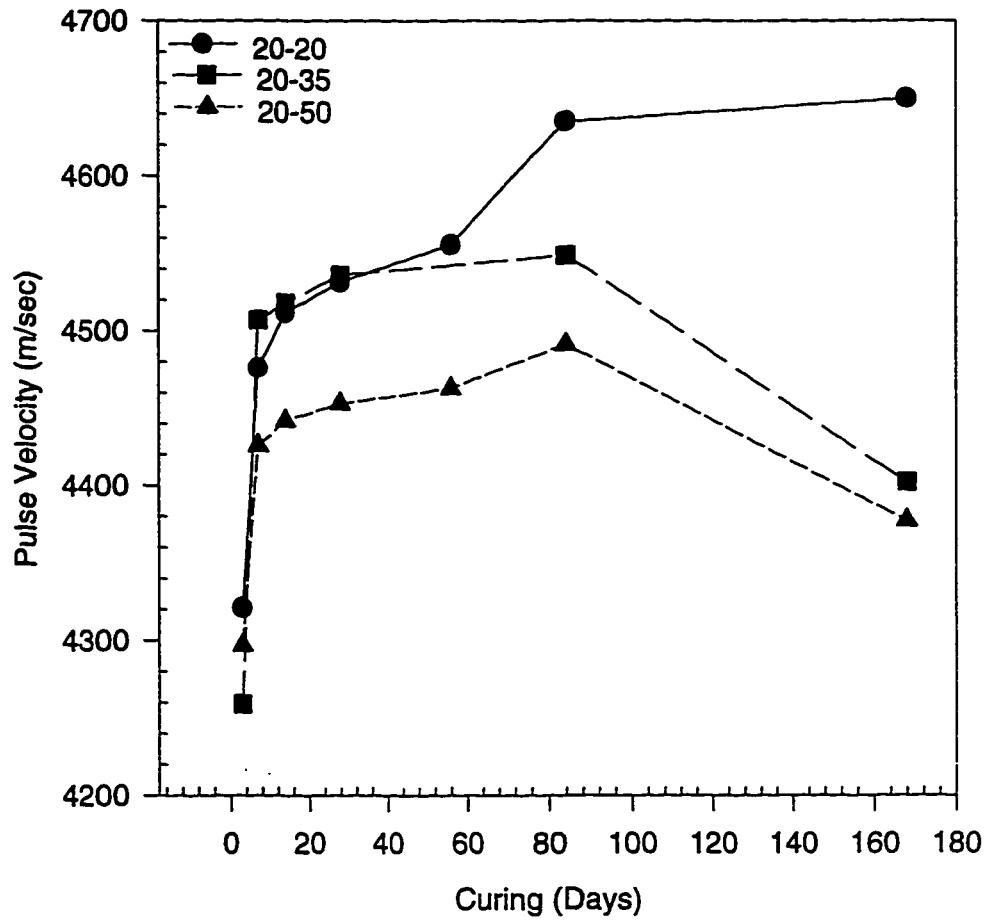


Fig. 4.18: Pulse Velocity in the Blast Furnace Slag Cement Concrete Specimens Cast at 20 °C and Cured at various Temperatures

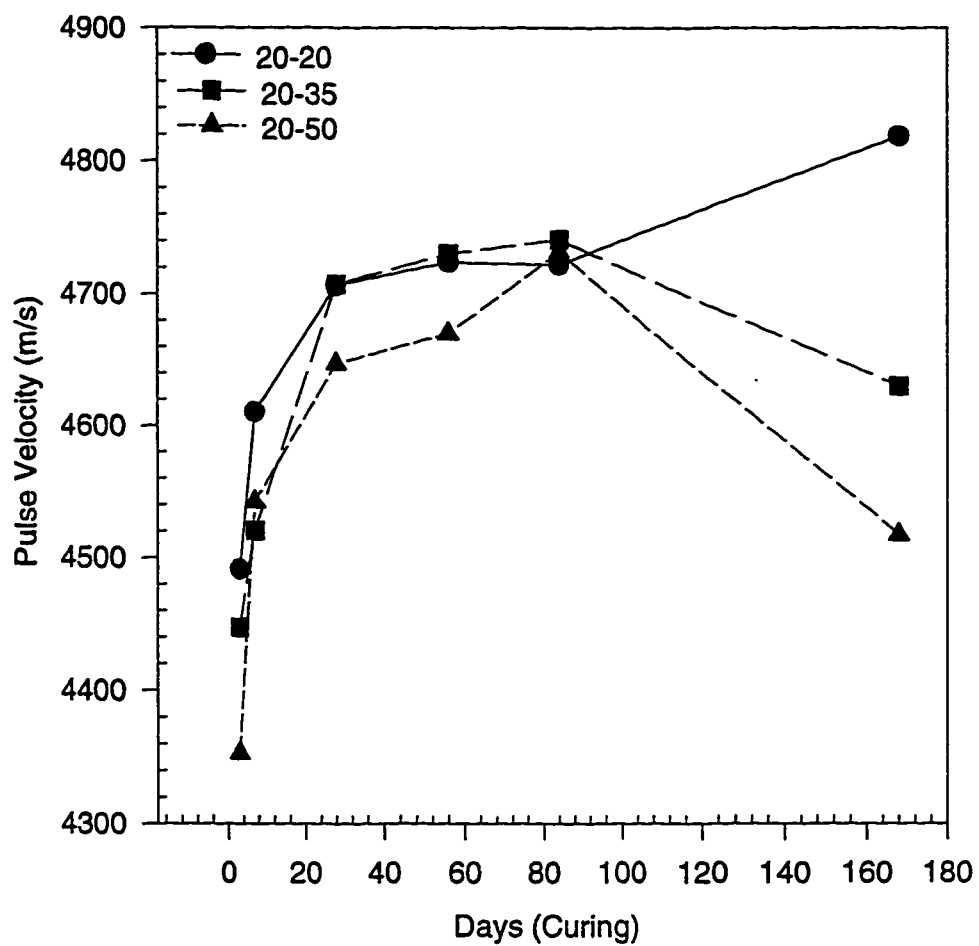


Fig. 4.19: Pulse Velocity in the Silica Fume Cement Concrete Specimens Cast at 20 °C and Cured at various Temperatures

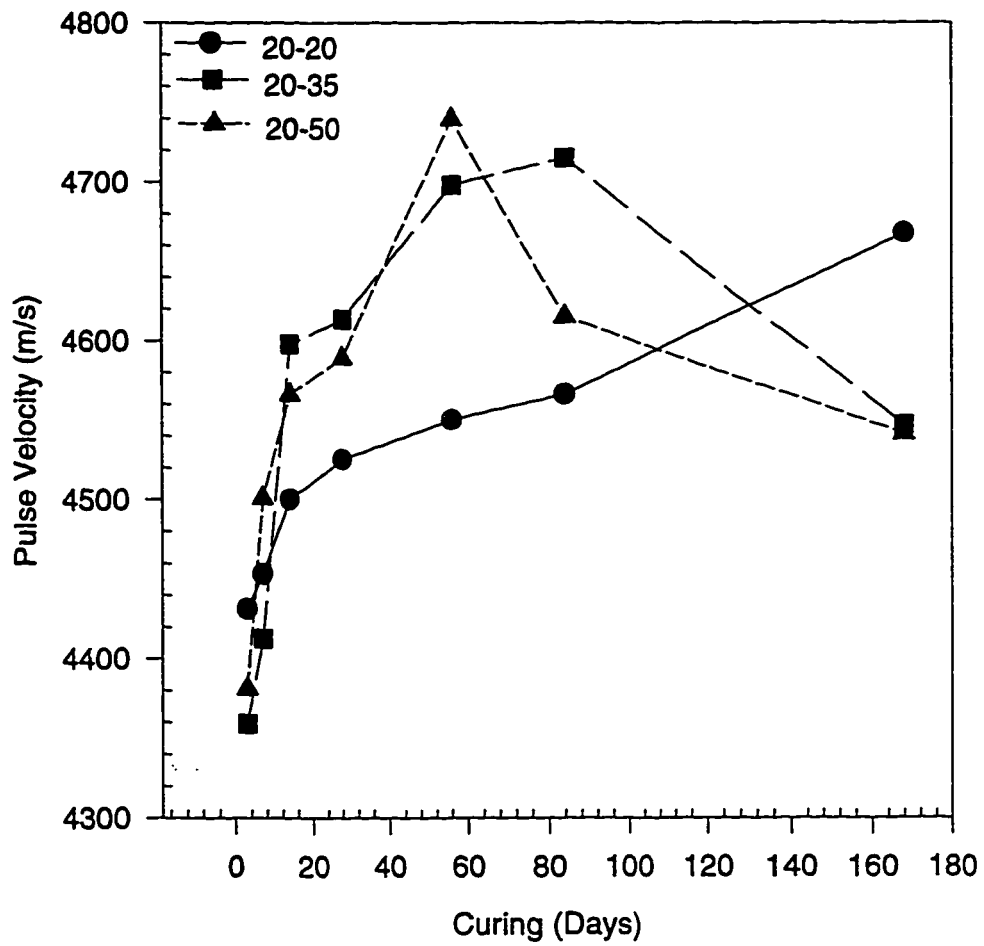


Fig. 4.20: Pulse Velocity in the Fly Ash Cement Concrete Specimens Cast at 20 °C and Cured at various Temperatures

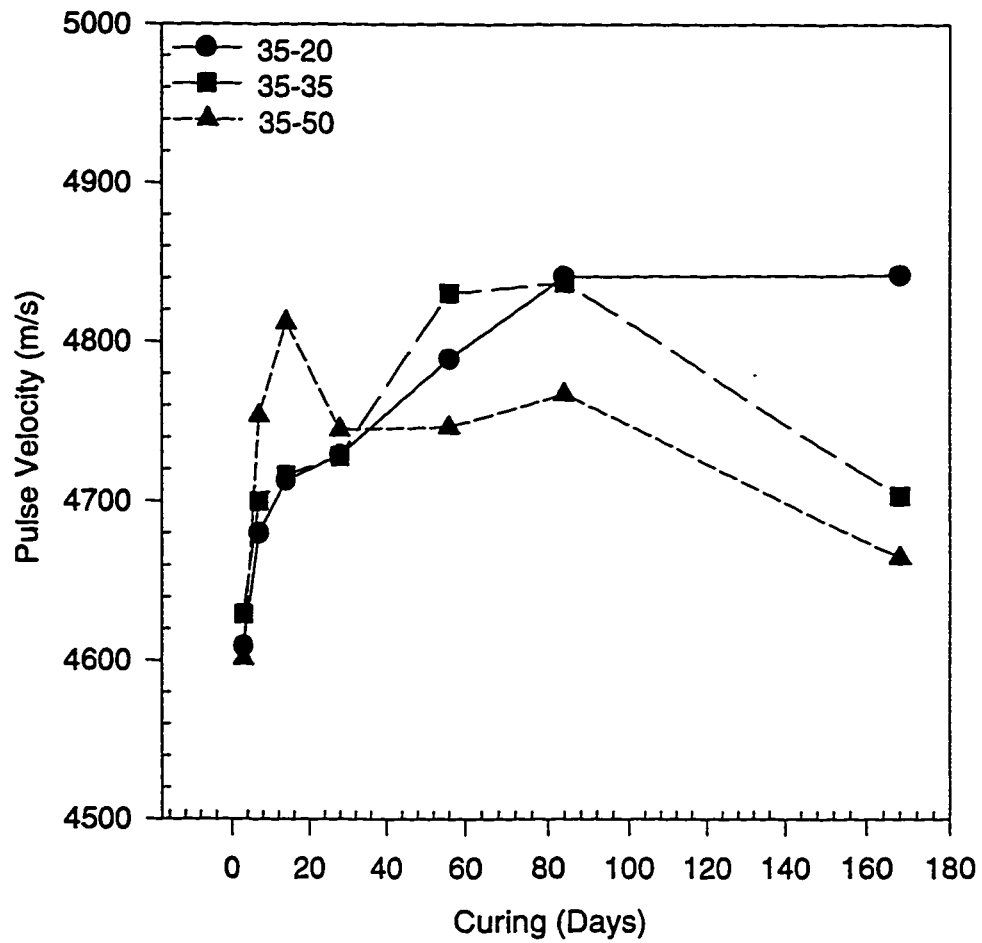


Fig. 4.21: Pulse Velocity in the Plain Cement Concrete Specimens Cast at 35 °C and Cured at various Temperatures

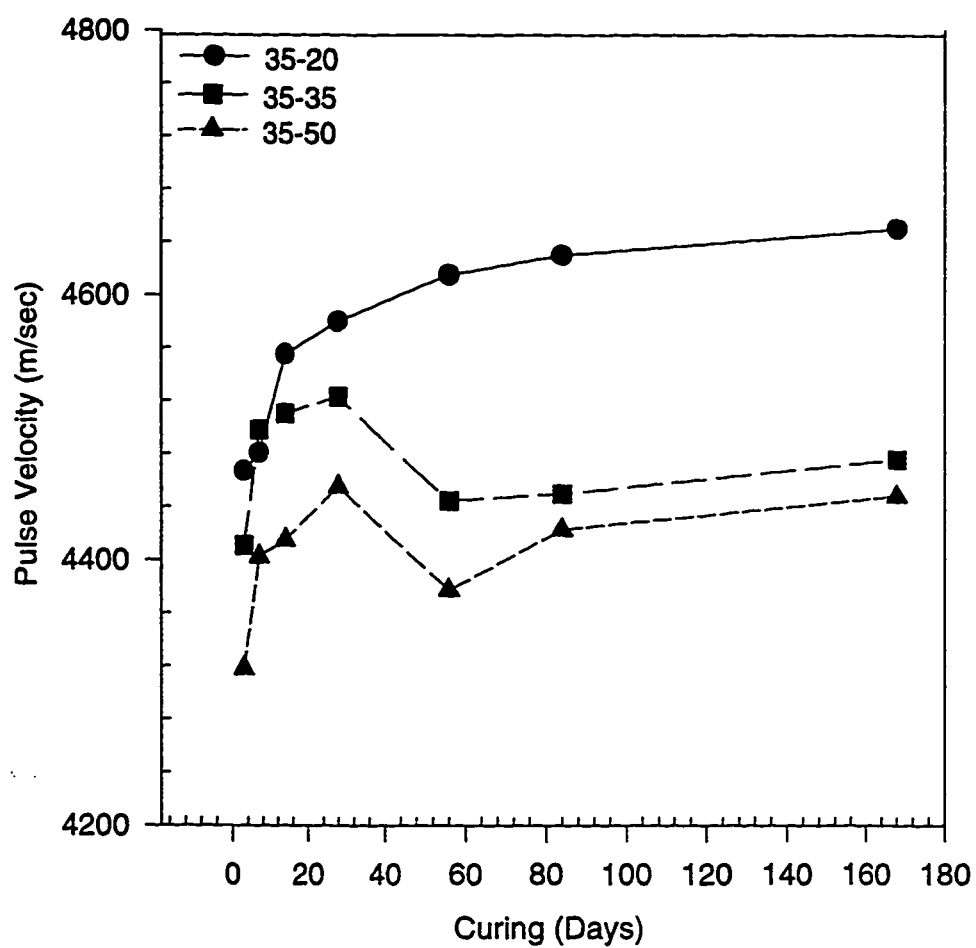


Fig. 4.22: Pulse Velocity in the Blast Furnace Slag Cement Concrete Specimens Cast at 35 °C and Cured at various Temperatures

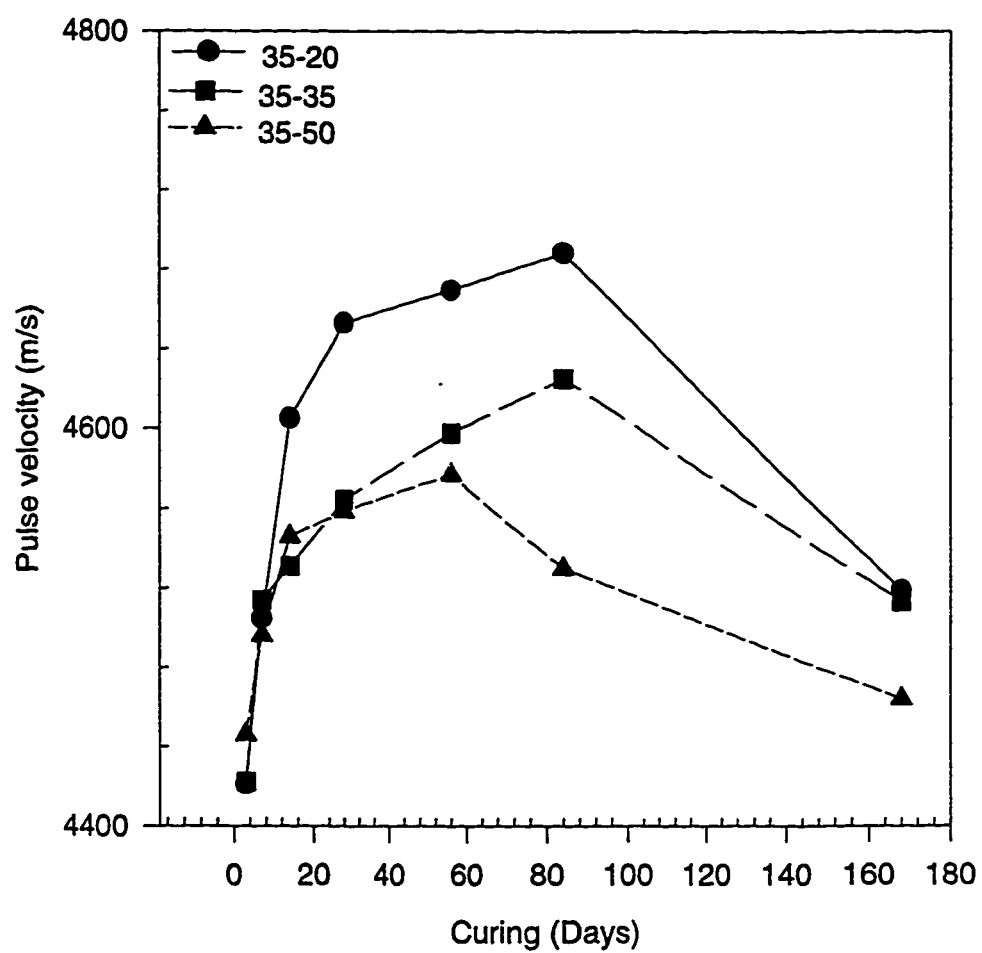


Fig. 4.23: Pulse Velocity in the Silica Fume Cement Concrete Specimens Cast at 35 °C and Cured at various Temperatures

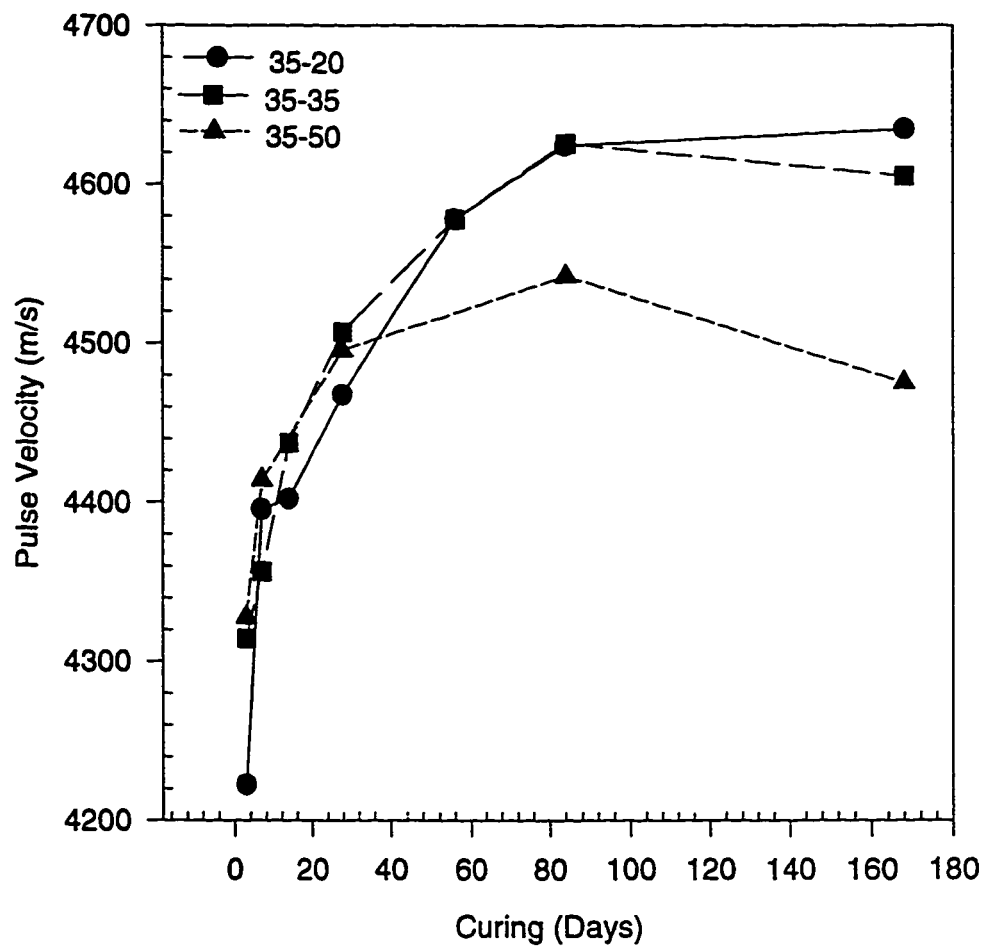


Fig. 4.24: Pulse Velocity in the Fly Ash Cement Concrete Specimens Cast at 35 °C and Cured at various Temperatures

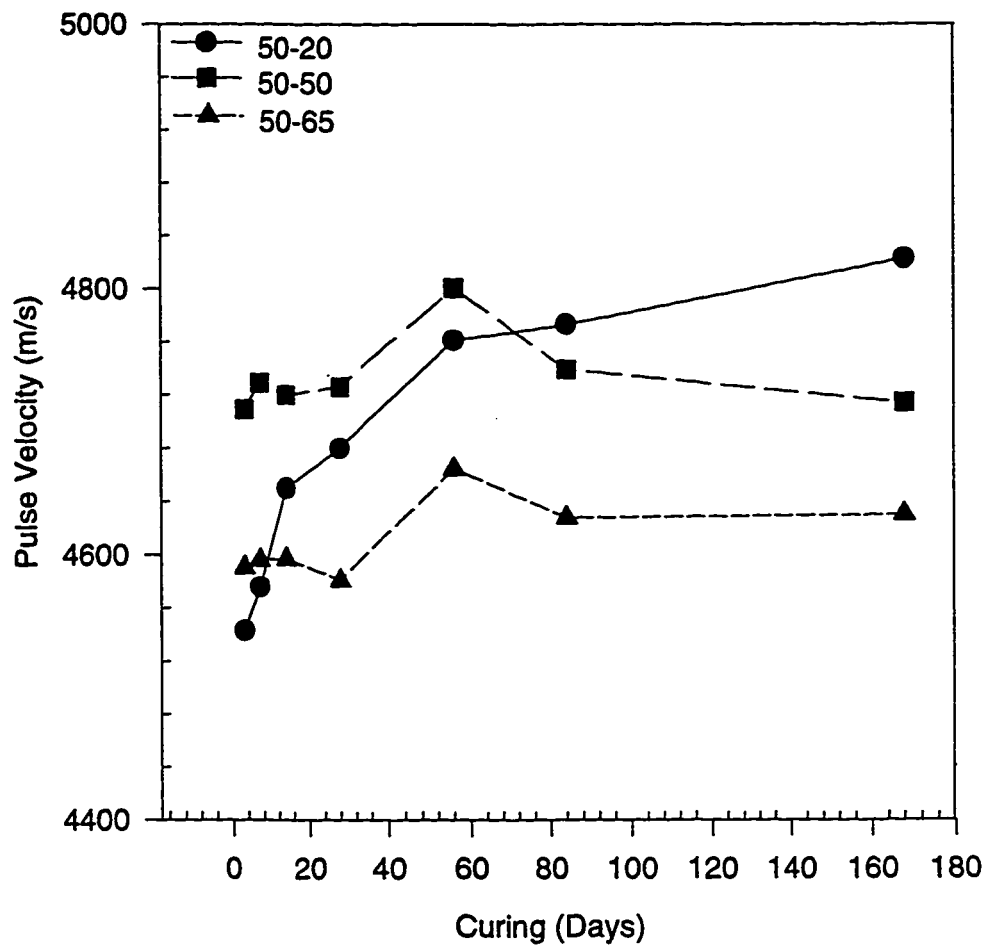


Fig. 4.25: Pulse Velocity in the Plain Cement Concrete Specimens Cast at 50 °C and Cured at various Temperatures

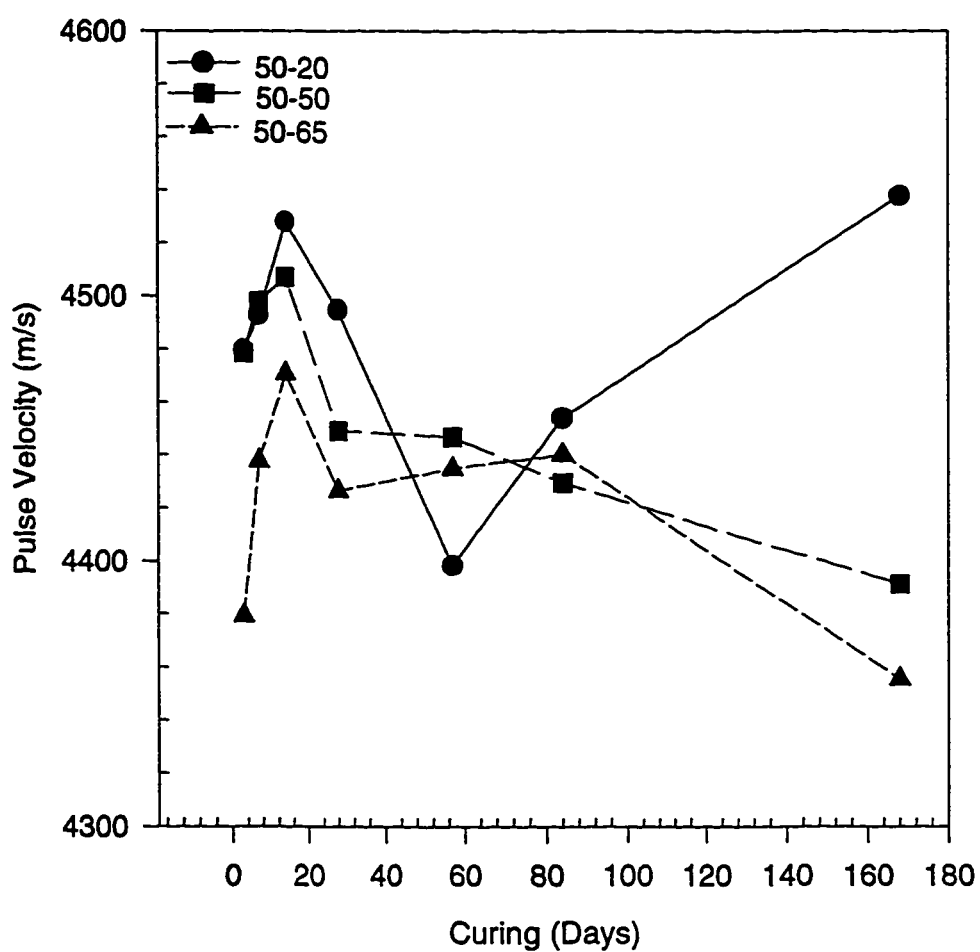


Fig. 4.26: Pulse Velocity in the Blast Furnace Slag Cement Concrete Specimens Cast at 50 °C and Cured at various Temperatures

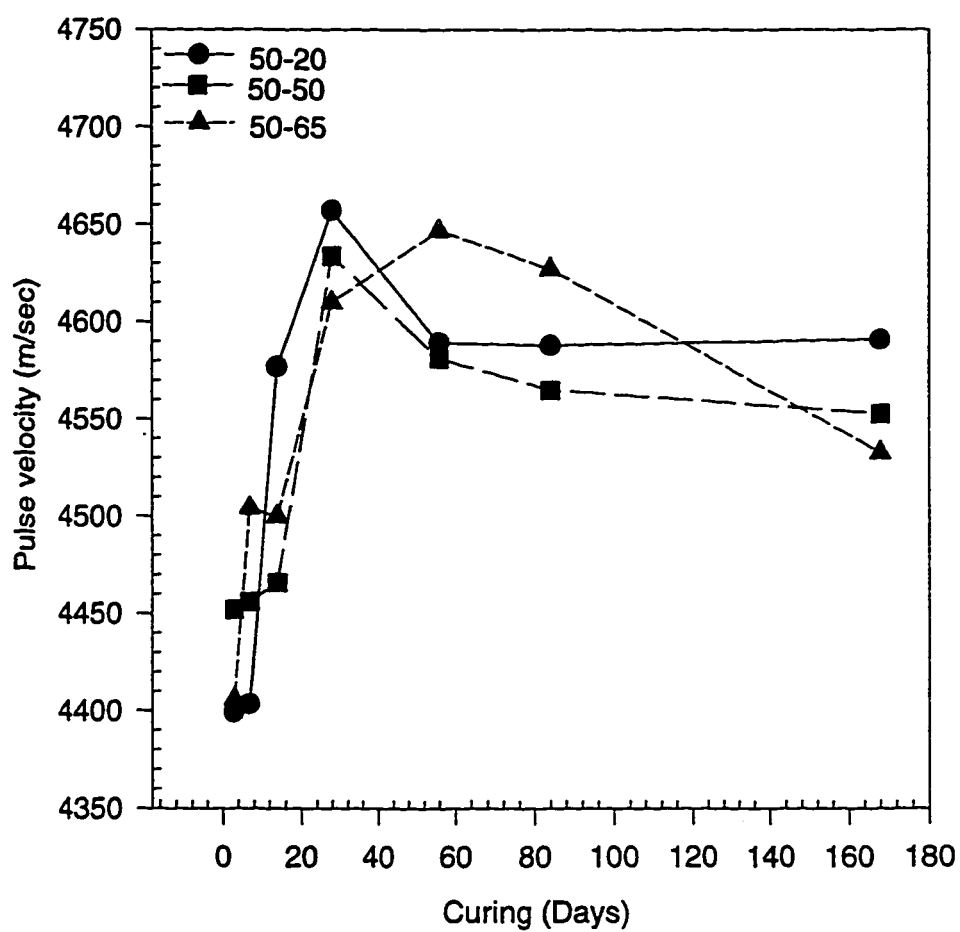


Fig. 4.27: Pulse Velocity in the Silica Fume Cement Concrete Specimens Cast at 50 °C and Cured at various Temperatures

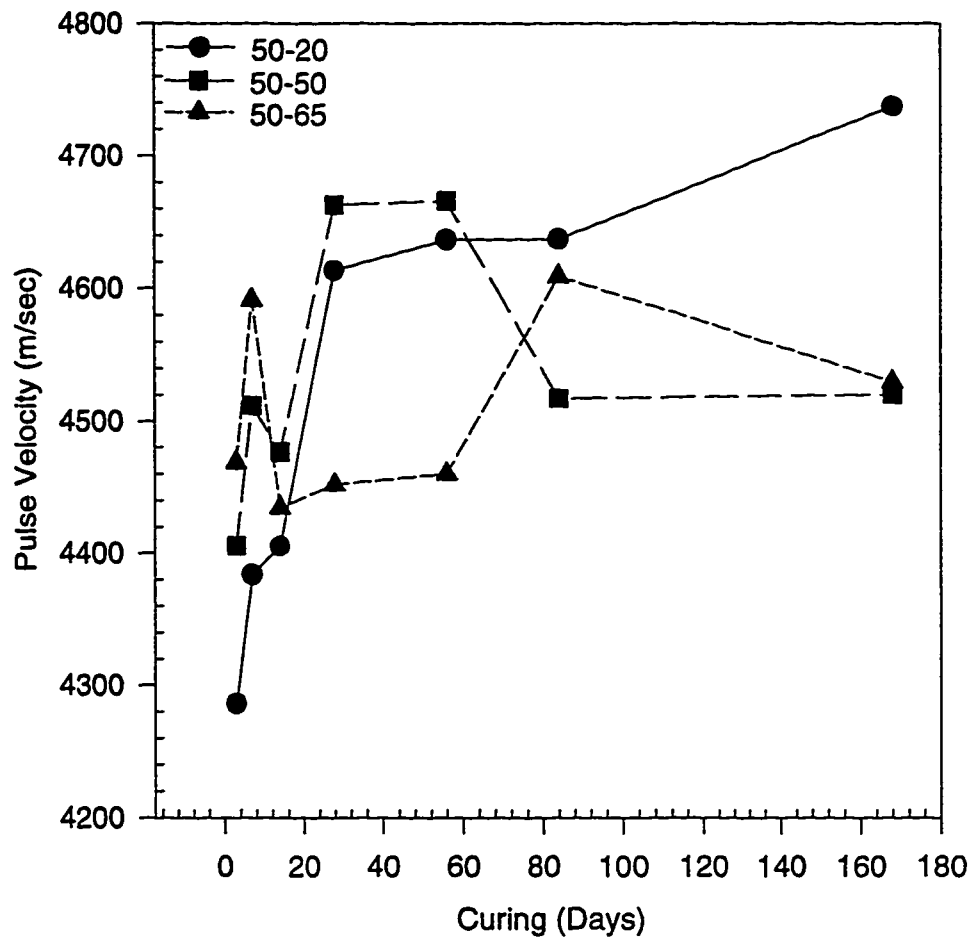


Fig. 4.28: Pulse Velocity in the Fly Ash Cement Concrete Specimens Cast at 50 °C and Cured at various Temperatures

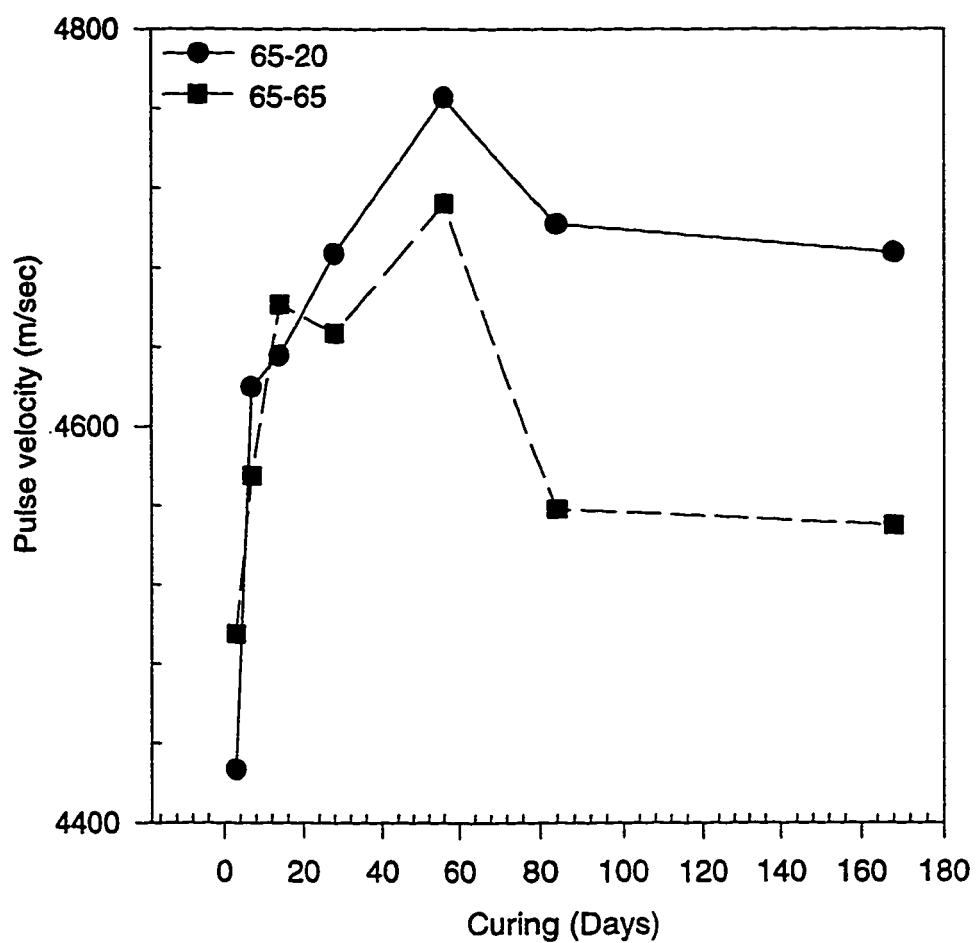


Fig. 4.29: Pulse Velocity in the Plain Cement Concrete Specimens Cast at 65 °C and Cured at various Temperatures

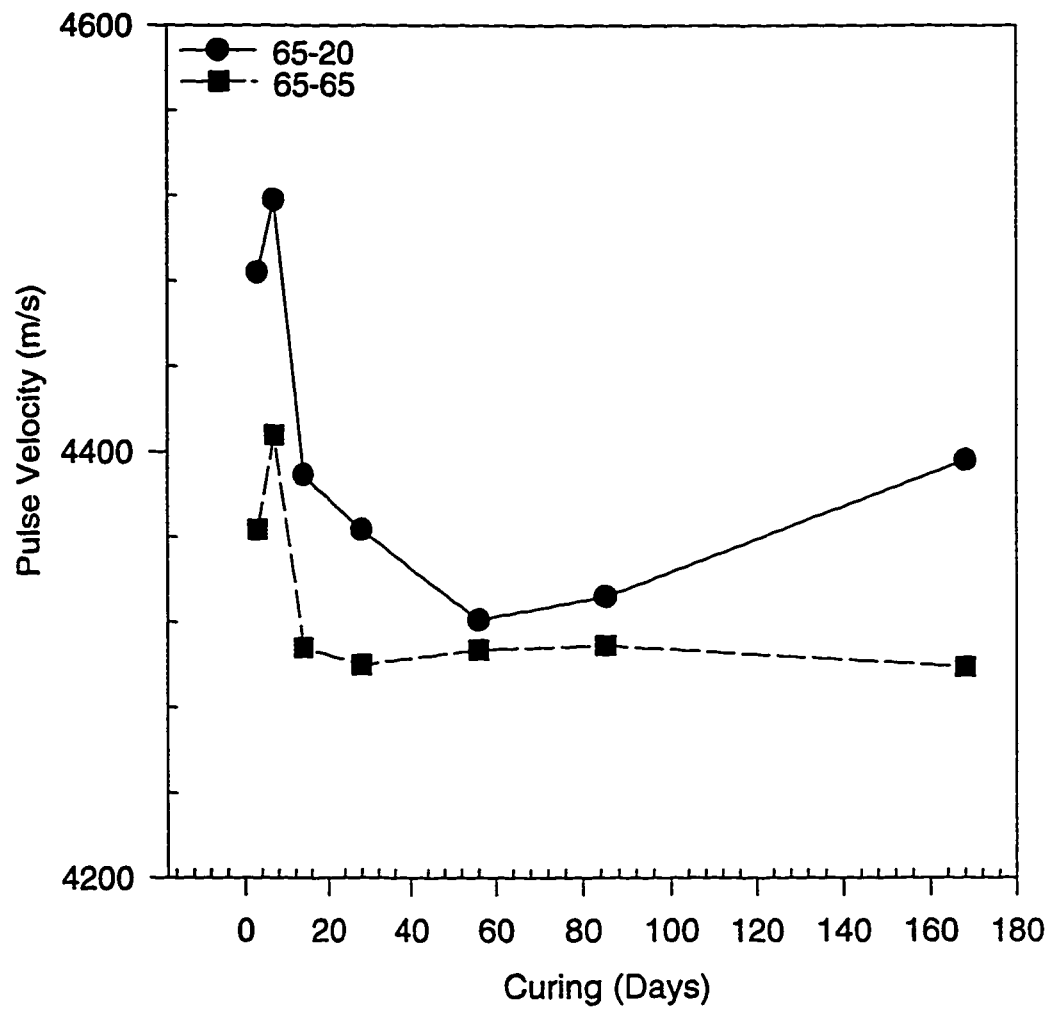


Fig. 4.30: Pulse Velocity in the Blast Furnace Slag Cement Concrete Specimens Cast at 65 °C and Cured at various Temperatures

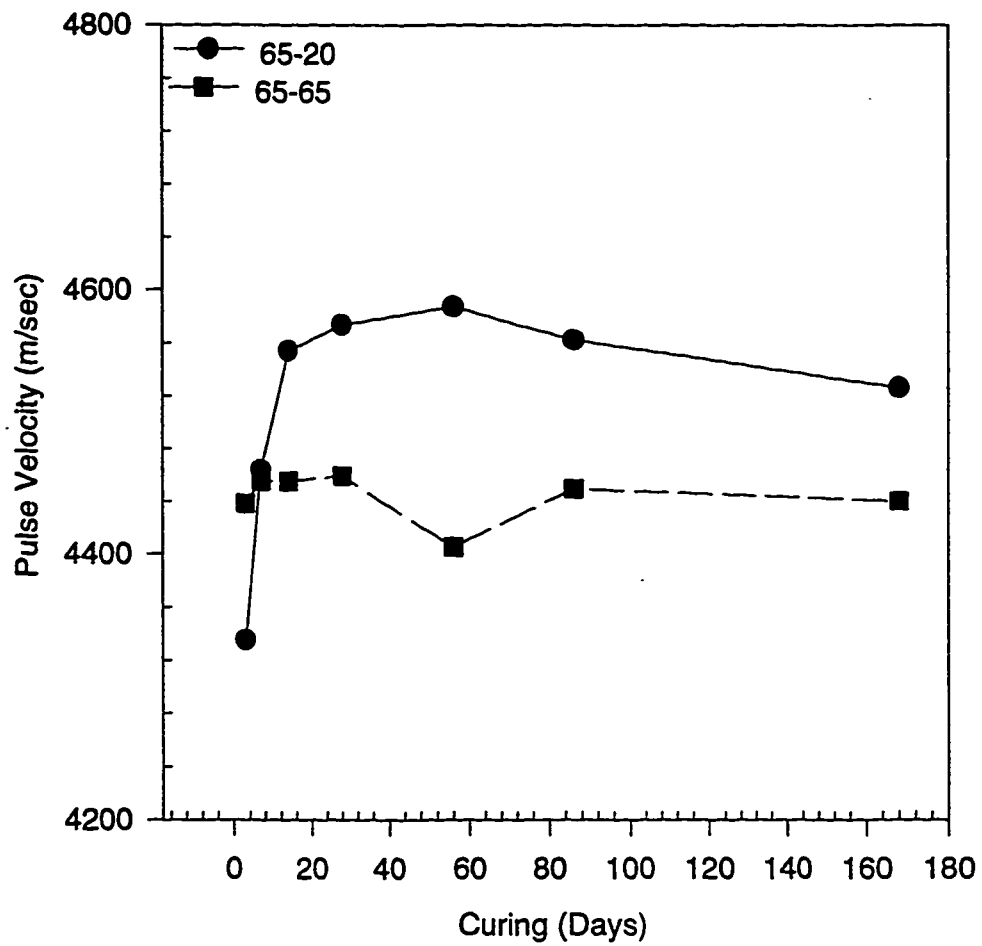


Fig. 4.31: Pulse Velocity in the Silica Fume Cement Concrete Specimens Cast at 65 °C and Cured at various Temperatures

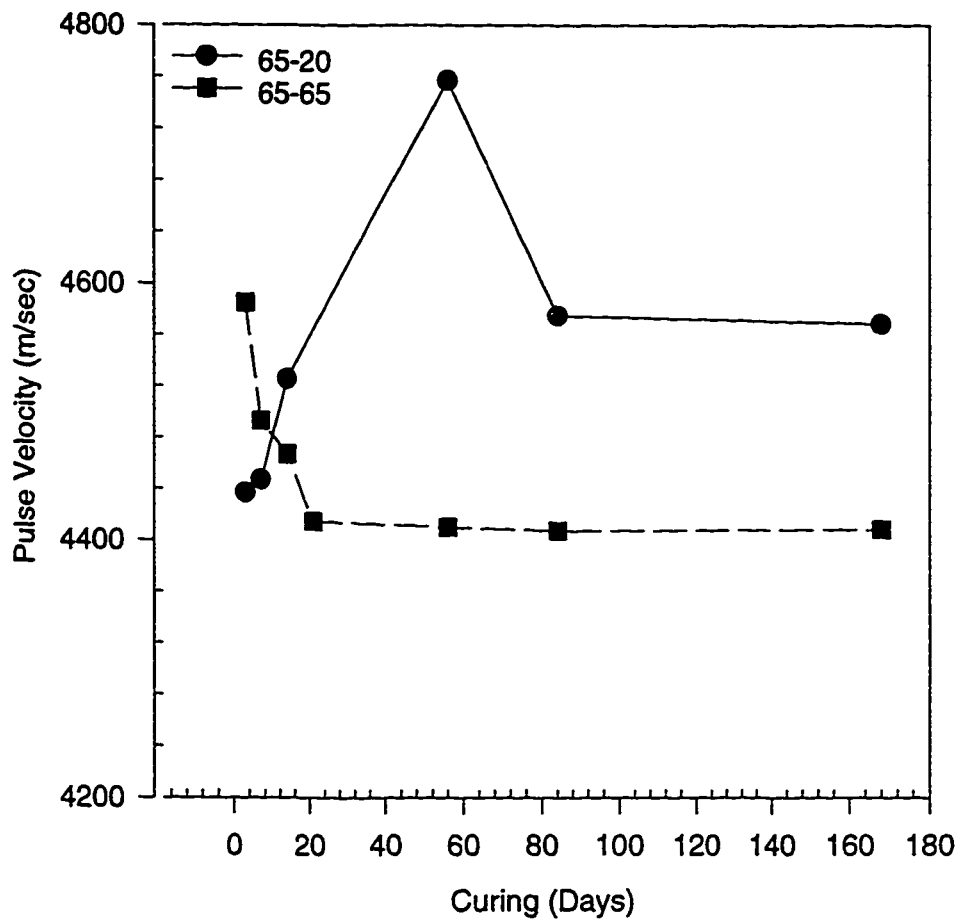


Fig. 4.32: Pulse Velocity in the Fly Ash Cement Concrete Specimens Cast at 65 °C and Cured at various Temperatures

4.3 EFFECT OF CASTING AND CURING TEMPERATURES ON WATER ABSORPTION

The water absorption in the plain cement concrete specimens cast at 20 °C and cured at various temperatures is shown in Figure 4.33. As expected, these values decreased with the age of curing in all the specimens. However, after 28 days of curing no significant change in the water absorption was noted in all the specimens. Further, the absorption increased with an increase in the curing temperature. After 168 days of curing the absorption in the concrete specimens cured at 20, 35, and 50 °C was 4.18, 4.44, and 4.71%, respectively.

Figure 4.34 shows the water absorption in the blast furnace slag cement concrete specimens cast at 20 °C and cured at various temperatures. In these specimens also, absorption decreased with the period of curing. The absorption values in the specimens cured at 20 and 50 °C were more or less similar up to 84 days. However, after 168 days of curing the absorption in the specimens cured at 50 °C was more than those cured at 20 and 35 °C. The lowest absorption was indicated in the specimens cured at 35 °C after about 14 days of curing. After 168 days of curing, the absorption in the specimens cured at 20, 35, and 50 °C was 3.67, 3.67, and 3.94%, respectively. The reduction in the absorption with increasing temperature may be attributed to the formation of a denser pore structure due to

elevated temperature curing. The reduction in the pore structure may be attributed to the acceleration of cement hydration in the blast furnace slag at elevated temperature. However, an increase in the absorption in the concrete specimens cured at 50 °C, for 168 days, may be attributed to the formation of microcracks due to elevated temperature curing.

Figure 4.35 shows the effect of curing at various temperatures on the absorption in the silica fume cement concrete specimens cast at 20 °C. While absorption in the concrete specimens cured at 20 °C decreased with age, in the concrete specimens cured at 35 and 50 °C it increased after 84 days of curing. The absorption in the concrete specimens cured at 35 and 50 °C was more than those cured at 20 °C. After 168 days of curing, the absorption in the specimens cured at 20, 35, and 50 °C was 4.67, 5.23, and 5.31%, respectively.

The absorption in the fly ash cement concrete specimens cast at 20 °C and cured at various temperatures are plotted in Figure 4.36. These values decreased with age in the specimens cured at 20 and 35 °C. However, in the specimens cured at 50 °C, they decreased with age up to 72 days, beyond which time they started to increase. The absorption in the concrete specimens cured at 20, 35, and 50 °C was 4.76, 4.71, and 5.2%, respectively.

Figure 4.37 shows the absorption in the plain cement concrete specimens cast at 35 °C and cured at various temperatures. These values decreased with age, the reduction in the specimens cured at 20 °C being more rapid after 84 days of curing, compared to those cured at 35 and 50 °C. After 168 days of curing, the absorption in the specimens cured at 20, 35, and 50 °C was 4.34, 4.46, and 4.55%, respectively. Figure 4.38 shows the absorption in the blast furnace slag cement concrete specimens cast at 35 °C and cured at various temperatures. The absorption values decreased with age and increased with the curing temperature. While there was a significant difference in the absorption between the concrete specimens cured at 20 and 35 °C, the margin between the concrete specimens cured at 35 and 50 °C was not significant. After 168 days, the absorption in the specimens cured at 20, 35, and 50 °C was 2.95, 3.14, and 3.19%, respectively.

Figure 4.39 shows the effect of curing temperature on the absorption in the silica fume cement concrete specimens cast at 35 °C and cured at various temperatures. The absorption in all the specimens decreased up to a curing period of 84 days. However, after 84 days an increase in the absorption capacity of the concrete specimens cured at 35 and 50 °C was indicated, while in the specimens cured at 20 °C, no significant change in the absorption was recorded. The absorption in the

specimens cured at 20, 35, and 50 °C was 5.0, 5.49, and 5.45%, respectively, after 168 days of curing.

Figure 4.40 shows the absorption in the fly ash cement concrete specimens cast at 35 °C and cured at various temperatures. Absorption in all the specimens decreased with the period of curing. The absorption in the specimens cured at 20, 35, and 50 °C was 5.42, 5.48, and 5.59%, respectively. Figure 4.41 shows the absorption in the plain cement concrete specimens cast at 50 °C and cured at various temperatures. A significant decrease in the absorption up to 56 days of curing, was observed in the specimens cured at 50 and 65 °C. However, after this time these values increased, to almost 3-day value, after 168 days of curing. However, the absorption in the concrete specimens cured at 20 °C decreased with the period of curing. The absorption in the specimens cured at 20, 50, and 65 °C after 168 days of curing was 4.55, 4.81, and 4.96%, respectively.

The absorption in the blast furnace slag cement concrete specimens cast at 50 °C and cured at various temperatures are plotted in Fig. 4.42. The absorption in the specimens cured at 50 and 65 °C did not decrease with time. However, the absorption in the specimens cured at 20 °C decreased with the period of curing. The absorption in the specimens cured at 20, 50, and 65 °C was 3.02, 4.42, and

4.48%, respectively. Figure 4.43 shows the absorption in the silica fume cement concrete specimens cast at 50 °C and cured at various temperatures. The absorption in the specimens cured at 50 and 65 °C decreased with age up to 84 and 28 days, respectively. After this curing period, an increase in the absorption was indicated. The absorption in the concrete specimens cured at 20 °C continued to decrease with the curing period. The absorption in the specimens cured at 20, 50, and 65 °C was 5.35, 5.28, and 5.41%, respectively.

Figure 4.44 shows the effect of curing on the absorption in the fly ash cement concrete specimens cast at 50 °C and cured at various temperatures. The absorption in the specimens cured at 20 and 65 °C decreased with age, while it increased after 84 days in the specimens cured at 50 °C. The absorption in the specimens cured at 20, 50, and 65 °C was 4.68, 5.06, and 5.0%, respectively, after 168 days of curing. Figure 4.45 shows the absorption in the plain cement concrete specimens cast at 65 °C and cured at 20 and 65 °C. A decrease in the absorption with the period of curing was observed in the specimens cured at both the temperatures. However, the absorption in the specimens cured at 20 °C was less than those cured at 65 °C. After 168 days of curing, the absorption in the specimens cured at 20 and 65 °C was 4.34 and 4.53%, respectively.

Figure 4.46 shows the absorption in the blast furnace slag cement concrete specimen cast at 65 °C and cured at 20 and 65 °C. A reduction in the absorption with the period of curing was indicated in the specimens cured at both the temperatures. Further, the absorption in the specimens cured at 20 °C was less than those cured at 65 °C at all the curing periods. After 168 days of curing, the absorption in the specimens cured at 20 and 65 °C was 3.43 and 3.64%, respectively.

Absorption in the silica fume cement concrete specimens cast at 65 °C and cured at 20 and 65 °C is presented in Figure 4.47. These values in the specimens cured at 20 and 65 °C decreased with age and were 3.68 and 3.82%, respectively, after 168 days of curing. Figure 4.48 shows the absorption in the fly ash cement concrete specimens cast at 65 °C and cured at 20 and 65 °C. Absorption in the specimens cured at 65 °C decreased up to 84 days. However, after this time, a significant increase was observed. Absorption values in the specimens cured at 20 °C decreased with age. After 168 days of curing, the absorption in the specimens cured at 20 and 65 °C was 5.43 and 5.6%, respectively.

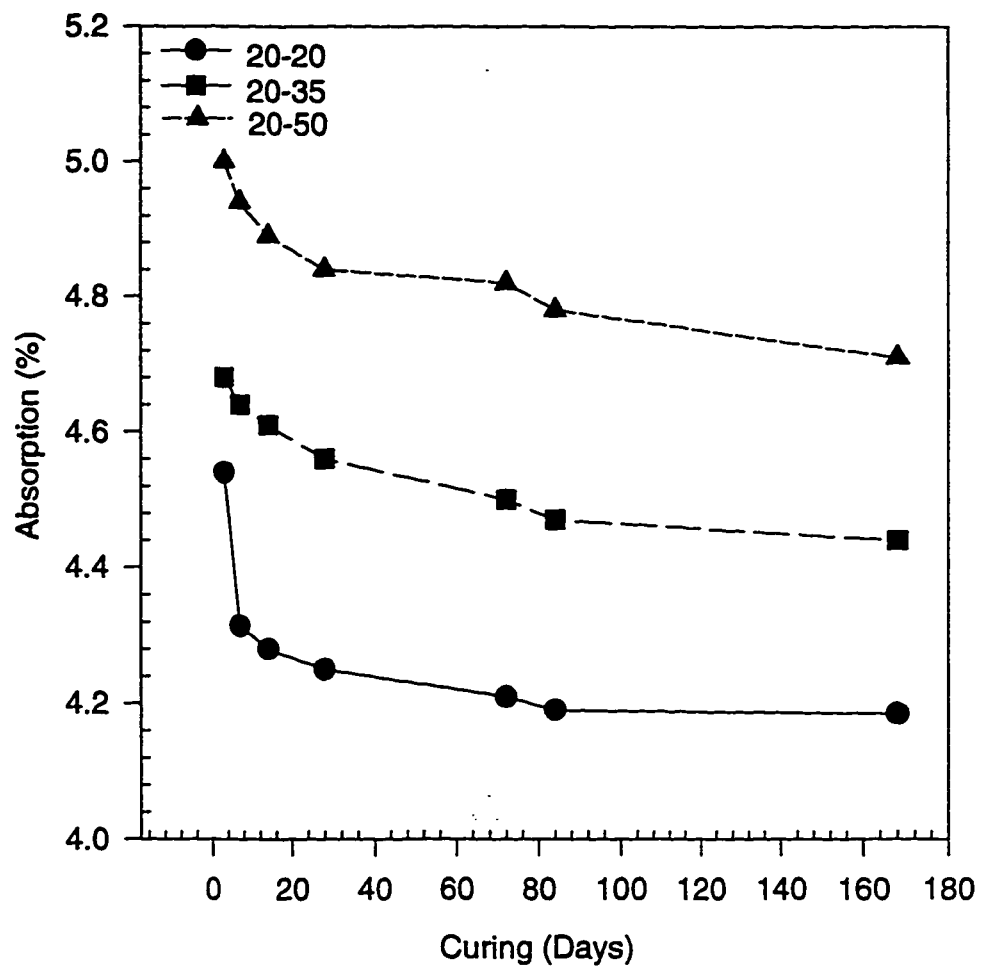


Fig. 4.33: Absorption in the Plain Cement Concrete Specimens Cast at 20 °C and Cured at various Temperatures

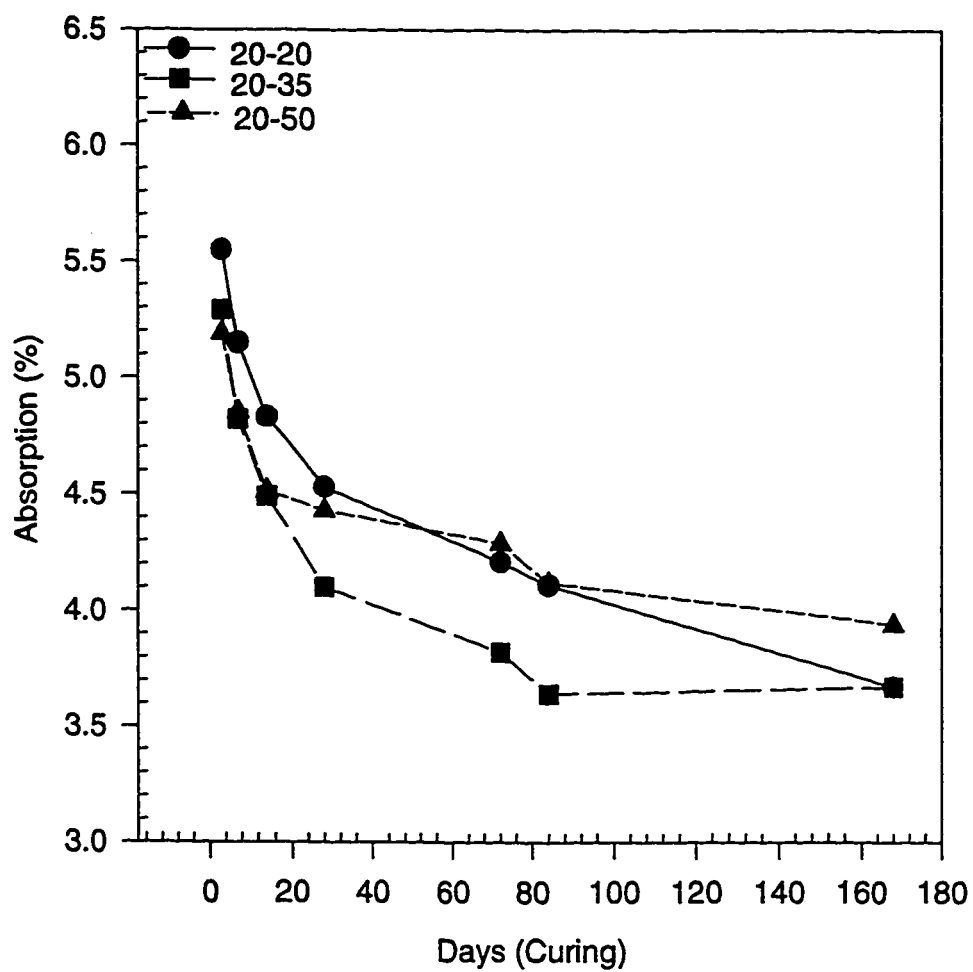


Fig. 4.34: Absorption in the Blast Furnace Slag Cement Concrete Specimens Cast at 20 °C and Cured at various Temperatures

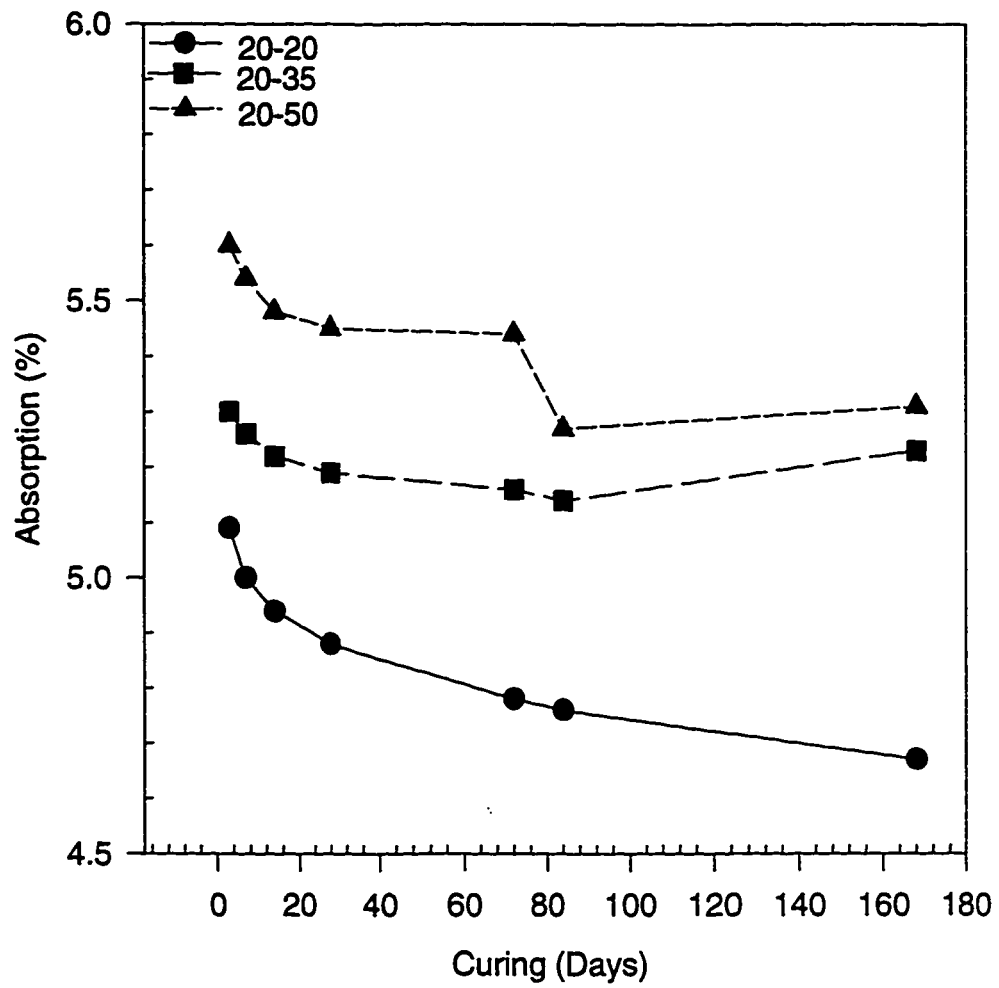


Fig. 4.35: Absorption in the Silica Fume Cement Concrete Specimens Cast at 20 °C and Cured at various Temperatures

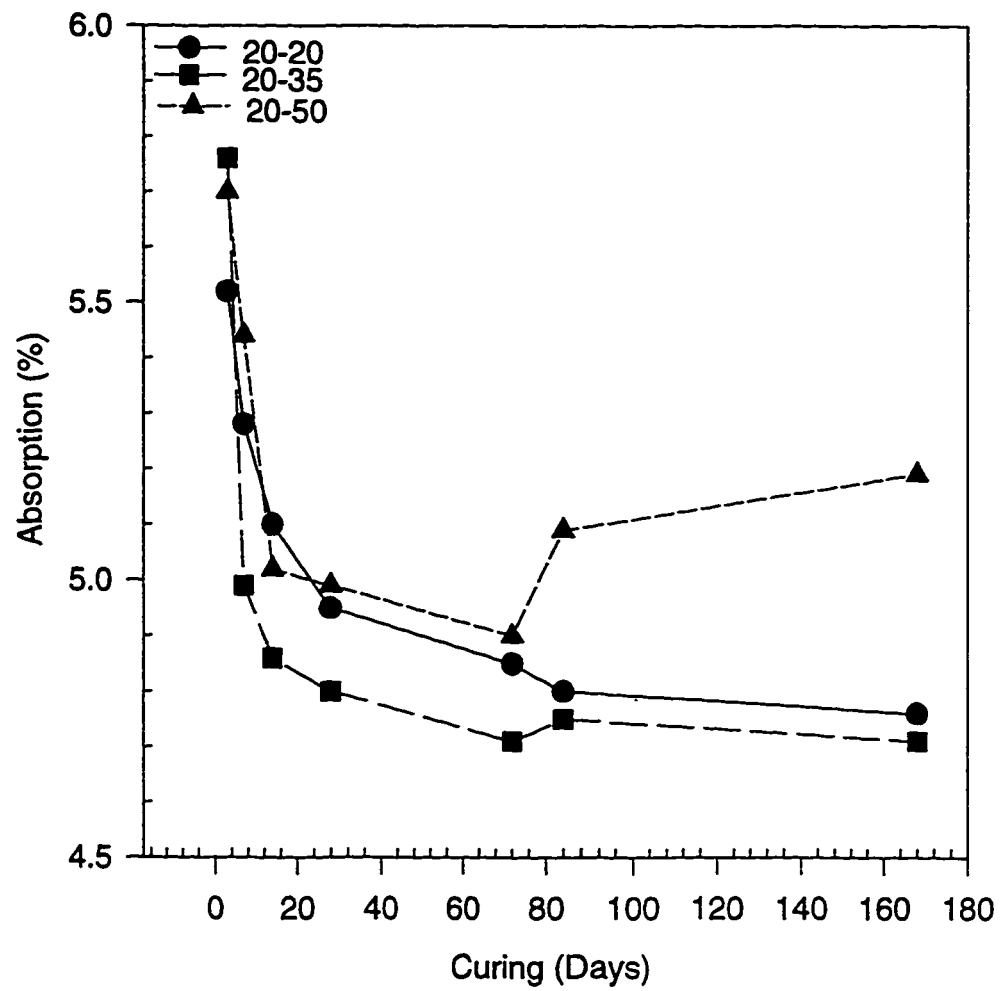


Fig. 4.36: Absorption in the Fly Ash Cement Concrete Specimens Cast at 20 °C and Cured at various Temperatures

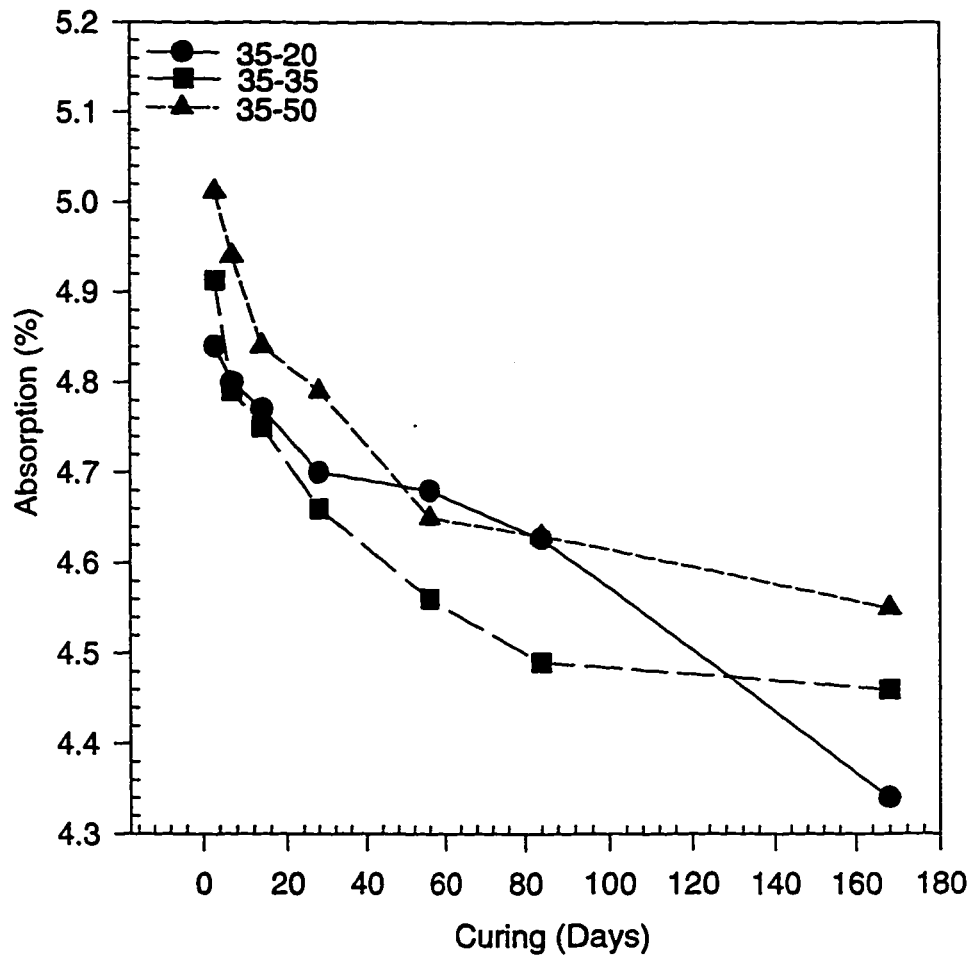


Fig. 4.37: Absorption in the Plain Cement Concrete Specimens Cast at 35 °C and Cured at various Temperatures

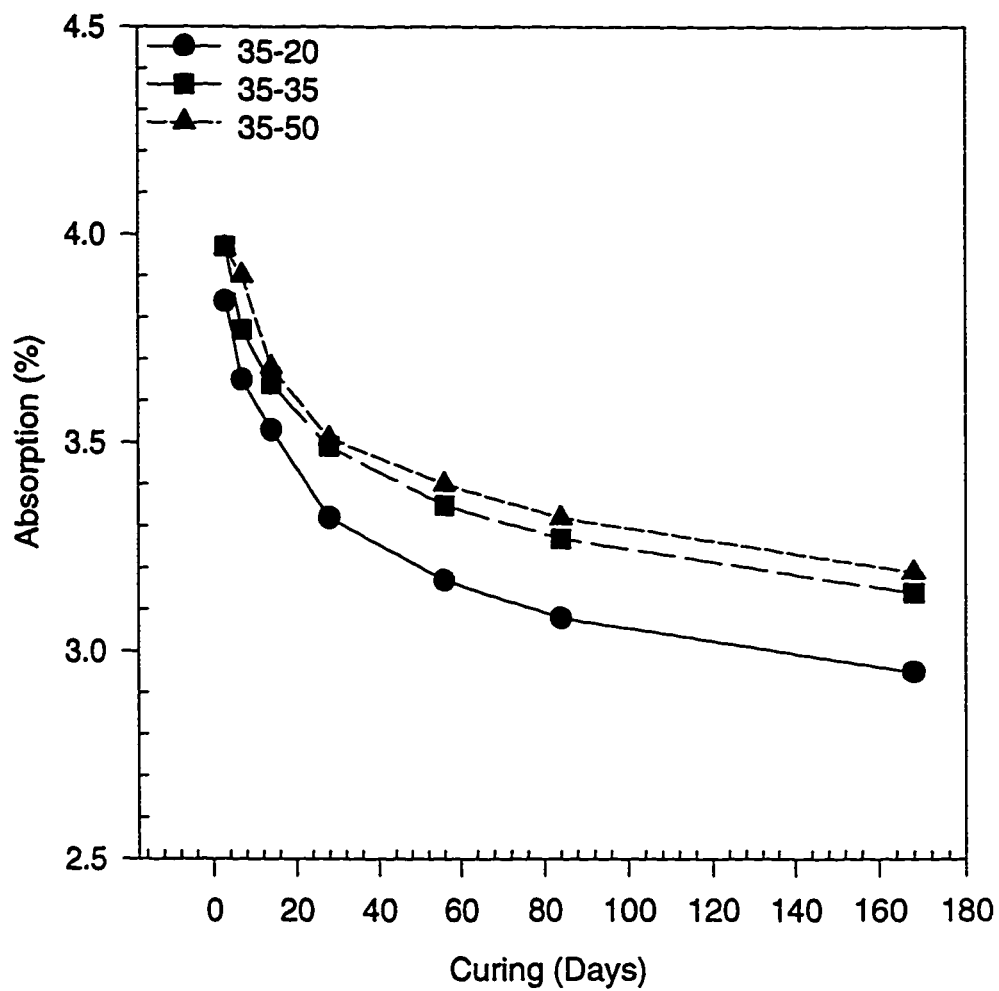


Fig. 4.38: Absorption in the Blast Furnace Slag Cement Concrete Specimens Cast at 35 °C and Cured at various Temperatures

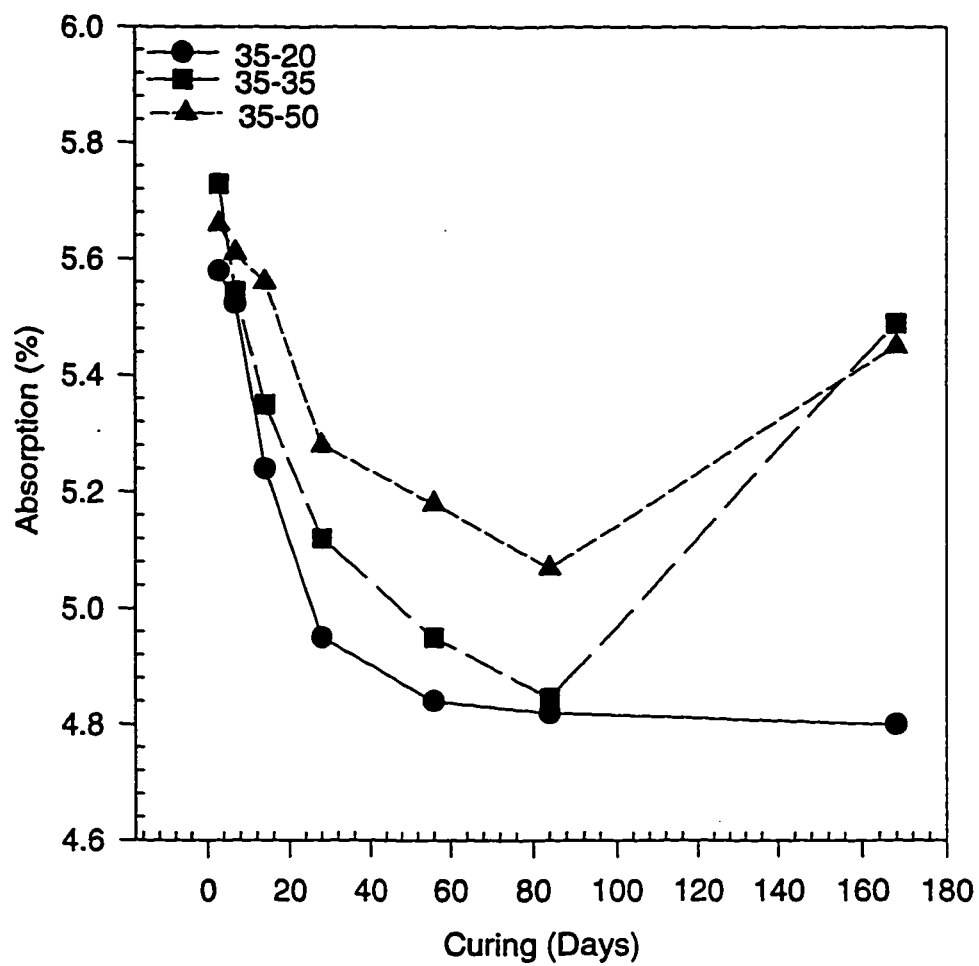


Fig. 4.39: Absorption in the Silica Fume Cement Concrete Specimens Cast at 35 °C and Cured at various Temperatures

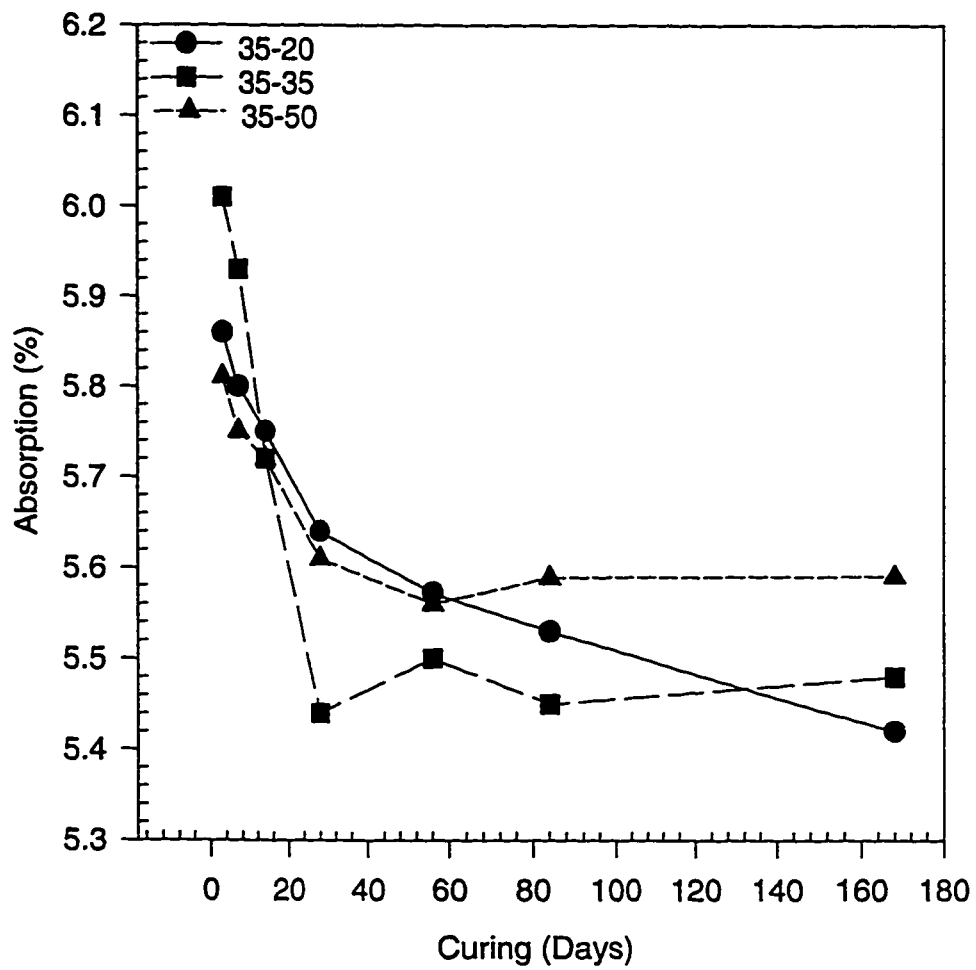


Fig. 4.40: Absorption in the Fly Ash Cement Concrete Specimens Cast at 35 °C and Cured at various Temperatures

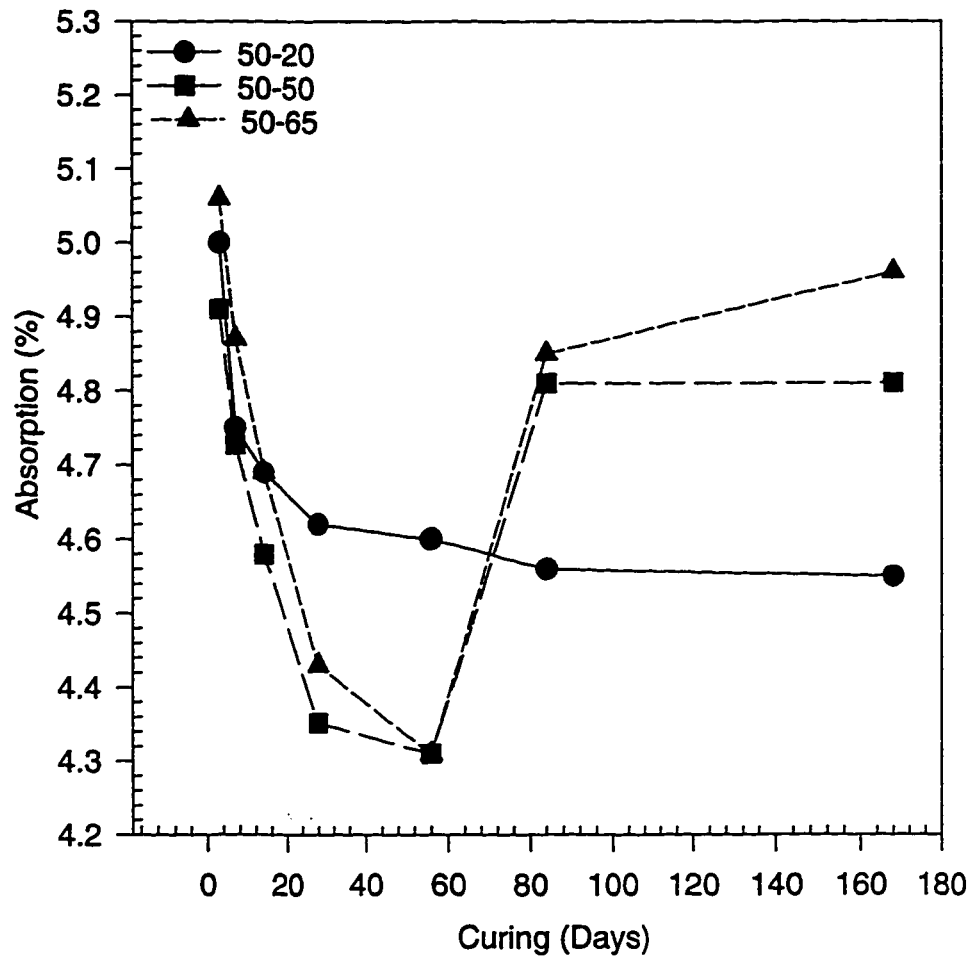


Fig. 4.41: Absorption in the Plain Cement Concrete Specimens Cast at 50 °C and Cured at various Temperatures

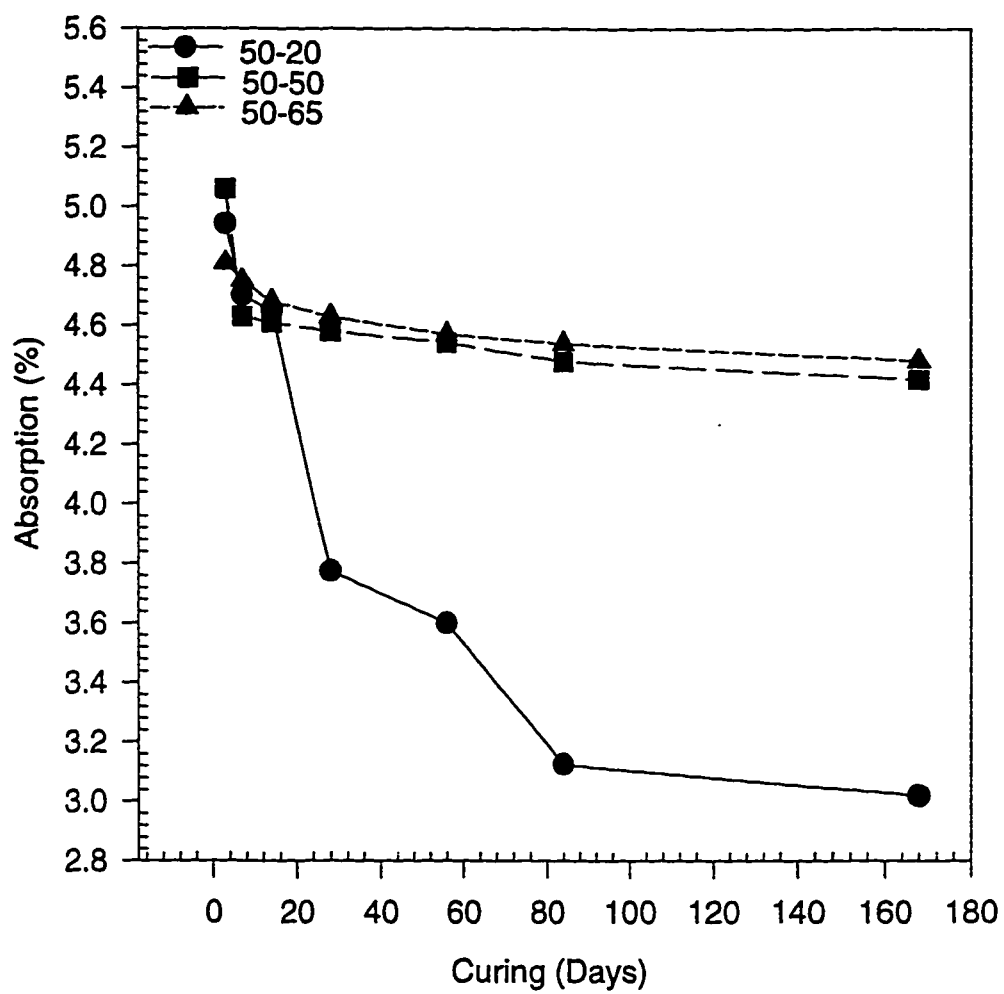


Fig. 4.42: Absorption in the Blast Furnace Slag Cement Concrete Specimens Cast at 50 °C and Cured at various Temperatures

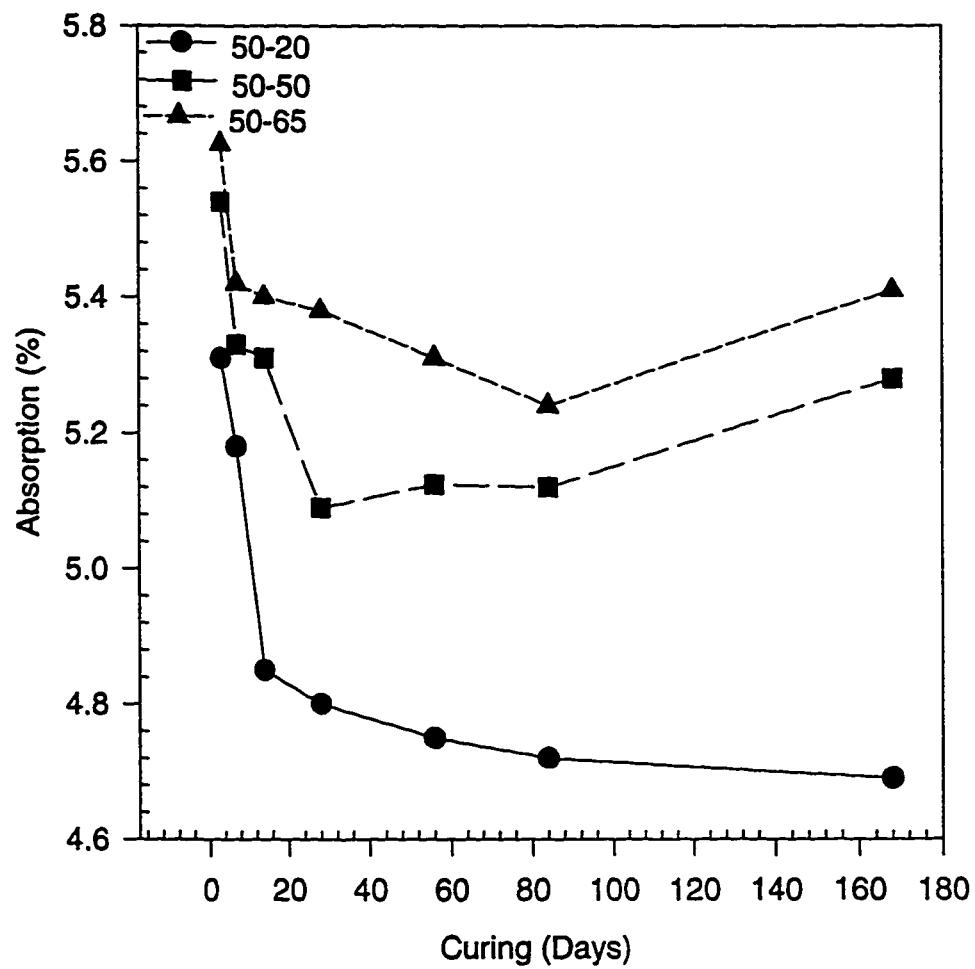


Fig. 4.43: Absorption in the Silica Fume Cement Concrete Specimens Cast at 50 °C and Cured at various Temperatures

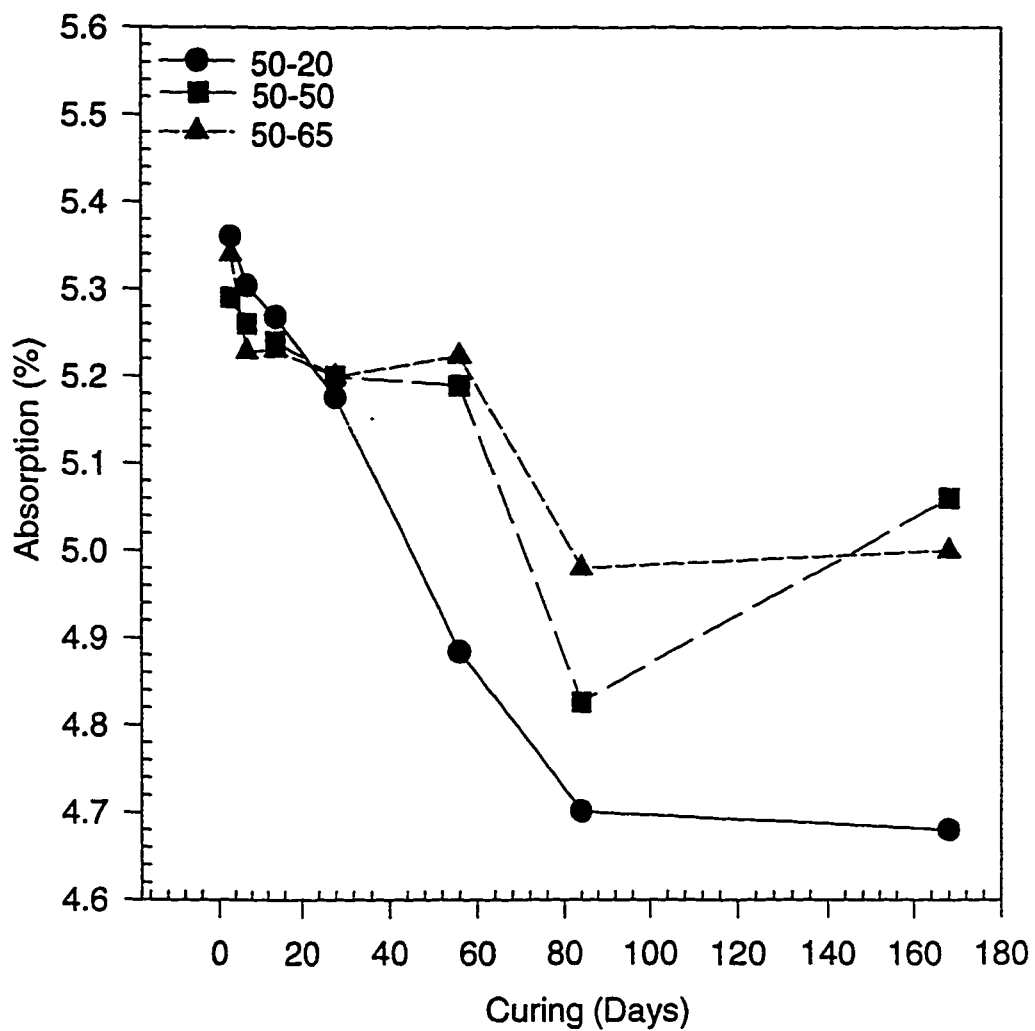


Fig. 4.44: Absorption in the Fly Ash Cement Concrete Specimens Cast at 50 °C and Cured at various Temperatures

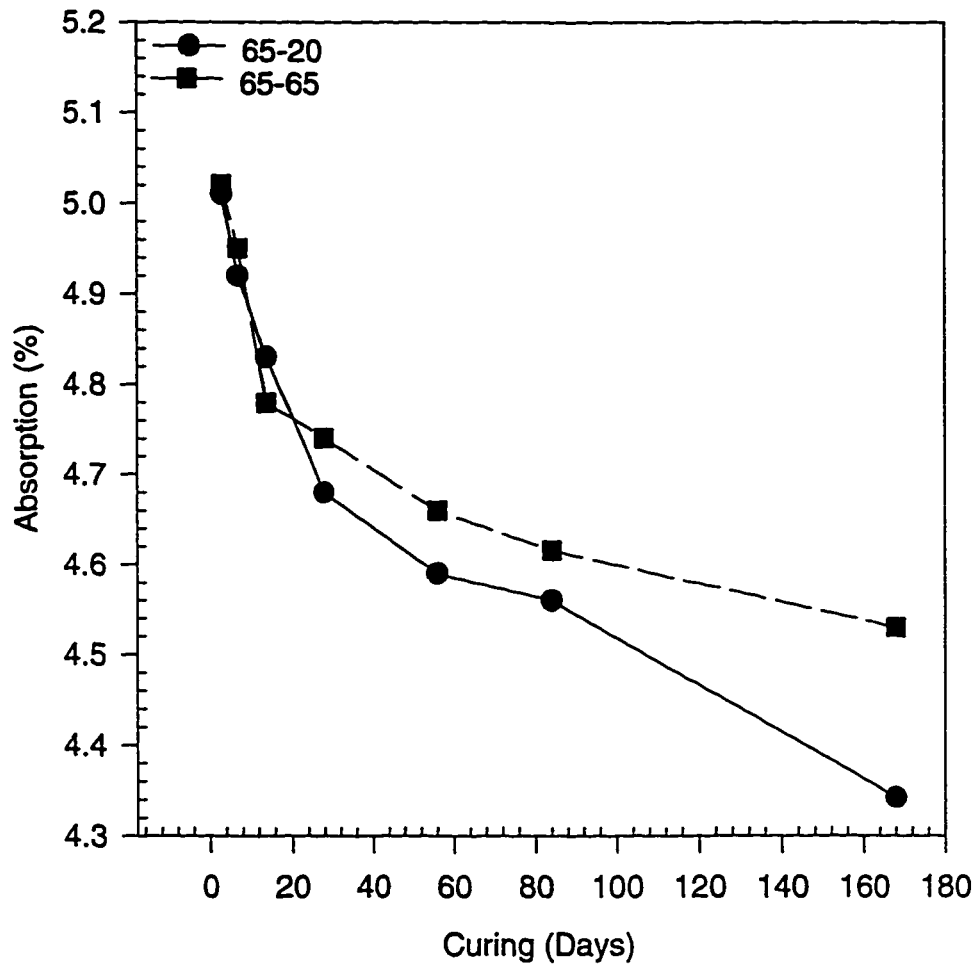


Fig. 4.45: Absorption in the Plain Cement Concrete Specimens Cast at 65 °C and Cured at various Temperatures

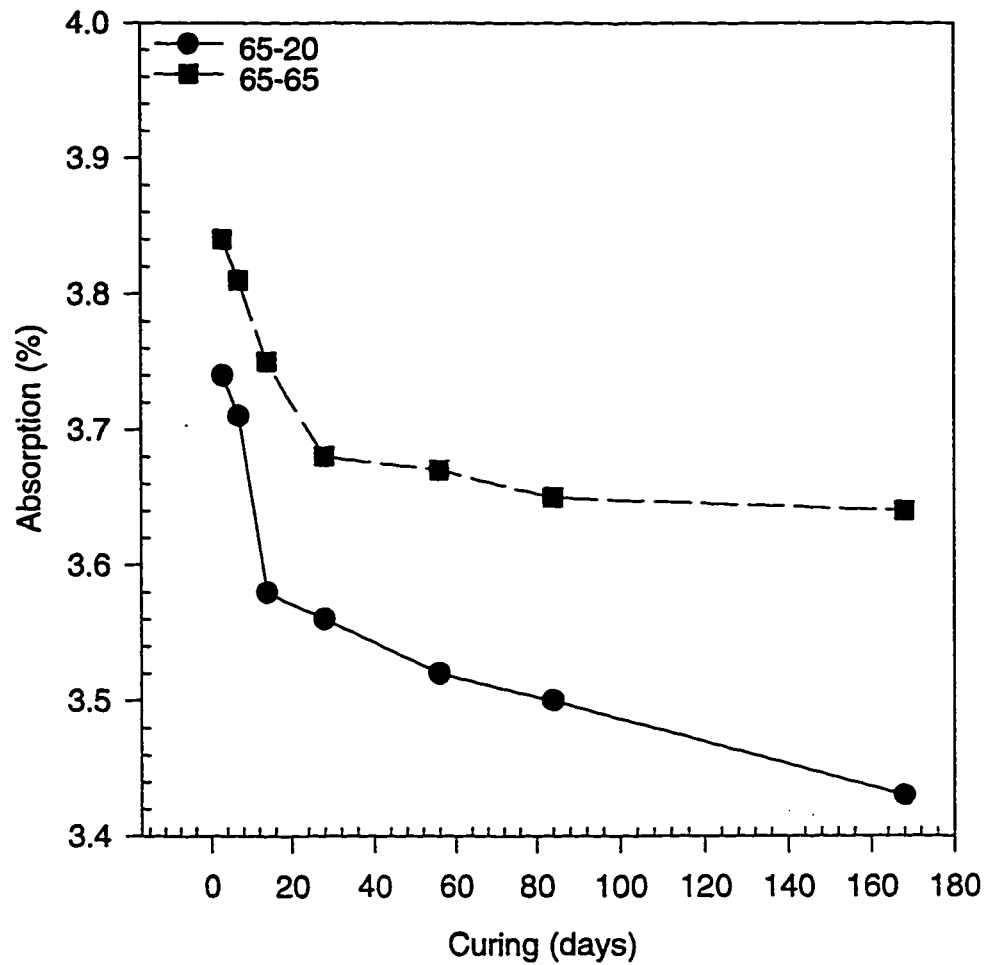


Fig. 4.46: Absorption in the Blast Furnace Slag Cement Concrete Specimens Cast at 65 °C and Cured at various Temperatures

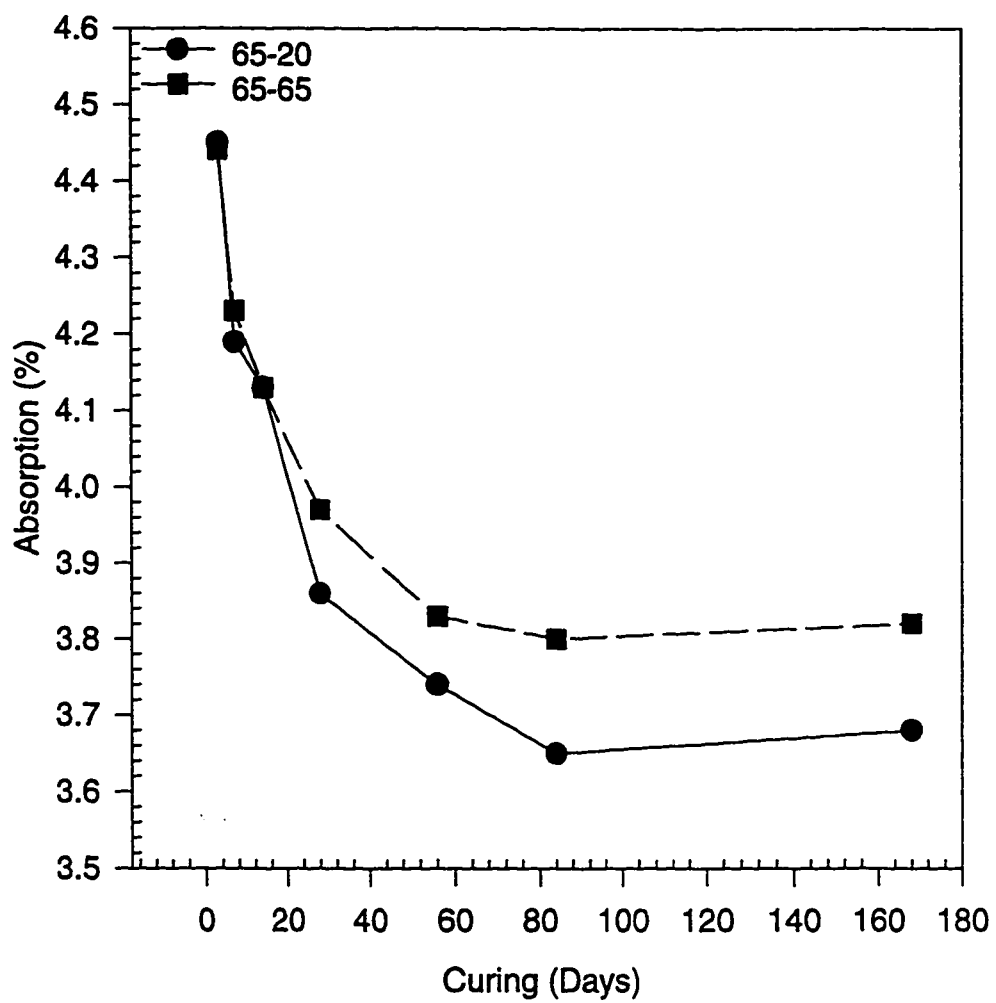


Fig. 4.47: Absorption in the Silica Fume Cement Concrete Specimens Cast at 65 °C and Cured at various Temperatures

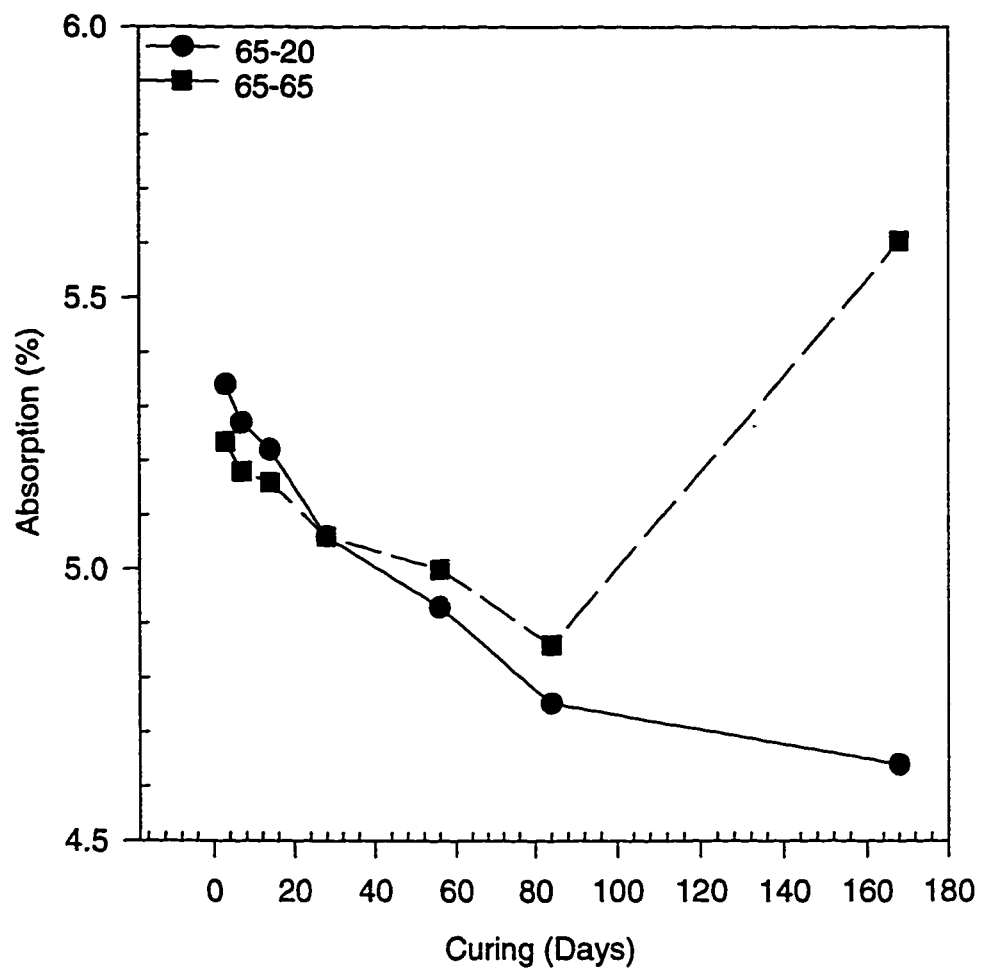


Fig. 4.48: Absorption in the Fly Ash Cement Concrete Specimens Cast at 65 °C and Cured at various Temperatures

4.4 EFFECT OF CASTING TEMPERATURE ON THE PORE SIZE DISTRIBUTION IN PLAIN AND BLENDED CEMENTS

The effect of casting and curing temperatures on the pore size distribution in the plain and blended cement mortar specimens cast at 20, 35, 50 °C and cured at 20 °C was determined by mercury intrusion porosimetry. For this purpose, representative samples from the mortar specimens cured up to 28 days were utilized.

Figure 4.49 shows the pore size distribution in the plain cement, while Figures 4.50 through 4.52 represents distribution of pores in the blended cements. These figures were used to evaluate the pore volume and distribution of coarse and fine pores. As suggested by Mehta and Manmohan [83] a pore radius of 1000 Å was used as a reference for distinguishing coarse pores from fine pores. The effect of casting temperature on the cumulative pore volume and the proportion of coarse and fine pores are shown in Table 4.1.

In the plain cement mortar specimens, the pore volume increased with the casting temperature. The pore volume in the specimens cast at 50 °C was about 1.4 times than that cast at 20 °C. Further, a reduction in the volume of fine pores,

consequently an increase in the coarse pores, was noted with increasing casting temperature in these specimens, even though these specimens were cured at 20 °C. The conjoint effect of both increase in the pore volume and proportion of coarse pores will increase the permeability of mortar. These results are in close agreement with the data developed by Marsh et al. [62] who reported that the plain cement pastes cured at elevated temperature resulted in increased permeability. The increase in the porosity of mortar specimens cast at elevated temperature may be attributed to the improper diffusion and sedimentation of the hydration products in the internal space between cement grains.

Villadsen [63] used low temperature colorimeter as an indirect measure of porosity for cement pastes cured at different temperatures. As the curing temperatures increased the amount of pore water frozen at -4 °C also increased. This may be attributed to the formation of coarser pore structure due to elevated curing temperature. Goto and Roy [54] found that total porosity of hydrated cement paste at 65 °C was greater than that hydrated at 27 °C. This difference in the porosity of cement paste was largely due to the difference in the pores with a radius in the range of 750-2300 Å

If the cement hydrates slowly, the hydration products require less time to diffuse and precipitate uniformly throughout the interstitial space, among the cement

grains. However, if the hydration is accelerated by increasing temperature there will be no uniform diffusion and sedimentation of the hydration products in the internal space between the cement grains. Consequently, the presence of a high concentrated, dense and encapsulated layer, forms an impermeable rim on the cement grains and retards subsequent hydration [22].

Knut et al. [84] reported that curing plain cement paste specimens at temperatures of 5, 20, and 50 °C resulted in increased porosity. It was more particularly effective for the pore radius in the range of 200-1000 Å. The authors compared these results with back scattered electron images and found that an increase in the temperature resulted in increased porosity, particularly for the pore radius of 2500-12,500 Å.

Cao and Detwiler [57] conducted back scattered electron imaging of cement pastes cured at elevated temperatures and reported that in the silica fume cement specimens hydrated at 23 °C, the Ca(OH)_2 was uniformly distributed. While in the slag cement paste the Ca(OH)_2 had more elongated crystalline form. Elevated temperature curing resulted in smaller and more numerous deposits of Ca(OH)_2 . They have also reported that the microstructure of pastes cured at 70 °C was more porous and less uniform than that of the paste specimens cured at 23 °C regardless

of the composition of the cement paste. The presence of additives, particularly silica fume had a pronounced effect in refining the pore structure and homogenizing the distribution of hydrates. Mangat and El-Khatib [85] reported that curing at higher temperature has a detrimental effect on the pore volume of silica fume cement paste specimens. Sellevold [53] found that steam curing at 97 °C resulted in a coarse pore structure.

The pore volume in the blast furnace slag cement mortar specimens also increased with the casting temperature. These values in the specimens cast at 20, 35, and 50 °C were 26.5, 42.5, and 48.5 mm³/g, respectively. The proportion of coarse to fine pores, however, remained the same. Therefore, it should be expected that the permeability of specimens cast at elevated temperature will not increase considerably, even though an increase in the pore volume was measured.

The pore volume in the silica fume cement mortar specimens cast at 20, 35, and 50 °C was 50.5, 49, and 53.4 mm³/g, respectively. The volume of coarse pores, in these specimens was 17.19, 26.53, and 25.73%, respectively. The increase in the volume of coarse pores, as the casting temperature increased from 20 to 35 °C indicates that the permeability of the specimens cast at the elevated temperature will be higher. These results are in agreement with the data developed by Reinhardt and Gaber [86]. They reported that at ordinary temperatures, silica fume

blended cements have greater tendency to form coarser pores. The volume of coarse pores in the mortar specimens cast at 35 °C was more or less similar to those cast at 50 °C. The effect of casting temperature on the pore volume in these specimens was not very significant.

The pore volume in the fly ash cement mortar specimens cast at 20, 35, and 50 °C was 58, 62, and 48 mm³/g, respectively. These consisted mainly of fine pores, for example the fine pores were 92, 94, and 85% of the total pore volume in the specimens cast at 20, 35, and 50 °C. The higher volume of coarser pores in the specimens cast at 50 °C, compared to the specimens cast at other temperatures indicates that the effect of elevated temperature casting in the fly ash cement mortar specimens can only be observed for temperatures as high as 50 °C.

In general, the data on pore size distribution, indicate that elevated temperature casting is not beneficial in the plain cements. Both the pore volume and the proportion of coarse pores increased with increasing casting temperature. In the blended cements, however, elevated temperature does not significantly influence the pore volume and the proportion of coarse pores. In the fly ash cement mortar specimens, the volume of coarse pores increased in the specimens cast at 50 °C, while, the total pore volume remained more or less similar.

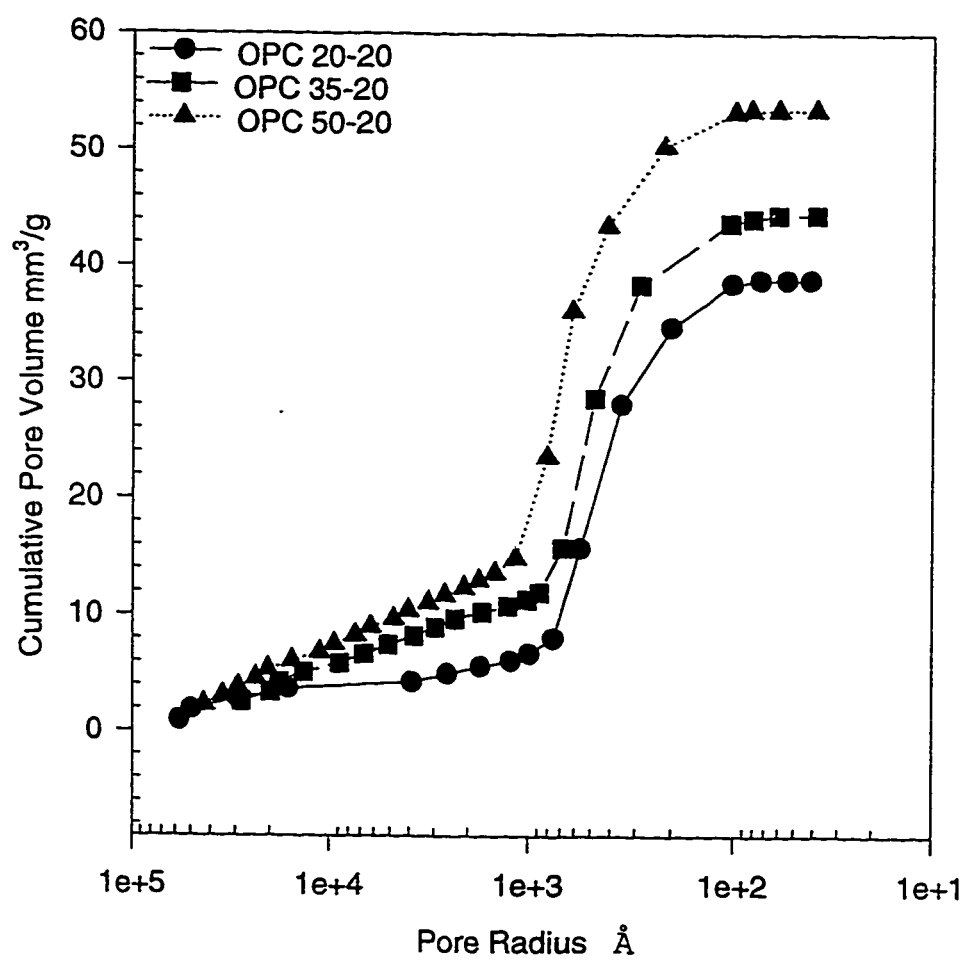


Fig. 4.49: Pore Size Distribution in the Plain Cement Mortar Specimens Cast at various Temperatures and Cured at 20 °C

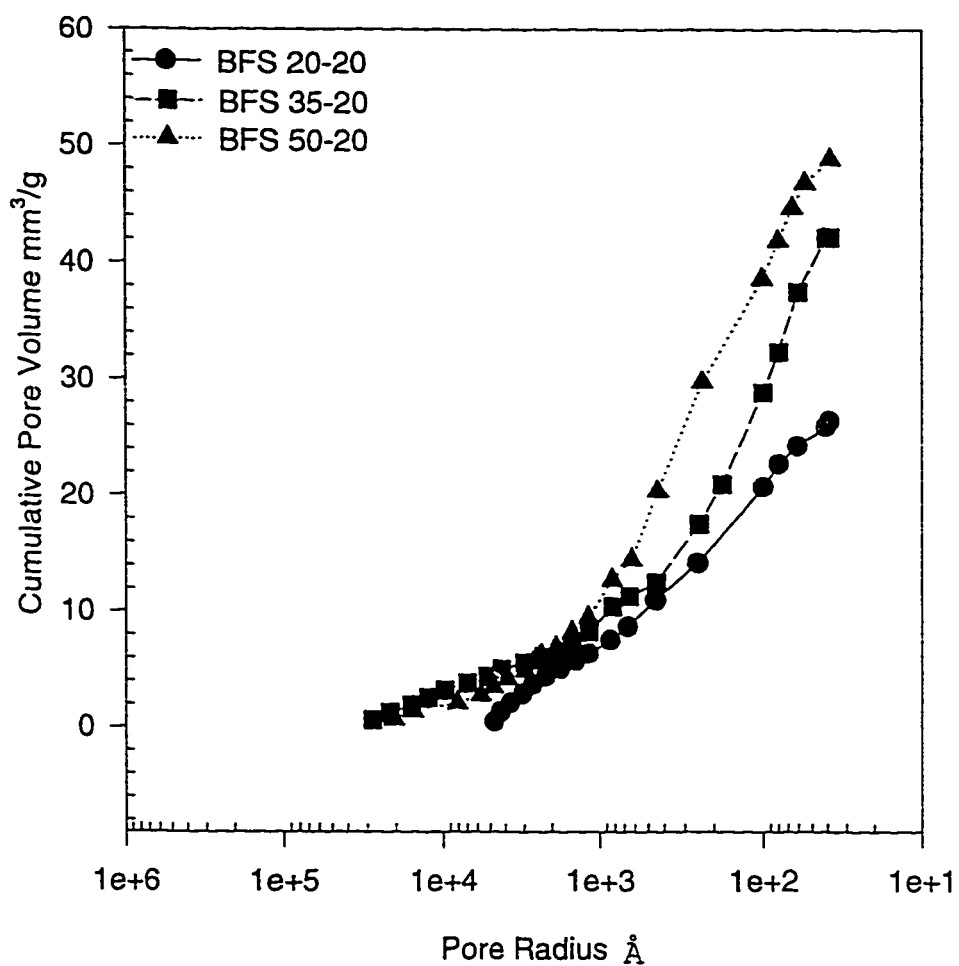


Fig. 4.50: Pore Size Distribution in the Blast Furnace Slag Cement Mortar Specimens Cast at various Temperatures and Cured at 20 °C

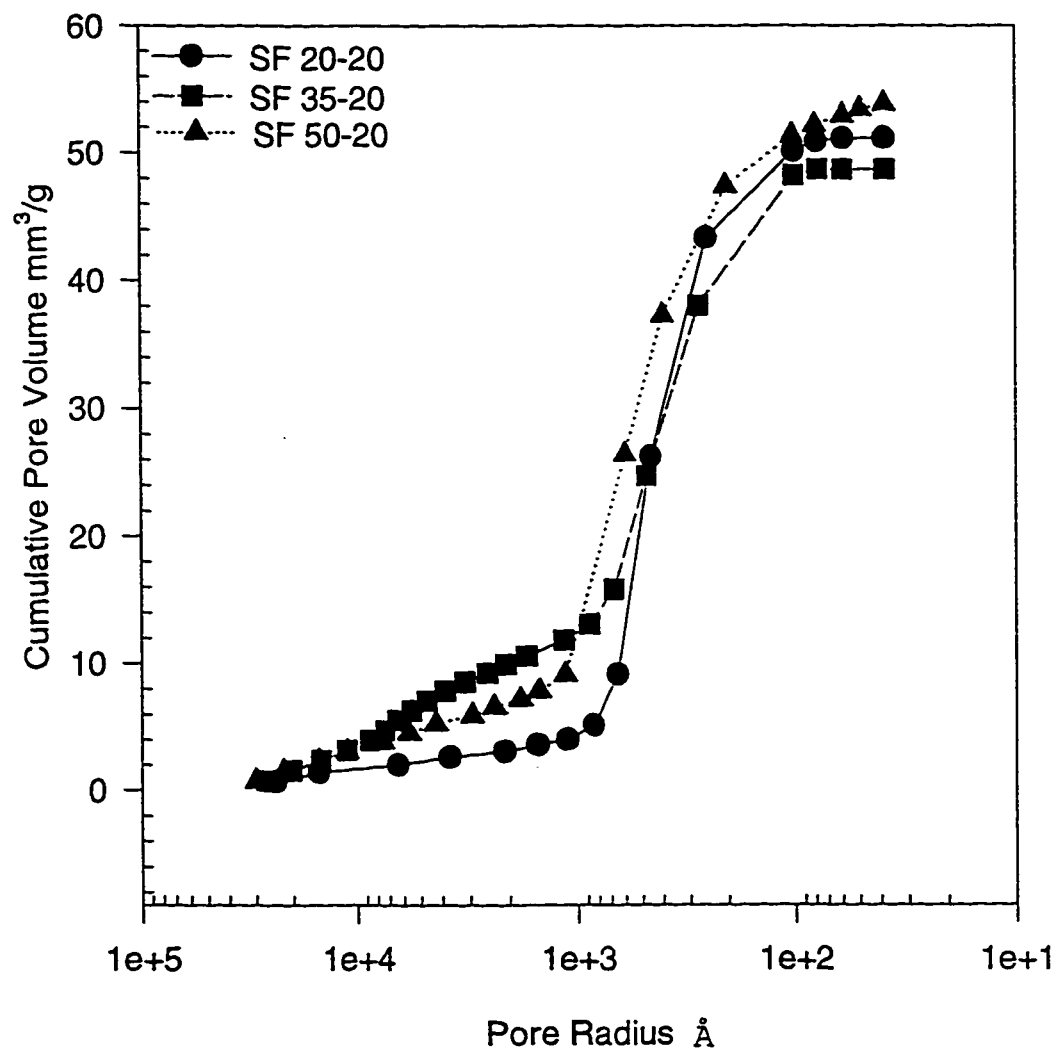


Fig. 4.51: Pore Size Distribution in the Silica Fume Cement Mortar Specimens Cast at various Temperatures and Cured at 20 °C

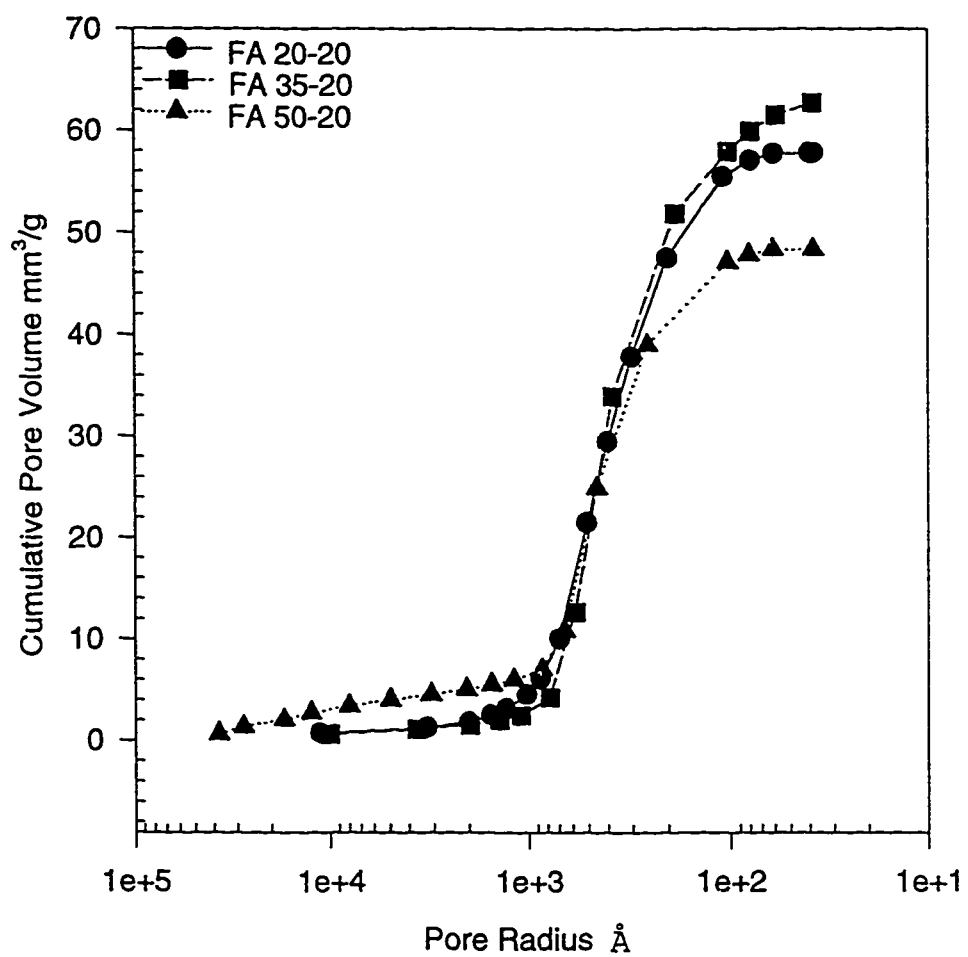


Fig. 4.52: Pore Size Distribution in the Fly Ash Cement Mortar Specimens Cast at various Temperatures and Cured at 20 °C

Table 4.1: Pore size distribution in the plain and blended cement mortar specimens

Cement	Casting Temperature (°C)*	Pore Volume mm ³ /g	Fine Pores (%)	Coarse Pores (%)
Type I	20	39	82.05	17.95
	35	44.5	73.04	26.96
	50	53.75	62.79	37.21
BFS	20	26.5	74.53	25.47
	35	42.5	78.83	21.17
	50	48.5	76.28	23.72
SF	20	50.5	82.81	17.19
	35	49	73.47	26.53
	50	53.4	74.27	25.73
FA	20	58	92.25	7.75
	35	62	94.35	5.64
	50	48	85.42	14.58

* Specimens were cured at 20 °C

4.5 EFFECT OF CASTING TEMPERATURE ON CALCIUM HYDROXIDE CONTENT IN PLAIN AND BLENDED CEMENTS

The effect of casting temperature on the calcium hydroxide Ca(OH)_2 content in the plain and blended cement mortars cast at 20, 35, and 50 °C and cured at 20 °C was determined using DTA/TG technique. For this purpose, mortar retrieved from concrete specimens cured for 28 days was utilized. Figures 4.53 through 4.64 show the DTA and TG curves for the plain and blended cements. The endothermic peaks at about 350 to 450 °C indicate the dehydration of Ca(OH)_2 resulting in the formation of CaO . The endothermic peak at 650 °C corresponds to the phase transformation from CaCO_3 to CaO , resulting in the liberation of CO_2 . The TGA curves were used to calculate the weight change due to the transformation of Ca(OH)_2 to CaO and similarly CaCO_3 to CaO . These weight changes were used to calculate the quantities of Ca(OH)_2 and CaCO_3 , respectively. These values are summarized in Table 4.2.

The data in Table 4.2 indicate that the quantity of Ca(OH)_2 in the plain cement was more than that in the blended cement mortar specimens. This may be attributed to the consumption of Ca(OH)_2 by the pozzolanic reaction. An increase in the Ca(OH)_2 content was noticed, in the plain cement when the casting temperature was increased from 20 to 35 °C. However, a further increase in the casting temperature to 50 °C indicated a decrease in the Ca(OH)_2

content. These results predict that at low temperatures of up to 35 °C the hydration products diffuse uniformly throughout the interstitial space among the cement grains and as a result, there is an increase in the quantity of Ca(OH)_2 . However, with further increase in temperature improper sedimentation of the hydration products takes place as a result further cement hydration is inhibited. The quantity of Ca(OH)_2 in the plain cement mortars cast at 20, 35, and 50 °C was 4.79, 4.97, and 3.62%, by weight of cement mortar, respectively.

The quantity of Ca(OH)_2 in the blended cement mortar specimens was less than that in the plain cement mortar specimens, it was the least in blast furnace slag cement mortar specimens. While no Ca(OH)_2 was detected in the blast furnace slag cement concrete specimens cast at 20 and 35 °C, it was 2.65% in the specimens cast at 50 °C. The higher Ca(OH)_2 in the blast furnace slag cement specimens cast at 50 °C may be attributed to the increase in the hydration in this cement. The quantity of Ca(OH)_2 in the silica fume and fly ash cement mortar specimens was less than that in the plain cements. This may be attributed to its consumption in the pozzolanic reaction. However, the data reveal that there was a slight increase in the weight of Ca(OH)_2 with an increase in the casting temperature in both of these cements. The weight of Ca(OH)_2 in the silica fume cement mortar specimens cast at 20, 35, and 50 °C was 2.36, 3.23, and 3.64%, respectively, while in the fly ash cement concrete it was 2.78, 3.1, and 3.27%, respectively.

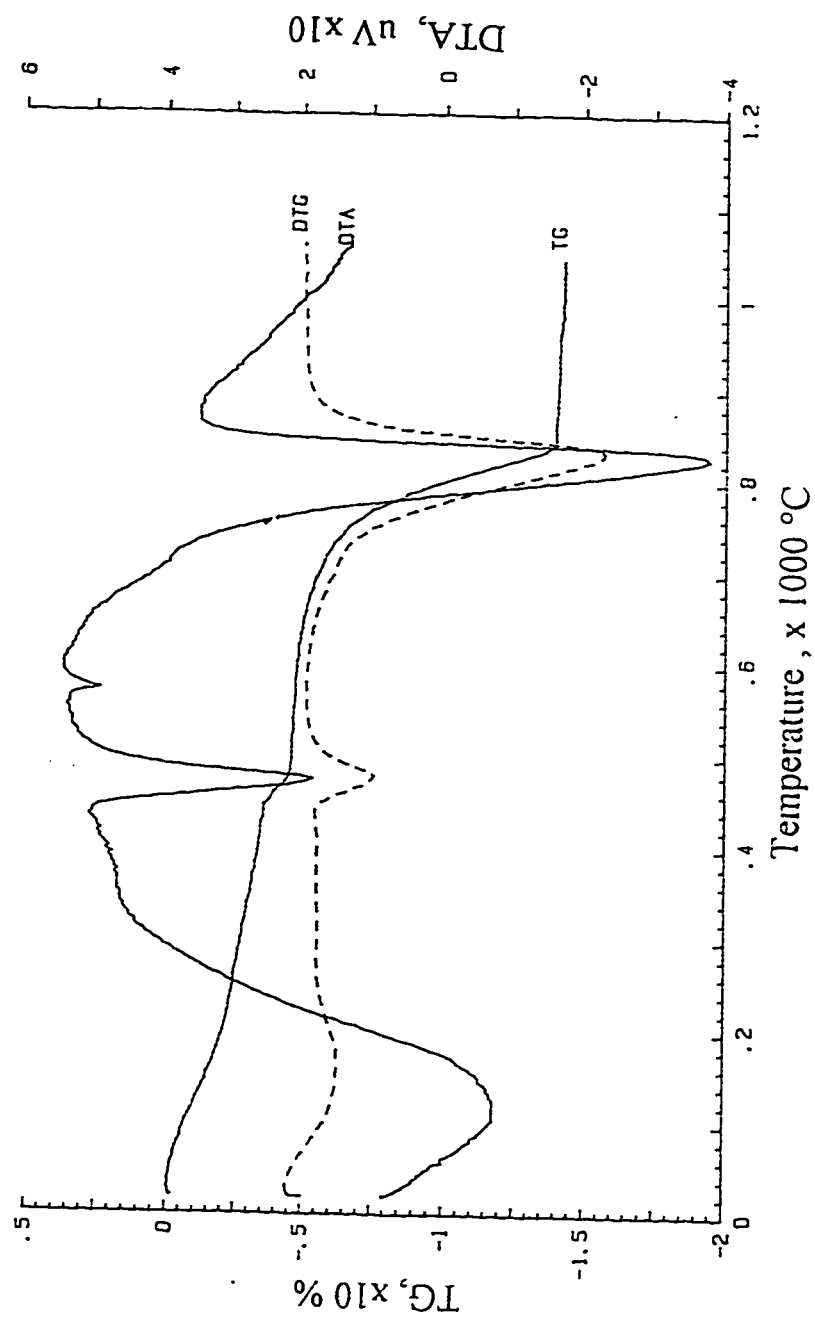


Fig. 4.53: Effect of Casting Temperature on the Ca(OH)_2 Content in the Plain Cement Mortar Specimens Cast and Cured at $20\text{ }^{\circ}\text{C}$

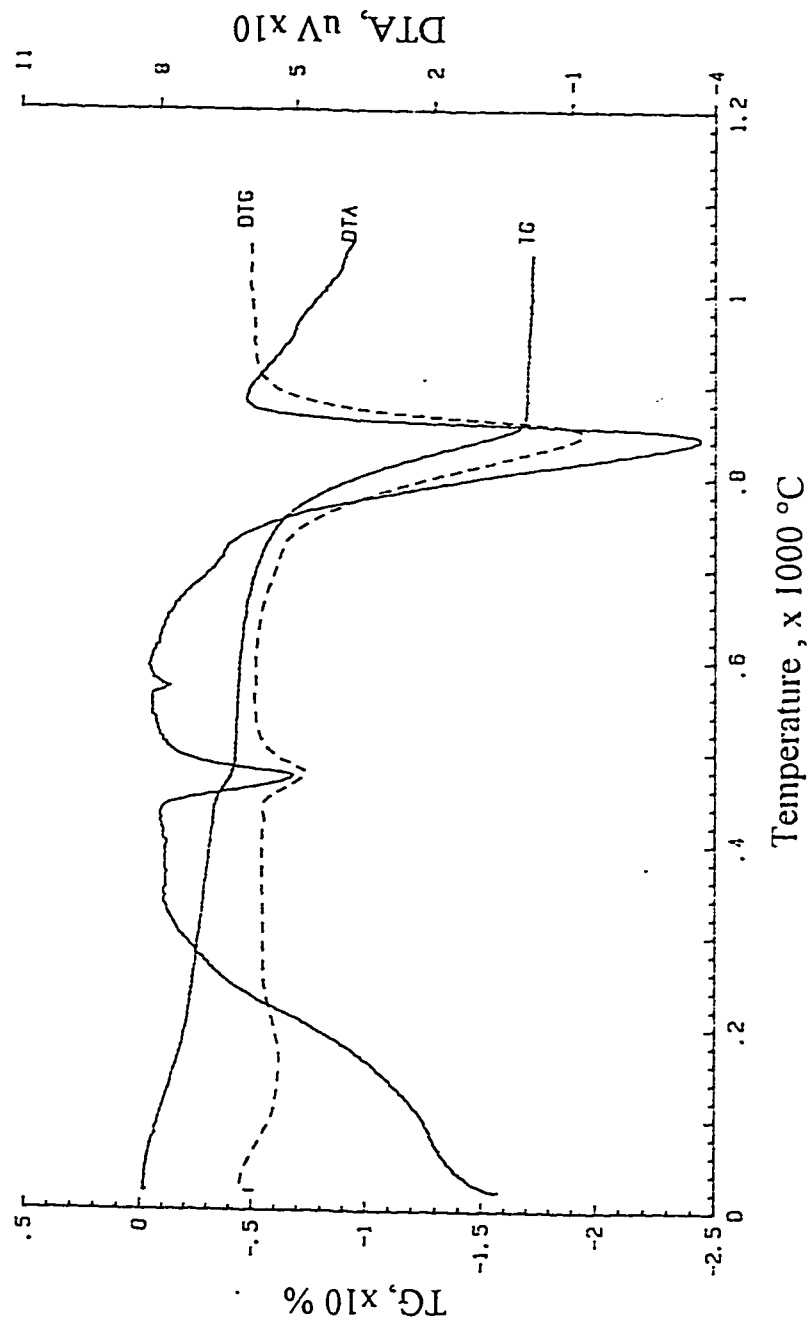


Fig. 4.54: Effect of Casting Temperature on the $\text{Ca}(\text{OH})_2$ Content in the Plain Cement Mortar Specimens Cast at 35 $^{\circ}\text{C}$ and Cured at 20 $^{\circ}\text{C}$

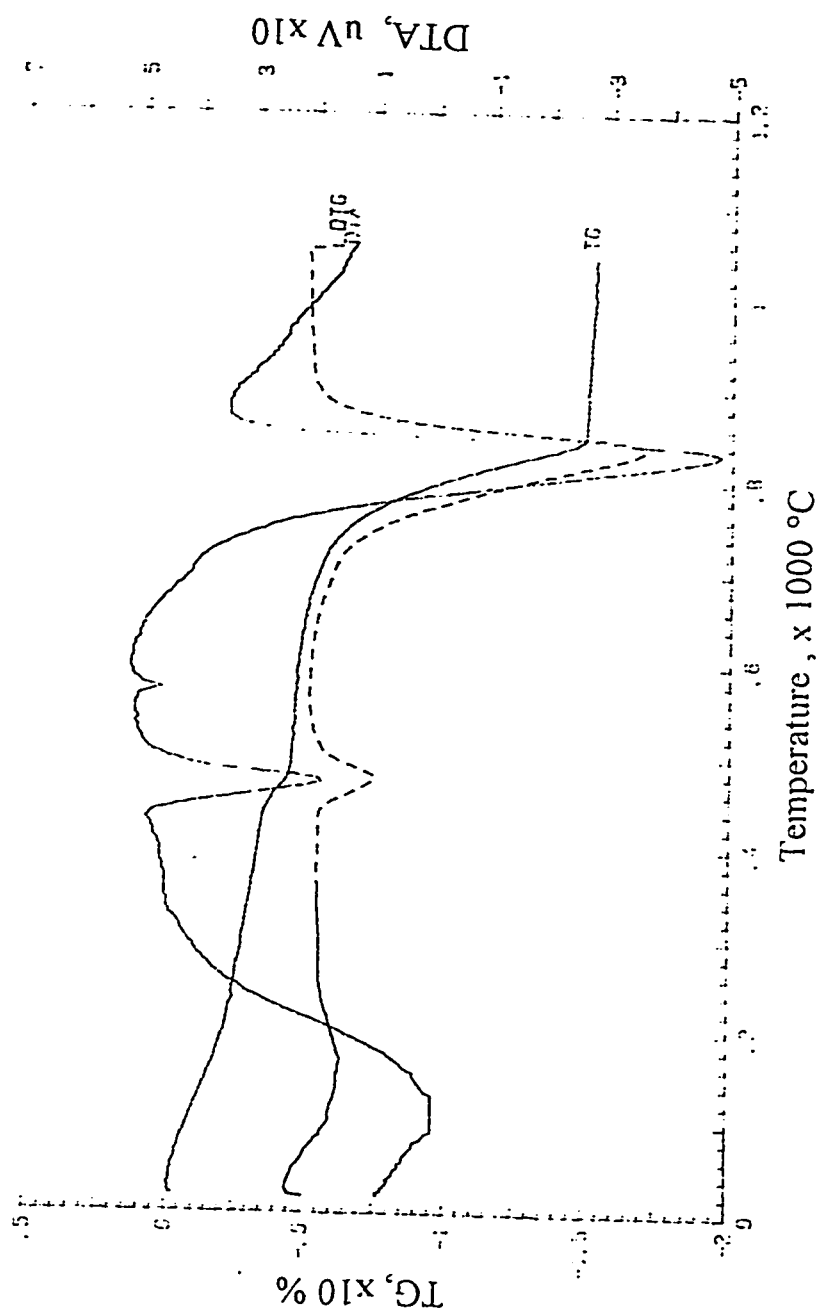


Fig. 4.55: Effect of Casting Temperature on the $\text{Ca}(\text{OH})_2$ Content in the Plain Cement Mortar Specimens Cast at $50\text{ }^{\circ}\text{C}$ and Cured at $20\text{ }^{\circ}\text{C}$

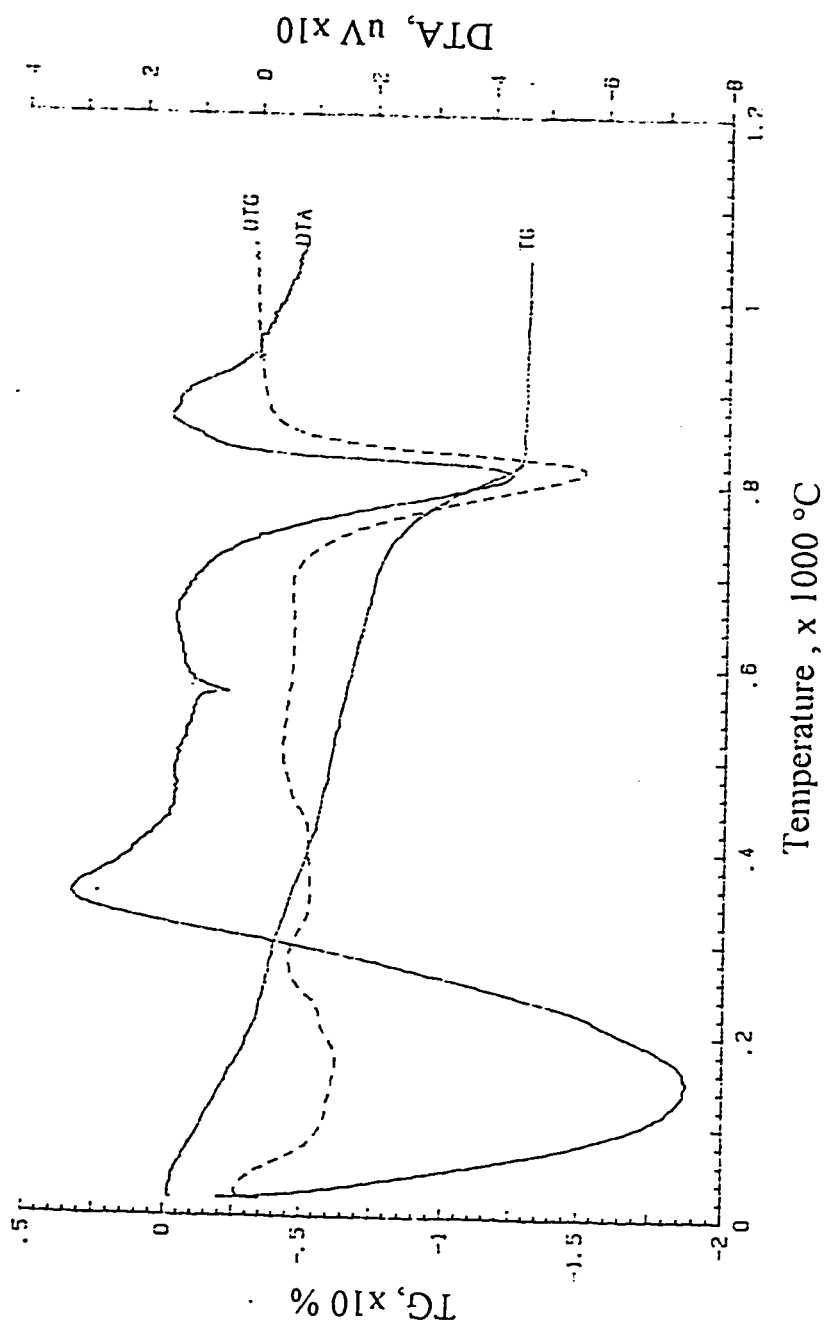


Fig. 4.56: Effect of Casting Temperature on the $\text{Ca}(\text{OH})_2$ Content in the Blast Furnace Slag Cement Mortar Specimens Cast and Cured at $20\text{ }^{\circ}\text{C}$

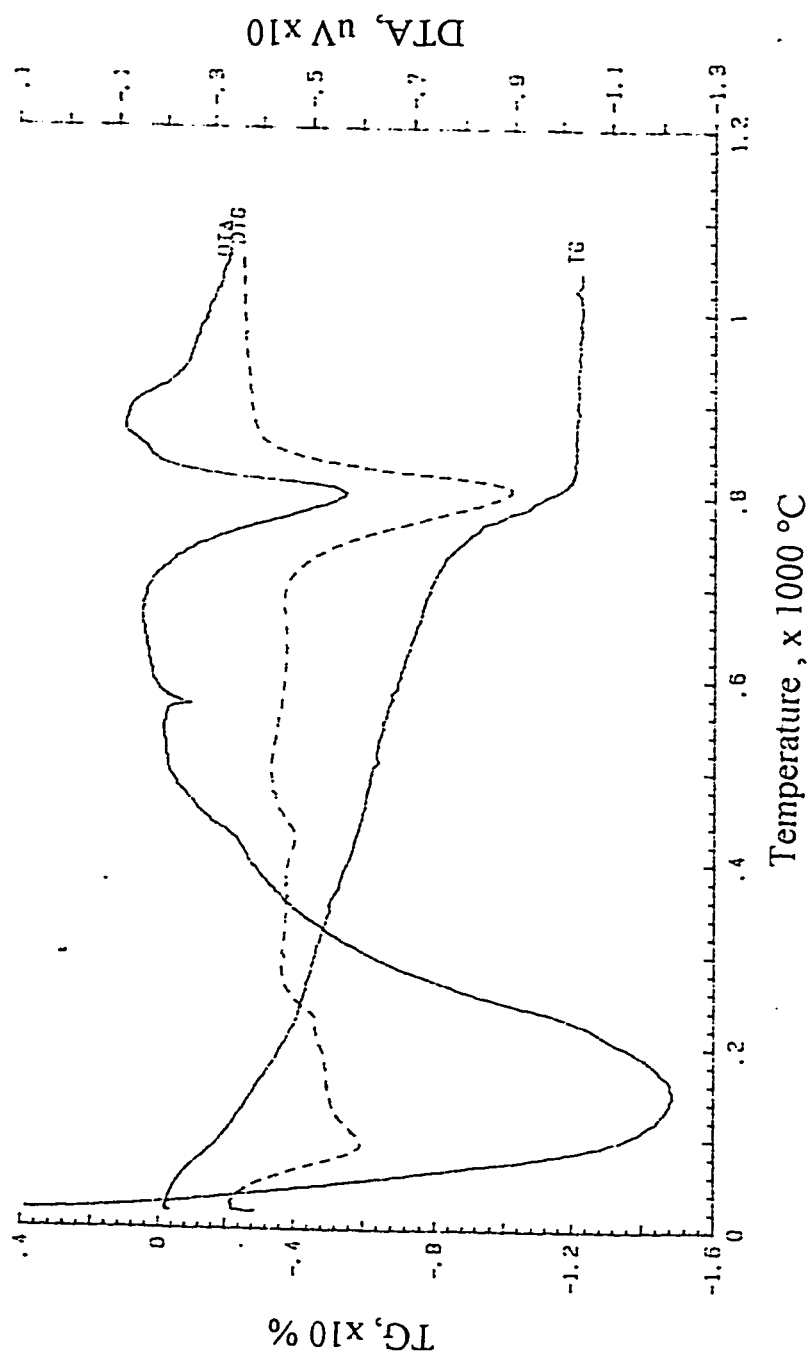


Fig. 4.57: Effect of Casting Temperature on the Ca(OH)_2 Content in the Blast Furnace Slag Cement Mortar Specimens Cast at 35 °C and Cured at 20 °C

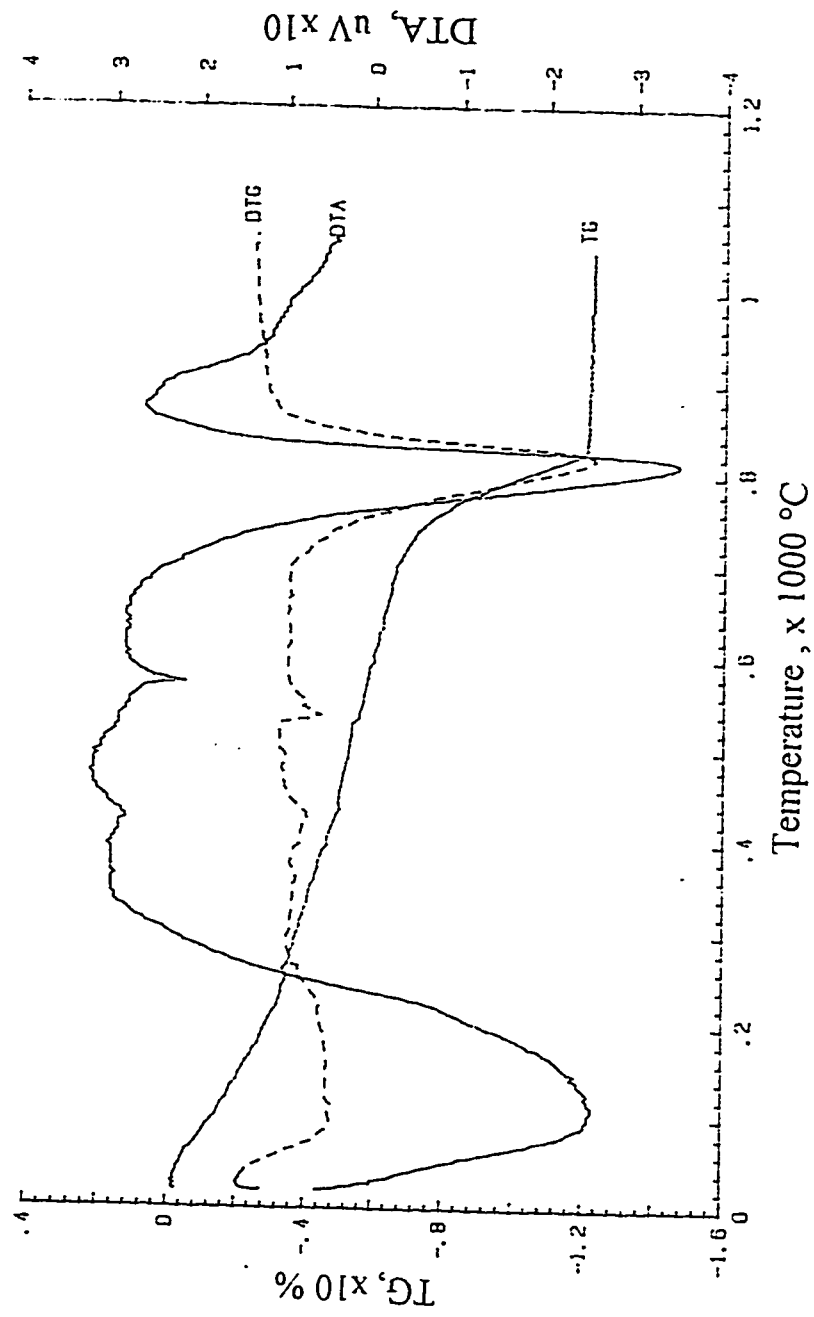


Fig. 4.58: Effect of Casting Temperature on the $\text{Ca}(\text{OH})_2$ Content in the Blast Furnace Slag Cement Mortar Specimens Cast at 50 °C and Cured at 20 °C

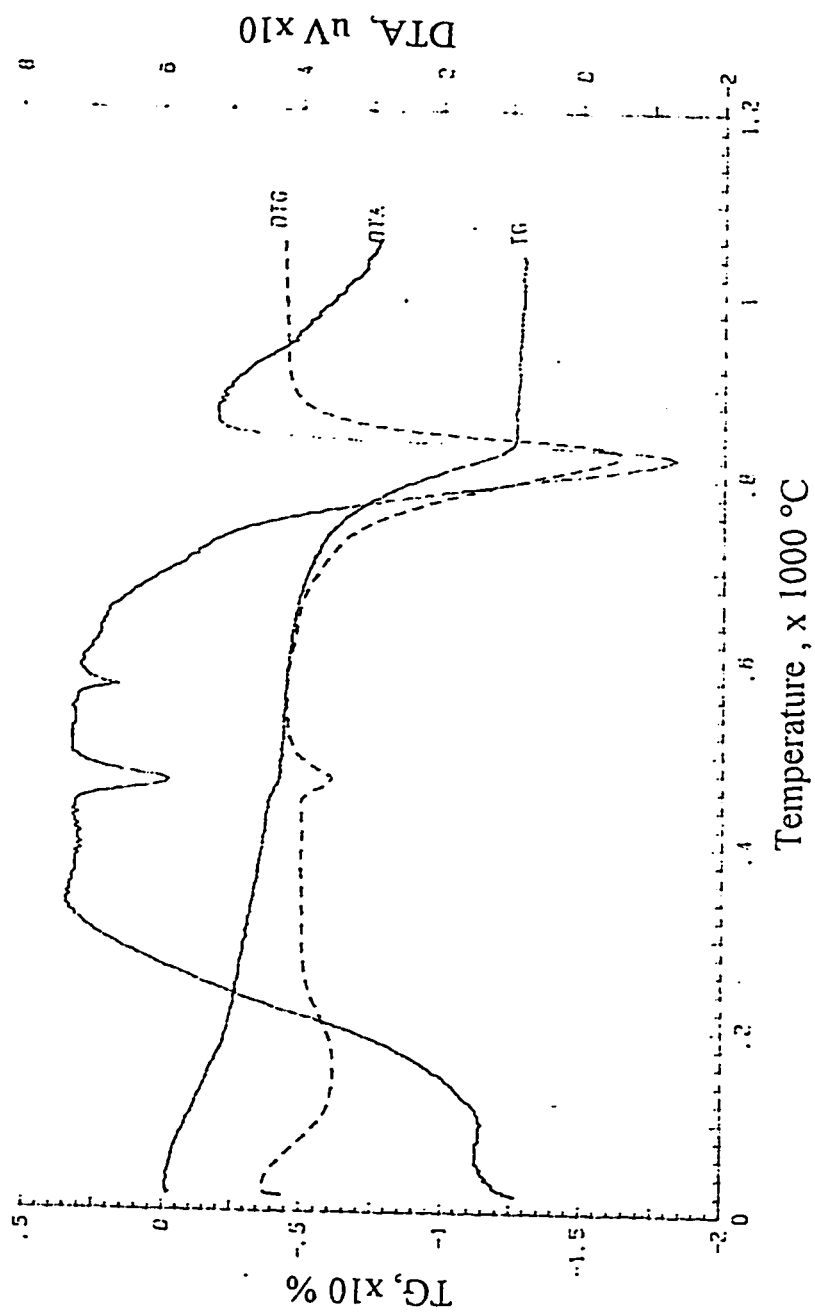


Fig. 4.59: Effect of Casting Temperature on the Ca(OH)_2 Content in the Silica Fume Cement Mortar Specimens Cast and Cured at 20 °C

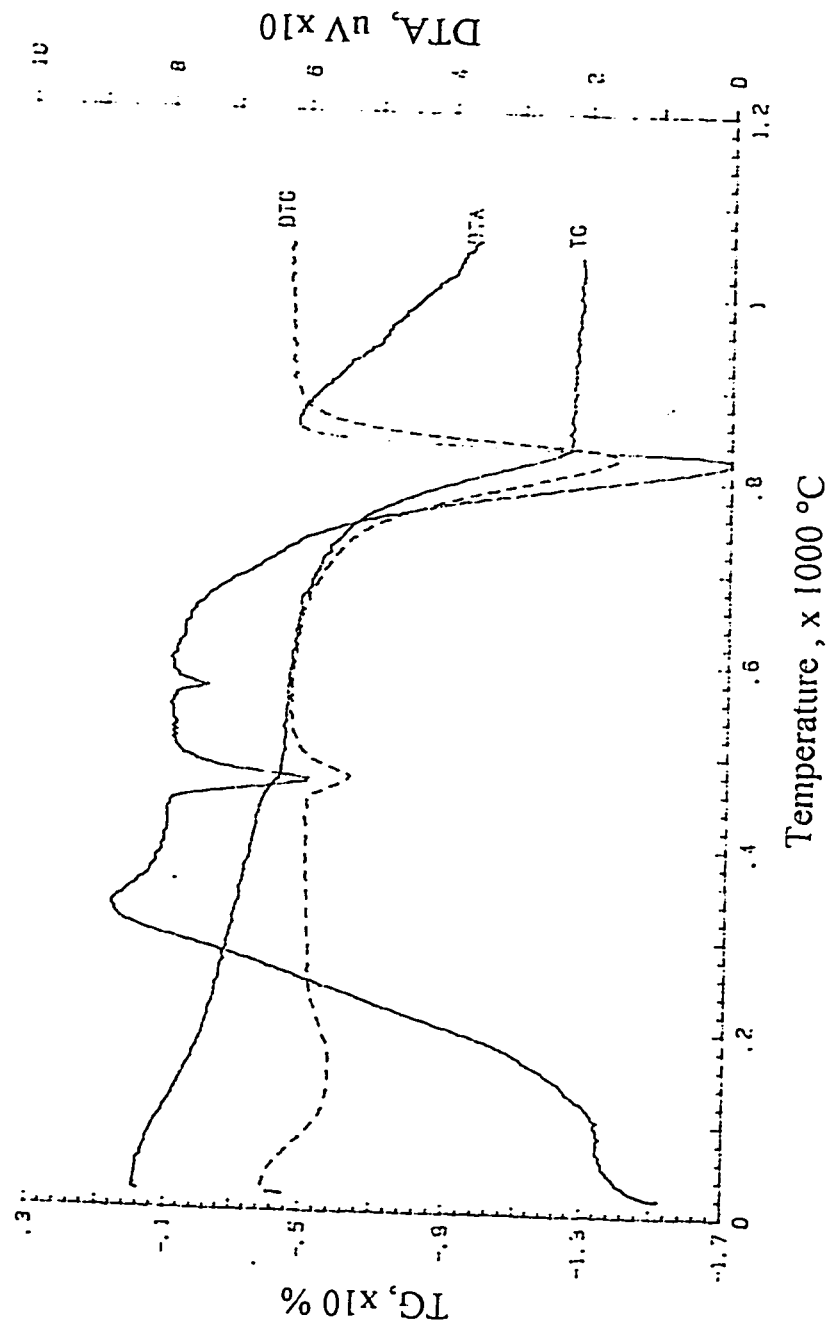


Fig. 4.60: Effect of Casting Temperature on the $\text{Ca}(\text{OH})_2$ Content in the Silica Fume Cement Mortar Specimens Cast at 35 °C and Cured at 20 °C

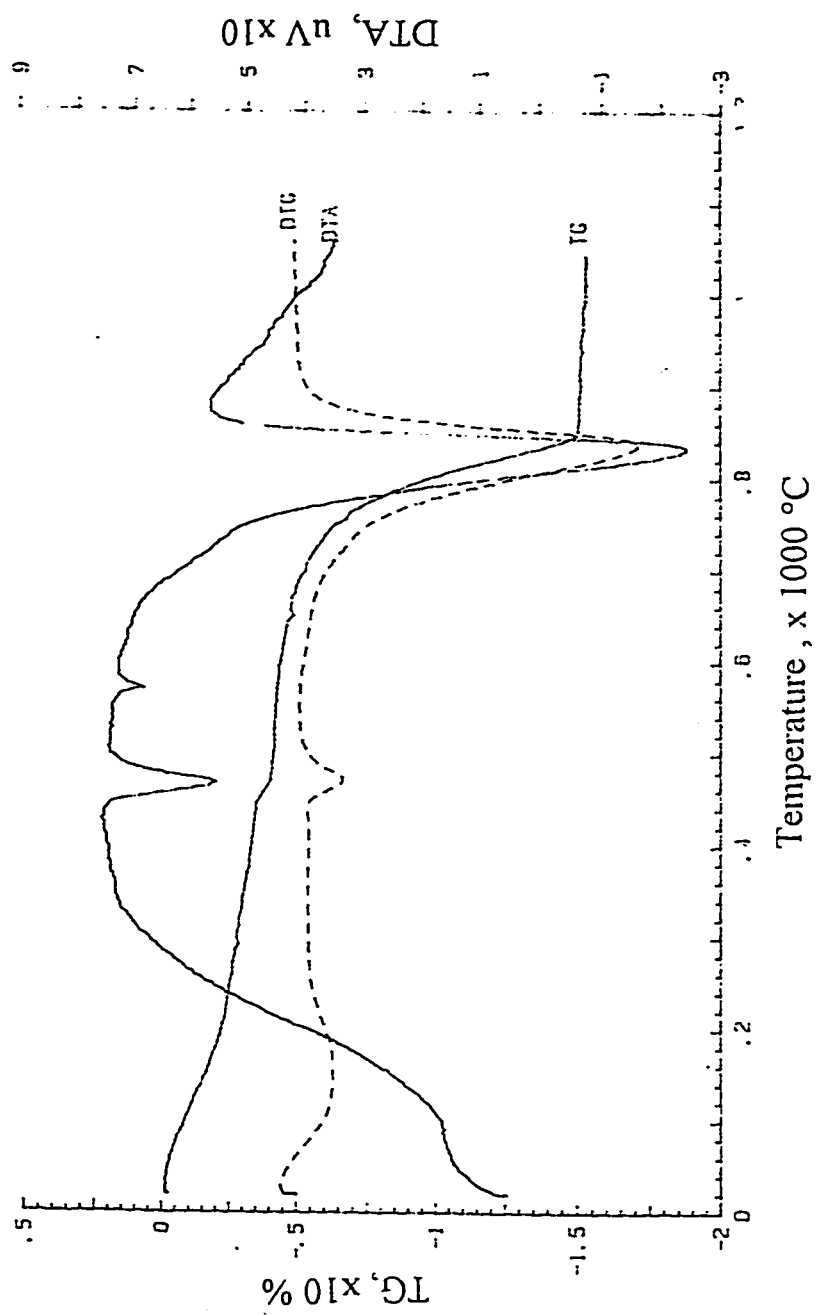


Fig. 4.61: Effect of Casting Temperature on the $\text{Ca}(\text{OH})_2$ Content in the Silica Fume Cement Mortar Specimens Cast at 50 °C and Cured at 20 °C

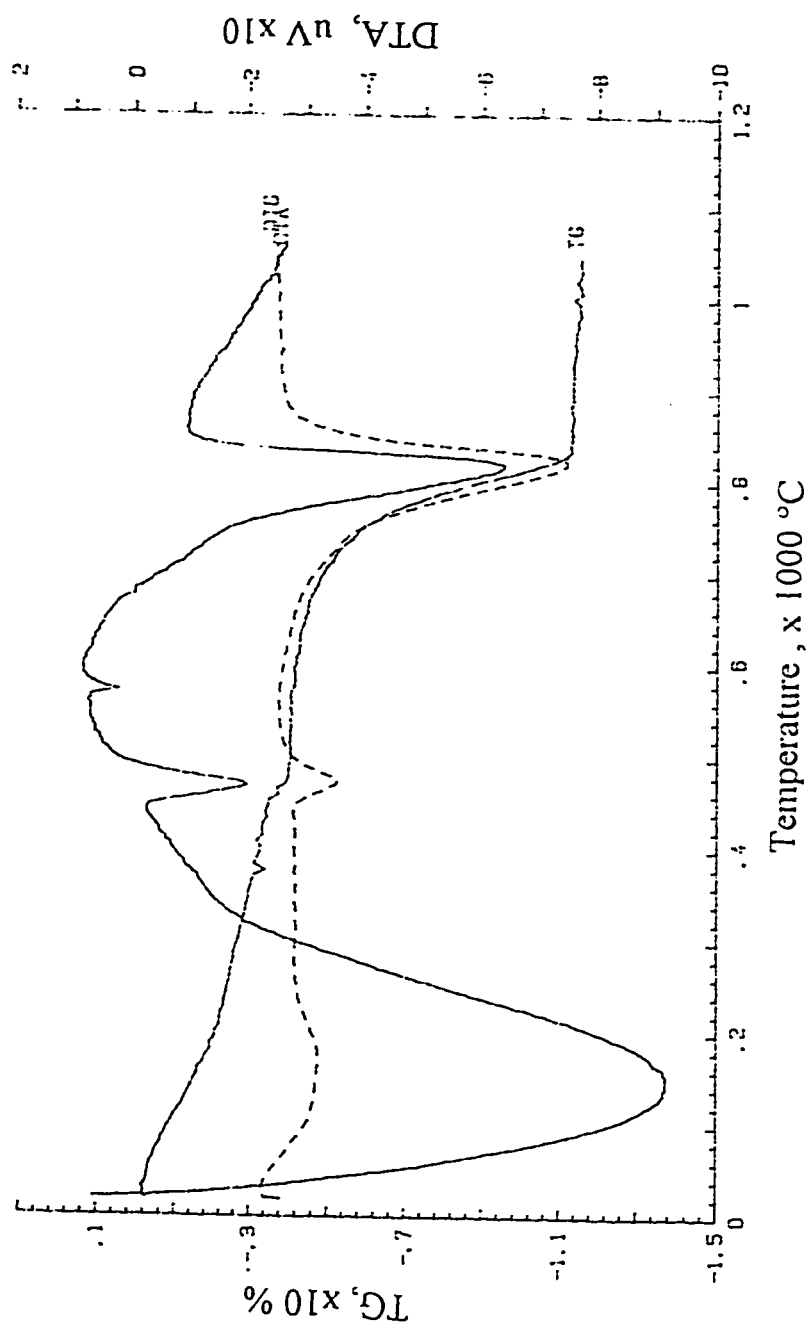


Fig. 4.62: Effect of Casting Temperature on the $\text{Ca}(\text{OH})_2$ Content in the Fly Ash Cement Mortar Specimens Cast and Cured at $20\text{ }^{\circ}\text{C}$

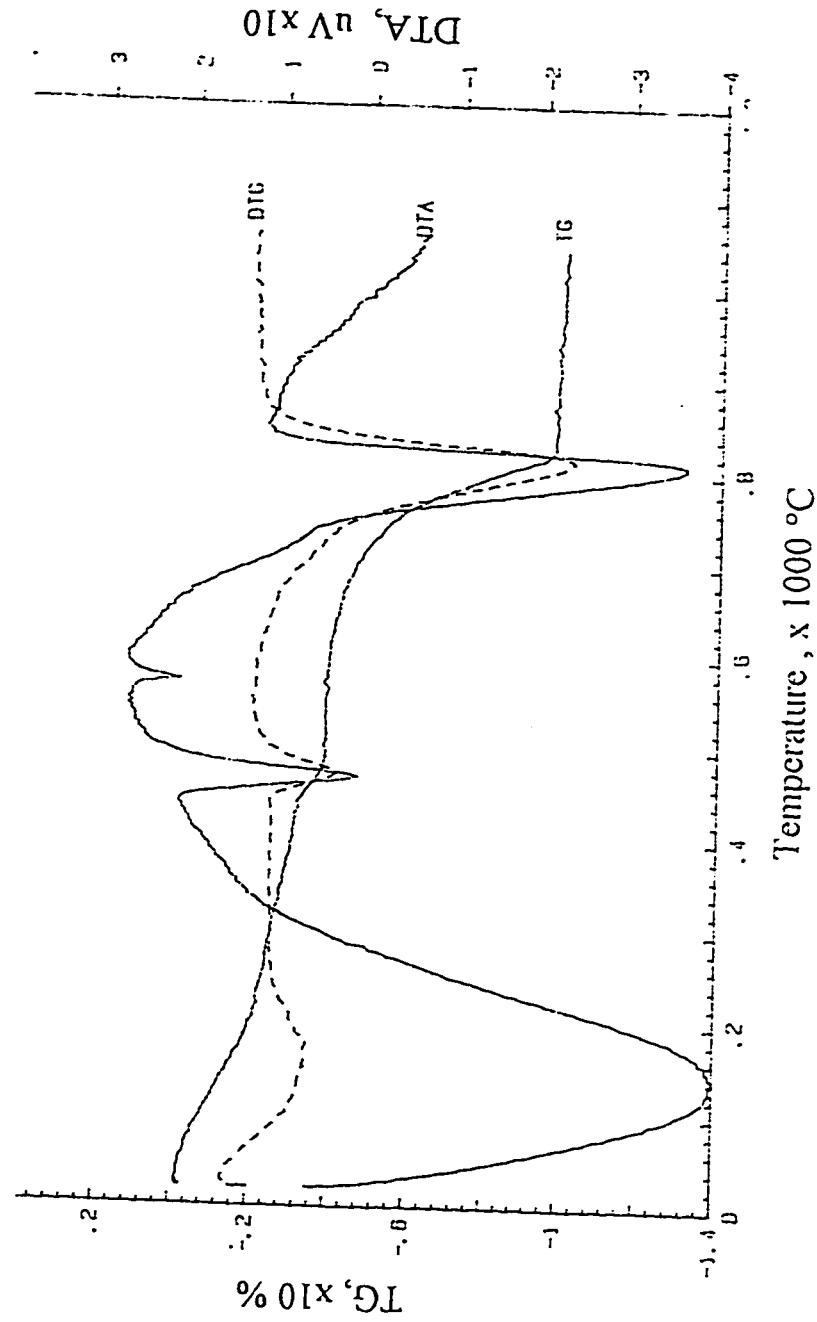


Fig. 4.63: Effect of Casting Temperature on the $\text{Ca}(\text{OH})_2$ Content in the Fly Ash Cement Mortar Specimens Cast at 35 °C and Cured at 20 °C

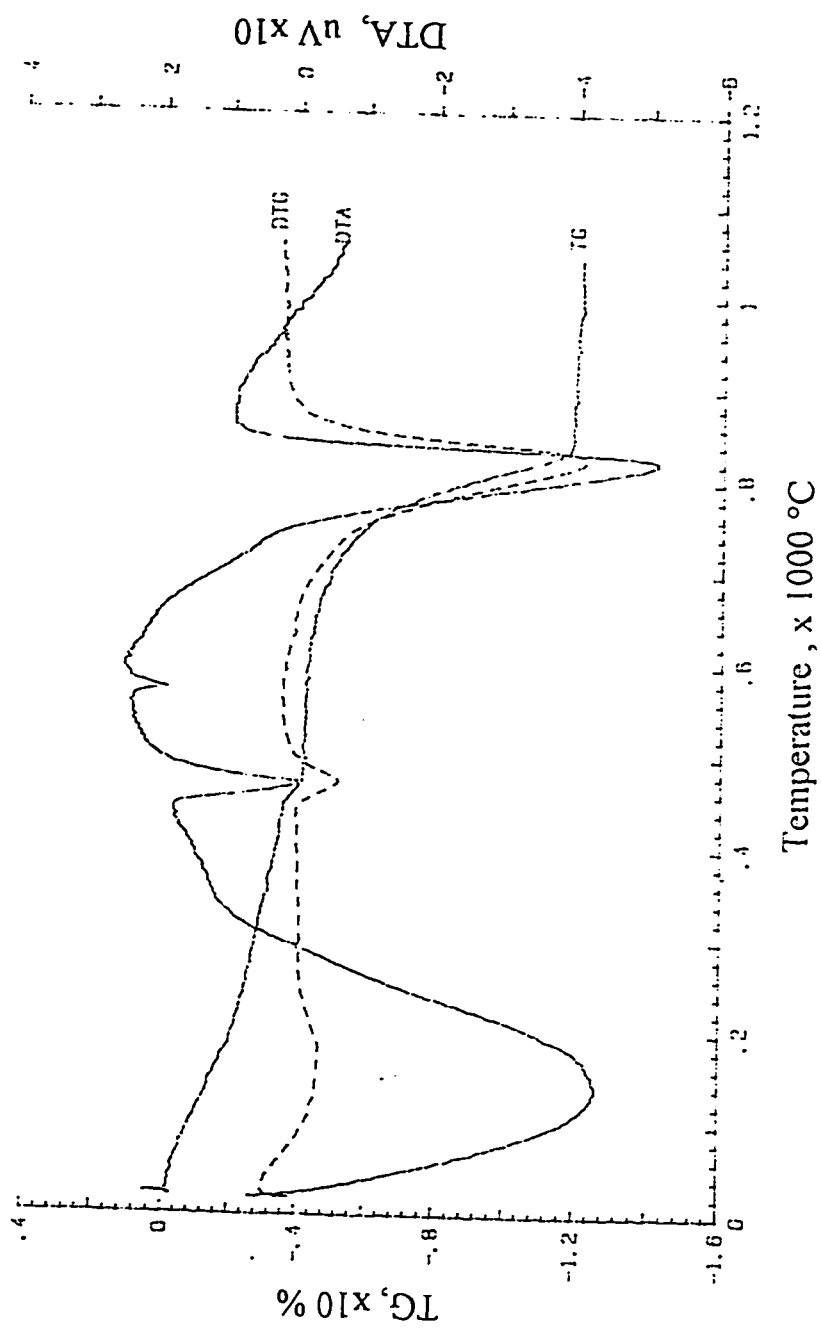


Fig. 4.64: Effect of Casting Temperature on the $\text{Ca}(\text{OH})_2$ Content in the Fly Ash Cement Mortar Specimens Cast at $50\text{ }^{\circ}\text{C}$ and Cured at $20\text{ }^{\circ}\text{C}$

Table 4.2: Calcium hydroxide content in the plain and blended cement mortar specimens

Cement	Casting Temperature (°C) *	Ca(OH)₂ % weight of mortar
Type I	20	4.79
	35	4.97
	50	3.62
BFS	20	---
	35	---
	50	2.65
SF	20	2.36
	35	3.23
	50	3.64
FA	20	2.78
	35	3.10
	50	3.27

* Specimens were Cured at 20 °C

4.6 EFFECT OF CASTING TEMPERATURE ON THE MINERALOGICAL COMPOSITION IN PLAIN AND BLENDED CEMENTS

Plain and blended cement mortar specimens cast at 20, 35, and 50 °C and cured at 20 °C were used to evaluate the effect of casting temperature on their mineralogical composition.

Figures 4.65 through 4.67 show the X-ray diffractograms for the plain cement mortar specimens cast at 20 to 50 °C and cured at 20 °C. The main compounds detected were Quartz, Portlandite [Ca(OH)_2], Calcium Silicate Hydrate (C-S-H), and Calcite (CaCO_3). The quantity of C-S-H formed in the mortar specimens cast at 35 and 50 °C was more than that detected in the specimens cast at 20 °C. The X-ray diffractograms for the blast furnace slag cement mortar specimens are shown in Figures 4.68 through 4.70. Quartz, C-S-H, and Calcite were the main compounds discerned in these specimens. Again, the quantity of C-S-H formed in the specimens cast at 35 and 50 °C was more than that in the specimens cast at 20 °C. As expected, the X-ray peaks for portlandite were not detected in these specimens. Furthermore, formation of calcite in the absence of portlandite can be attributed to the carbonation of C-S-H. Figures 4.71 through 4.73 show the X-ray diffractograms for the silica fume cement mortar specimens cast at 20 to 50 °C. The main compounds detected were Quartz, Portlandite, C-S-H, and Calcite. The

quantity of C-S-H in the specimens cast at 35 °C was more than those cast at 20 and 50 °C.

The X-ray diffractograms for the fly ash cement concrete specimens cast at 20 to 50 °C and cured at 20 °C are shown in Figures 4.74 through 4.76. The main compounds detected in these specimens were Quartz, Portlandite, C-S-H and Calcite. The quantity of C-S-H in the specimens cast at 20 and 35 °C was more than that in the specimens cast at 50 °C. Table 4.3 shows the approximate weight fraction of mineralogical phases present in various cement mortars.

4.6.1 Effect of Casting Temperature on the Transition Zone

The ratio of peak intensity of calcium hydroxide at a bragg angle of 18.1° [20] (I_{001}) and 36.2° [20] (I_{101}) is often utilized to evaluate the orientation of calcium hydroxide at the aggregate-mortar interface [87]. A value of this ratio of more than one indicates that the orientation of the transition zone is parallel to the plain of the aggregate. The (I_{001}/I_{101}) values for the plain and blended cement concrete specimens cast at various temperatures are shown in Table 4.4. These results show that an increase in the casting temperature decreases the peak intensity of portlandite. The orientation ratio in the plain cement mortar specimens cast at 20, 35, and 50 °C was 1.19, 0.76, and 0.73, respectively. Therefore, preferred

orientation of the Ca(OH)_2 at the interfacial zone was observed in the concrete specimens cast and cured at 20 °C and the orientation of the Ca(OH)_2 was less preferred in the specimens cast at 35 and 50 °C.

Since Calcium hydroxide could not be detected in the blast furnace slag cement concrete specimens, the orientation of the interfacial zone could not be determined.

In the silica fume cement mortar specimens the ratio of peak intensities of calcium hydroxide was similar at all the casting temperatures and less preferentially oriented. Another reason for such a behavior may be the consumption of Ca(OH)_2 due to the pozzolanic reaction.

In the fly ash cement mortar specimens the ratio of peak intensity of Ca(OH)_2 in the specimens cast at 20 and 35 °C was 0.86 and 0.74, respectively. However, this ratio was 1.16 in the specimens cast at 50 °C which indicates that orientation of calcium hydroxide is highly preferential in these specimens at elevated temperatures.

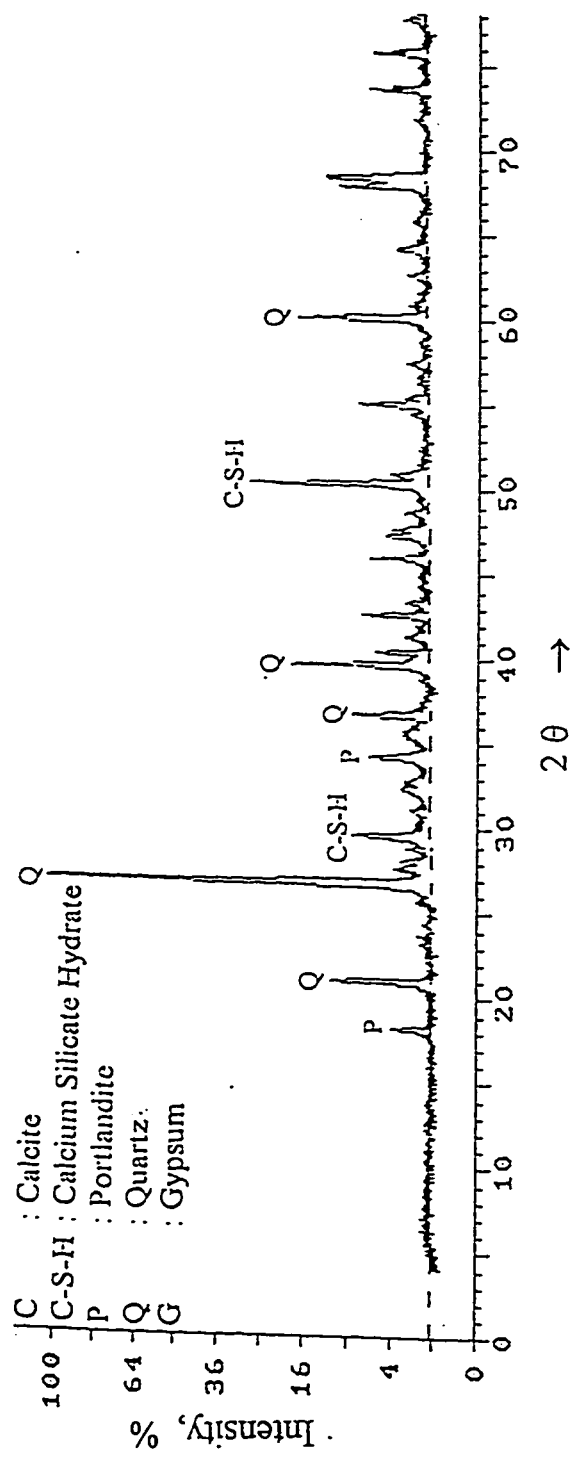


Fig. 4.65: Effect of Casting Temperature on the X-ray Diffraction in the Plain Cement Mortar Specimens Cast and Cured at 20 °C

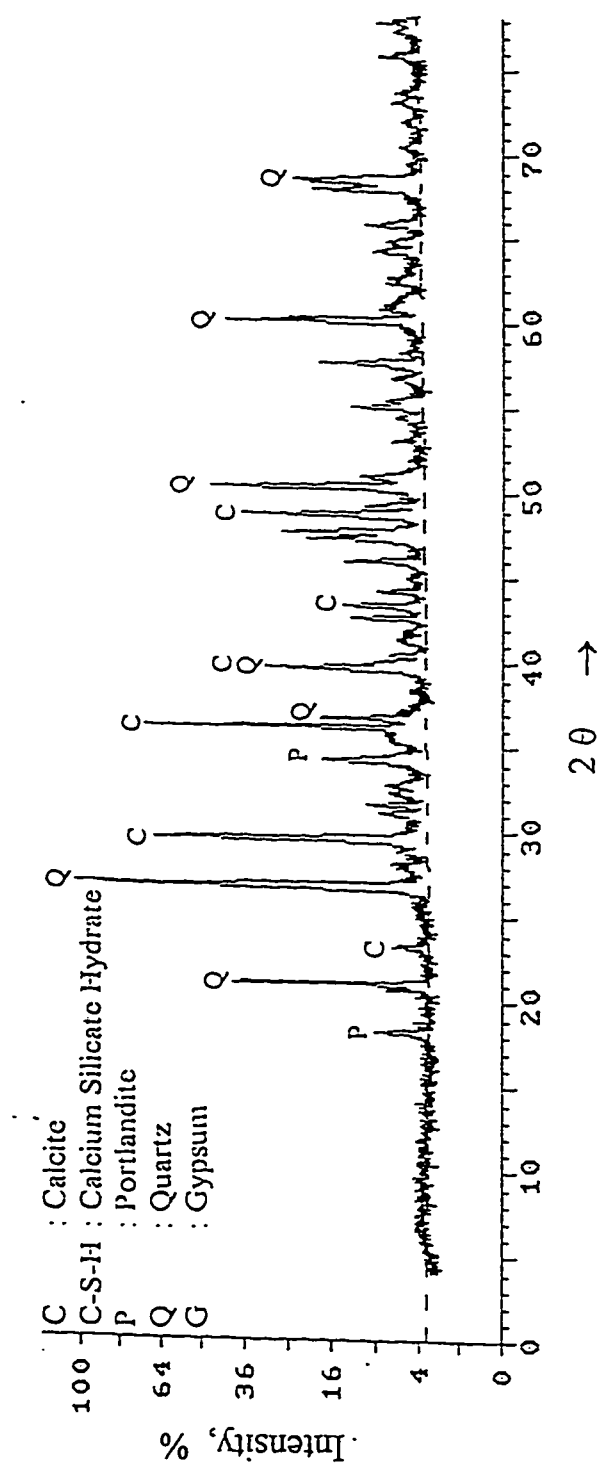


Fig. 4.66: Effect of Casting Temperature on X-ray Diffraction in the Plain Cement Mortar Specimens Cast at 35 °C and Cured at 20 °C

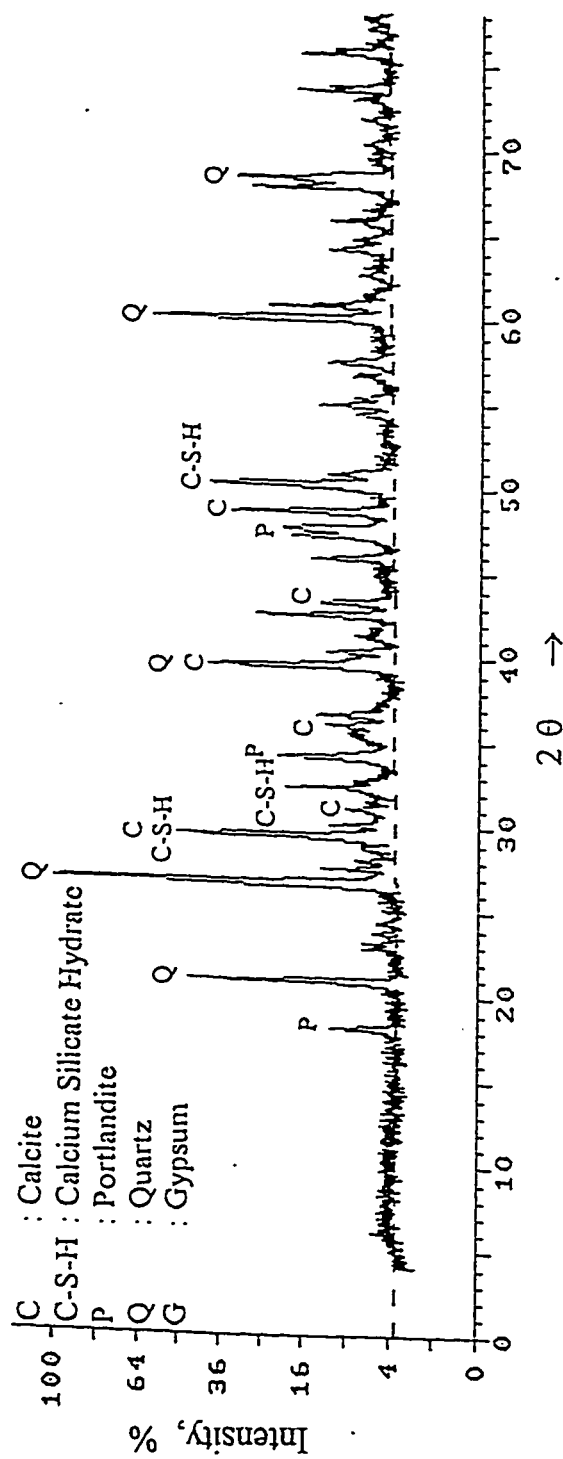


Fig. 4.67: Effect of Casting Temperature on X-ray Diffraction in the Plain Cement Mortar Specimens Cast at 50 °C and Cured at 20 °C

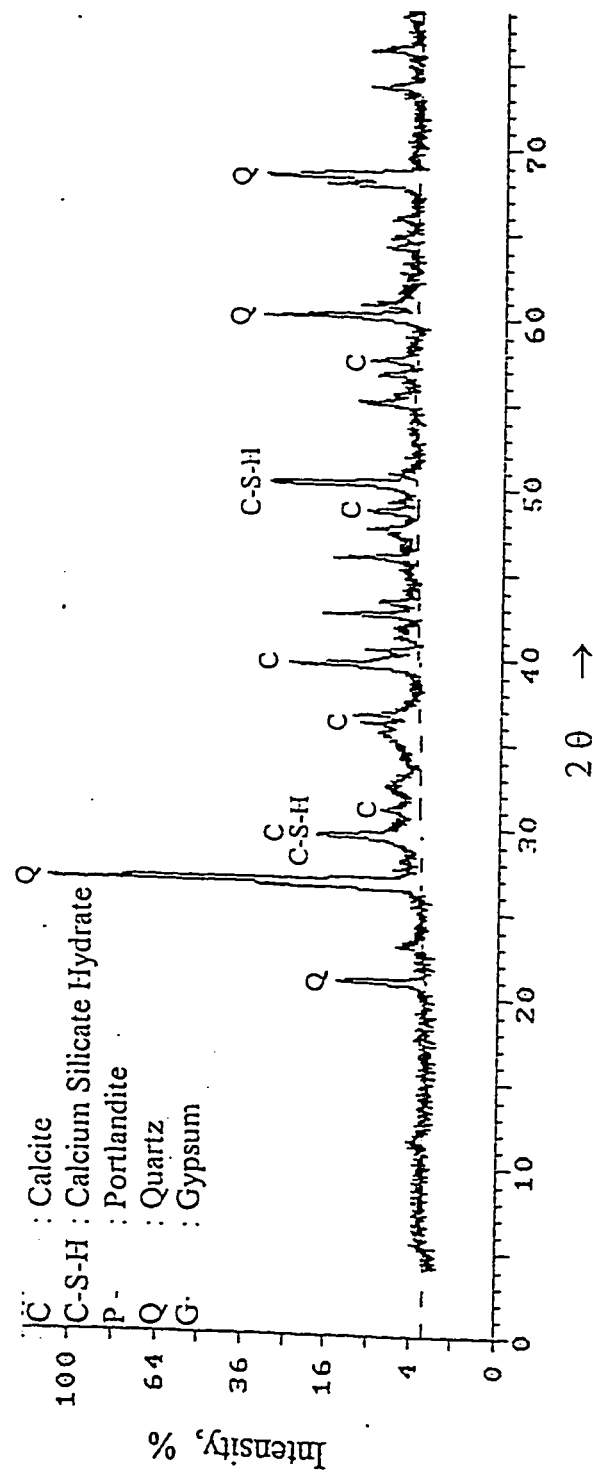


Fig. 4.68: Effect of Casting Temperature on X-ray Diffraction in the Blast Furnace Slag Cement Mortar Specimens Cast and Cured at 20 °C

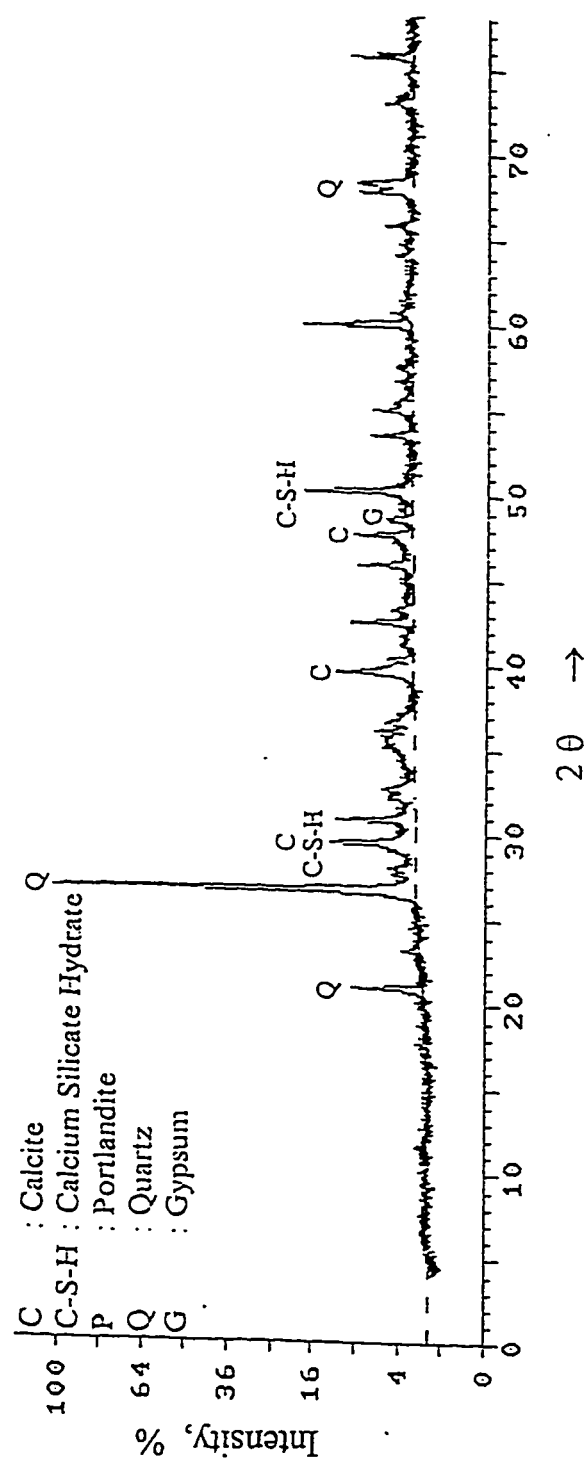


Fig. 4.69: Effect of Casting Temperature on X-ray Diffraction in the Blast Furnace Slag Cement Mortar Specimens
Cast at 35 °C and Cured at 20 °C

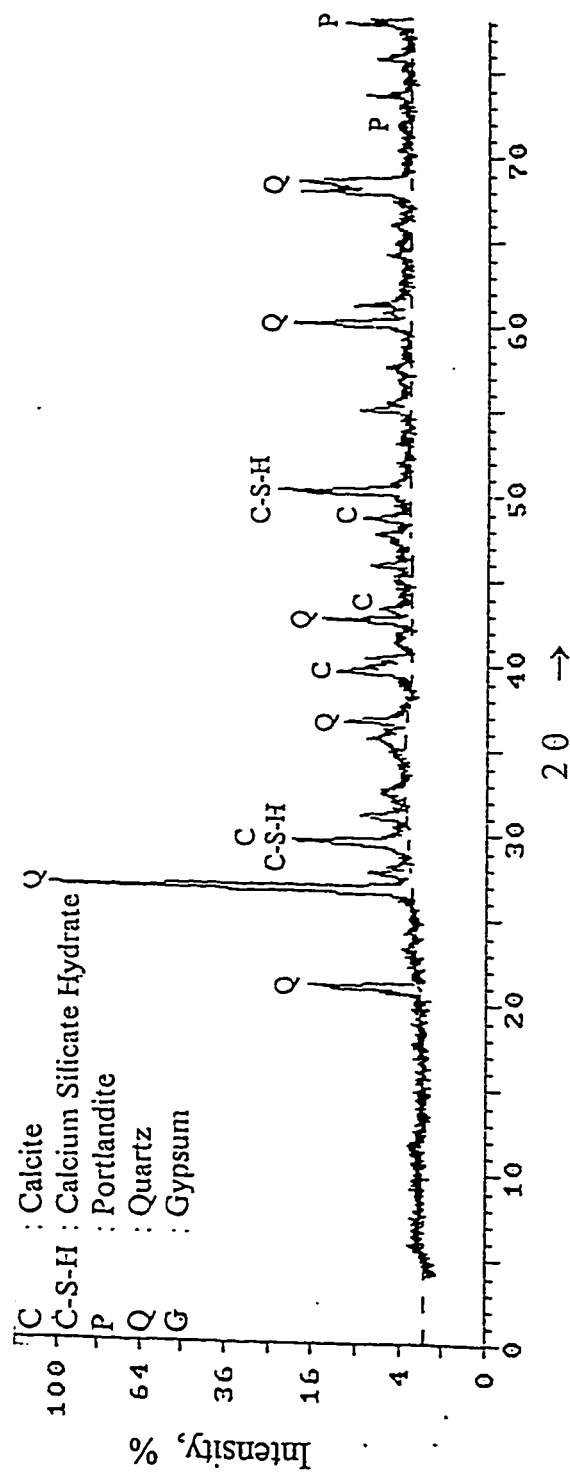


Fig. 4.70: Effect of Casting Temperature on X-ray Diffraction in the Blast Furnace Slag Cement Mortar Specimens
Cast at 50 °C and Cured at 20 °C

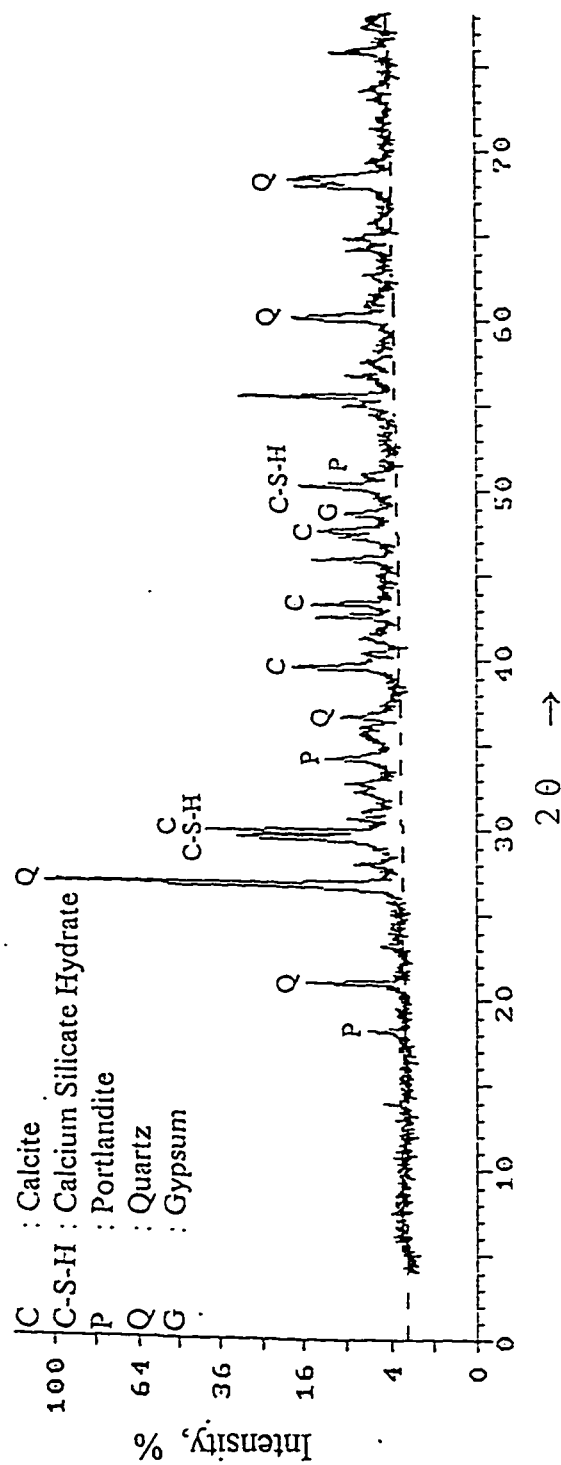


Fig. 4.71: Effect of Casting Temperature on X-ray Diffraction in the Silica Fume Cement Mortar Specimens Cast and Cured at 20 °C

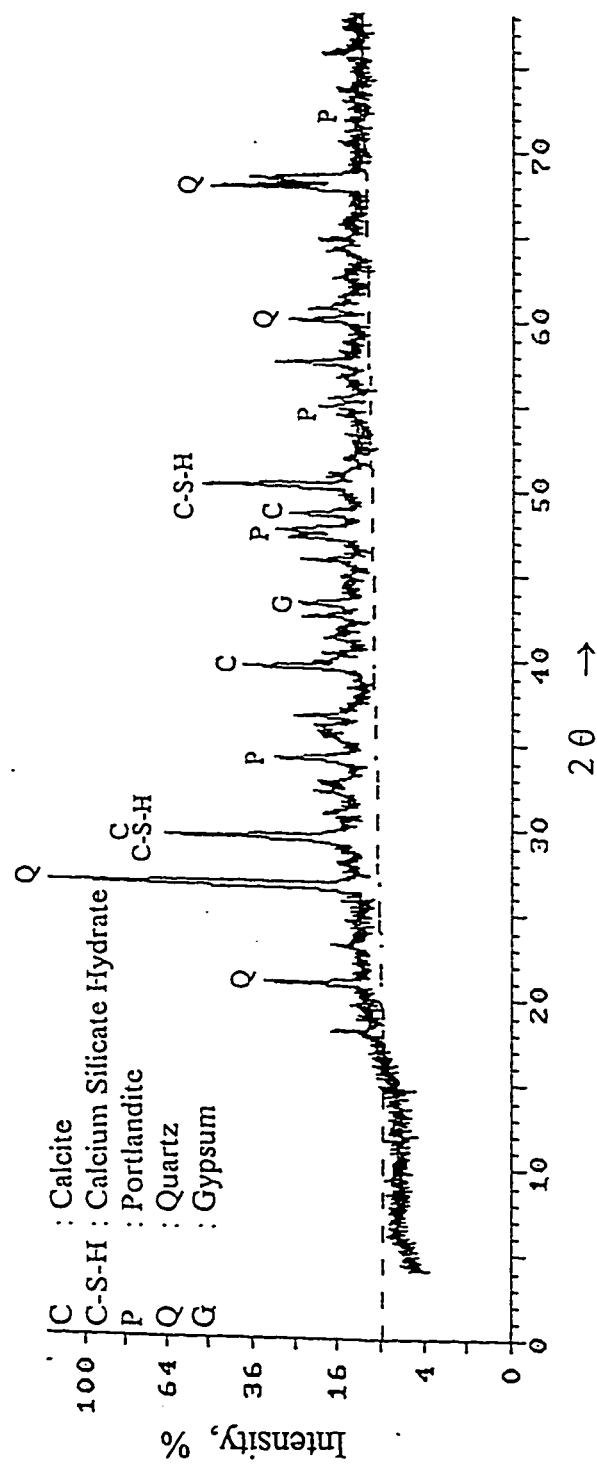


Fig. 4.72: Effect of Casting Temperature on X-ray Diffraction in the Silica Fume Cement Mortar Specimens Cast at 35 °C and Cured at 20 °C

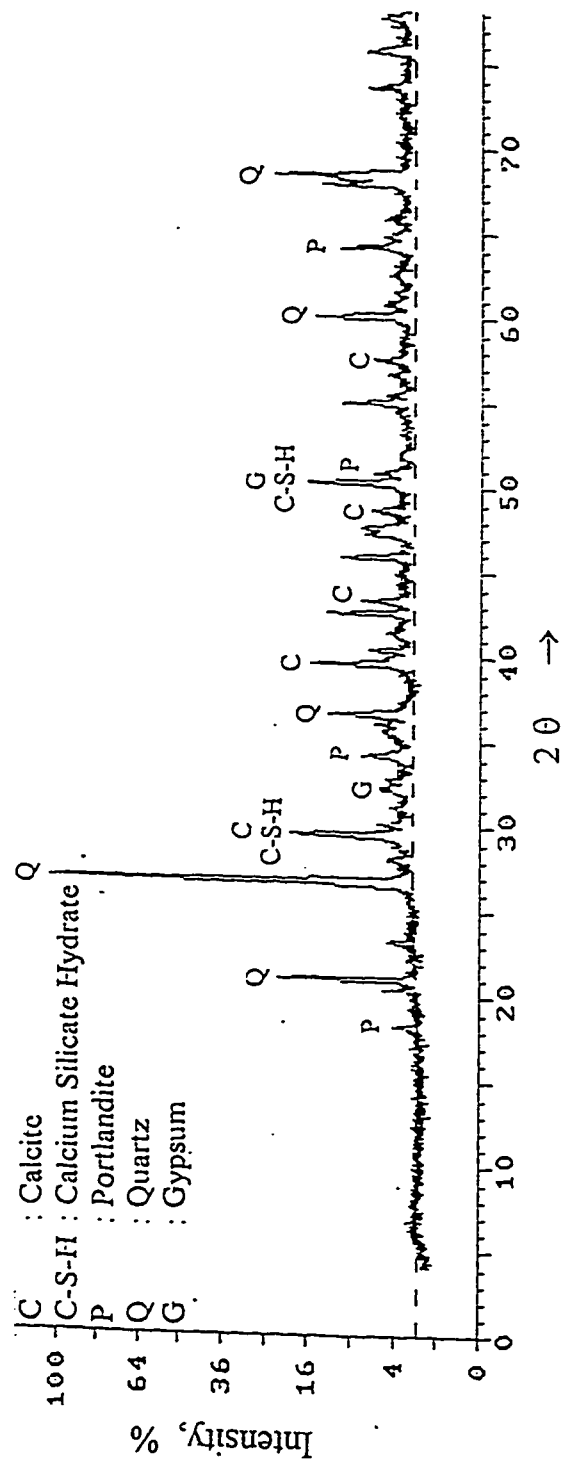


Fig. 4.73: Effect of Casting Temperature on X-ray Diffraction in the Silica Fume Cement Mortar Specimens Cast at 50 °C and Cured at 20 °C

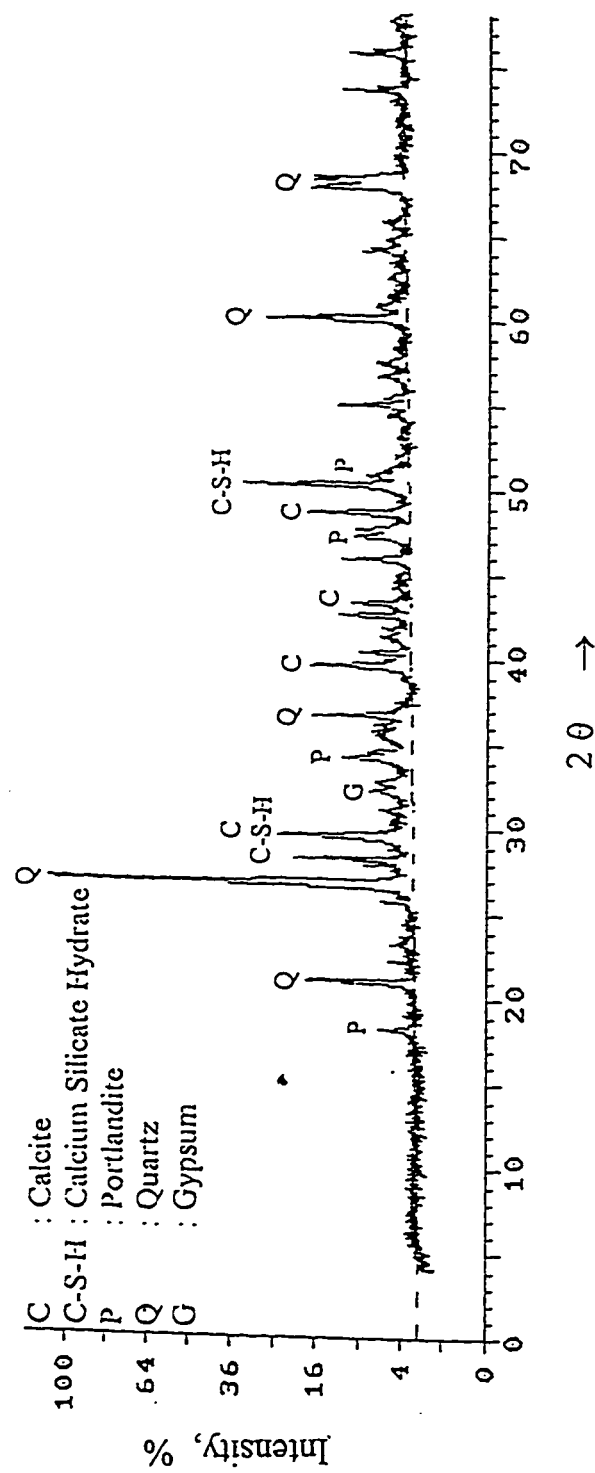


Fig. 4.74: Effect of Casting Temperature on X-ray Diffraction in the Fly Ash Cement Mortar Specimens Cast and Cured at 20 °C

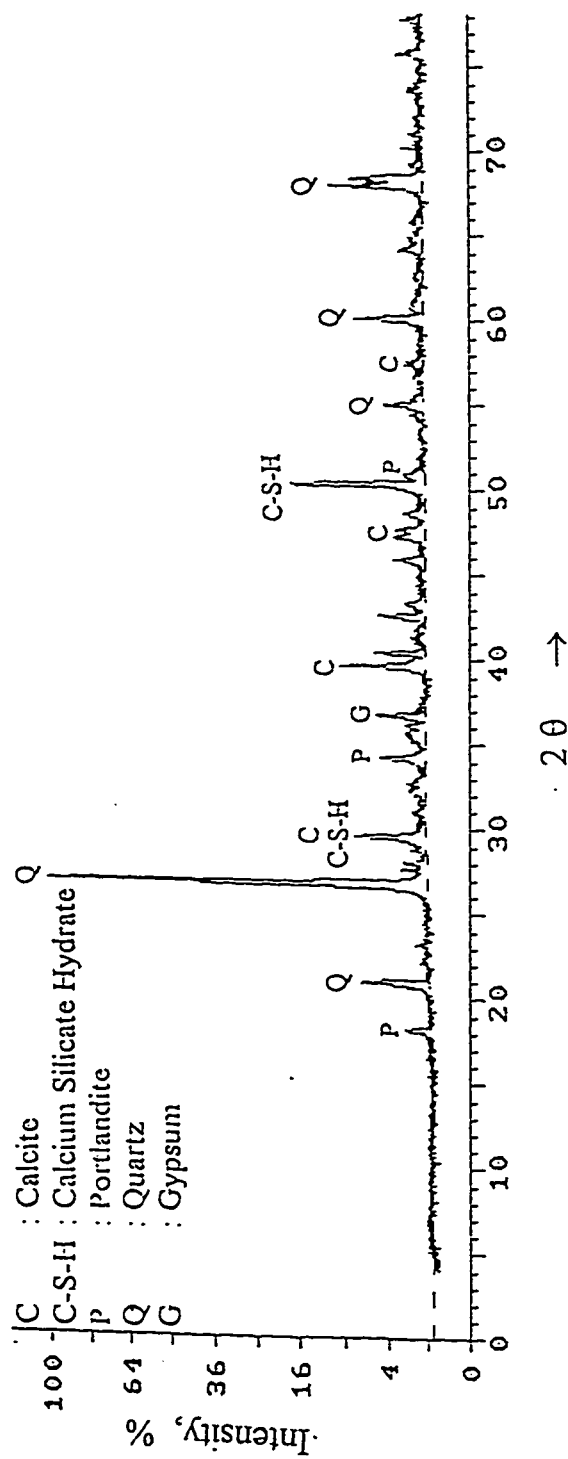


Fig. 4.75: Effect of Casting Temperature on X-ray Diffraction in the Fly Ash Cement Mortar Specimens Cast at 35 °C and Cured at 20 °C

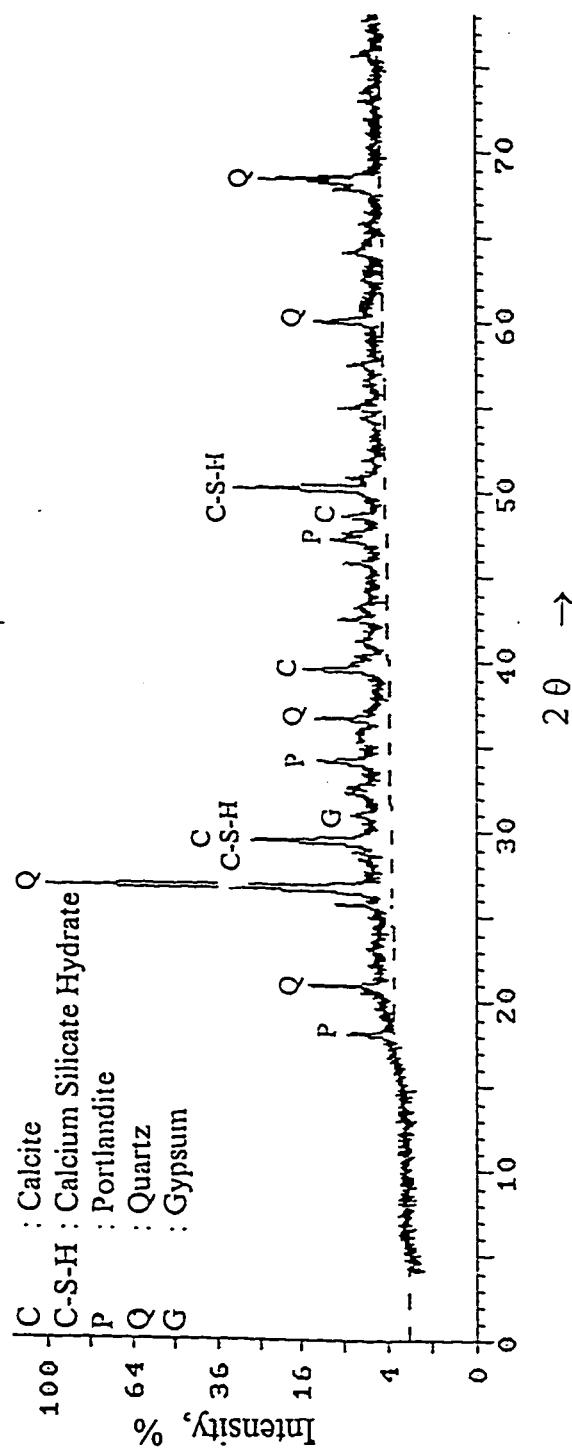


Fig. 4.76: Effect of Casting Temperature on X-ray Diffraction in the Fly Ash Cement Mortar Specimens Cast at 50 °C and Cured at 20 °C

Table 4.3: Approximate weight fraction of mineralogical phases present in the cement mortars by X-ray Diffraction method

Weight Fraction	O20-20	O35-20	O50-20	B20-20	B35-20	B50-20	SF20-20	SF35-20	SF50-20	F20-20	F35-20	F50-20
CSH	14	12	15	8	13	10	8	11	7	9	8	15
Ca(OH) ₂	9	12	7	1	-	-	6	6	4	5	6	8
Quartz	66	60	53	69	61	75	63	60	71	71	66	55
Calcite	9	12	22	16	16	10	17	20	16	9	14	18
C ₂ S	2	4	3	-	-	-	-	-	-	-	-	-
Gypsum	-	-	-	6	10	5	6	3	2	6	6	4

Table 4.4: Orientation of the transition zone

Cement	Casting Temperature (°C)	$(I_{001}) / (I_{101})$	Orientation
Plain	20	1.19	Highly preferential
	35	0.76	Less preferential
	50	0.73	Less preferential
BFS	20	-	-
	35	-	-
	50	-	-
SF	20	0.64	Less preferential
	35	0.71	Less preferential
	50	0.58	Less preferential
FA	20	0.86	Less preferential
	35	0.74	Less preferential
	50	1.16	Highly preferential

CHAPTER 5

DISCUSSION OF RESULTS

5.1 PROPERTIES OF PLAIN AND BLENDED CEMENT CONCRETES CAST AT 20 °C AND CURED AT 20, 35, AND 50 °C

5.1.1 Compressive Strength

The effect of curing temperature on the compressive strength development in plain and blended cement concrete specimens cast at 20 °C is shown in Figures 4.1 through 4.4. An early age compressive strength development was more evident in the specimens cured at temperatures greater than 20 °C, in both plain and blended cements. This increase in the early strength may be attributed to the accelerated hydration reactions due to elevated temperature exposure [88, 89]. Several researchers [90,91] have shown that early strength gain, in the plain and blended cement concretes is a function of initial temperature of the concrete. After 168 days of curing, the compressive strength in the concrete specimens cured at 50 °C was more than those cured at 20 and 35 °C (Fig. 4.1). The compressive strength of concrete specimens cured at 50 °C was 6% more than those cured at 20 °C. However, the compressive strength of concrete specimens cured at 35 °C was approximately 4% lower than those cured at 20 °C. This indicates that the curing temperature does not significantly affect the compressive strength of plain cement concrete specimens cast at 20 °C. These results contradict the findings of

Brunauer and Kantro [92] who indicated that the composition of C-S-H gel varies with curing temperature. According to them gel coating formed at lower temperature appears to be more denser than that formed at higher temperatures. The results of that study indicated that the compressive strength increases with initial casting and curing temperatures. However, at later ages, the specimens cast and cured at higher temperature had lower strengths than those cast and cured at lower temperatures. In a study conducted by Zivkovic [28] on the effect of temperature on the properties of fresh and hardened concrete, the author indicated that the 28 day compressive strength of concrete cast and cured at 8 °C was 40% more than those cast and cured at 60 °C.

Temperature had an insignificant effect on the compressive strength development in the blast furnace slag cement concrete specimens (Fig. 4.2). The compressive strength of these concrete specimens cured at 35 and 50 °C was slightly more than those cured at 20 °C. This indicates that curing temperature has an insignificant effect on the hydration of blast furnace slag. The highest early and later-age compressive strength was recorded in the silica fume cement concrete specimens cured at 50 °C (Fig. 4.3). This may be attributed to the conjoint effect of accelerated hydration of cement and the pozzolanic reaction between silica fume and the calcium hydroxide. The 28 and 84 days compressive strength in the

specimens cured at 50 °C was 43.5 and 44.12 Mpa, respectively, while in the specimens cured at 20 °C it was 36.6 and 38 Mpa, respectively.

The elevated temperature curing, beyond 20 °C, was not beneficial for compressive strength development in the fly ash cement concrete specimens (Fig. 4.4). While, the compressive strength of the specimens cured at 20 and 35 °C was more or less similar, after 168 days of curing, a reduction in the strength was observed in the specimens cured at 50 °C. These data are in agreement with those reported by Ravina [23]. He reported that strength of constant workability mix was reduced in the specimens cured at elevated temperature. According to Sybertz and Weins [67] the pozzolanic reaction slows down after 28 days of curing at elevated temperature. Whatever may be the cause, the data developed in this study indicated that a long-term strength reduction should be expected in the concrete specimens cured at elevated temperature, even though the concrete may be cooled at the time of casting.

5.1.2 Pulse Velocity

Figures 4.17 through 4.20 show the pulse velocity in the plain and blended cement concrete specimens cast at 20 °C and cured at 20, 35, and 50 °C. Maximum pulse velocity was indicated in the plain and blended cement concrete specimens cast at 20 °C. However, the pulse velocity in the specimens cured at

35 °C was not significantly different from than those cured at 20 °C. Also, the pulse velocity in the specimens cured at 50 °C was less than those cured at 20 and 35 °C. Another important observation that could be derived from these specimens is that the pulse velocity in plain cement concrete specimens did not decrease with age, even in those specimens cured at a high temperature of 50 °C. In the blended cements (Fig. 4.18 through 4.20) the pulse velocity decreased after 84 days of curing, in the specimens cured at 35 and 50 °C, while no retrogression in the pulse velocity in the specimens cured at 20 °C was noted, even after 168 days of curing. This reduction in the pulse velocity may be attributed to microcracking caused due to elevated temperature curing. This indicates that curing of blended cement concrete specimens at elevated temperature produces a more porous structure. Jones and Facaoaru [93] reported that ambient temperature between 5 and 30 °C does not significantly affect the pulse velocity in concrete. However, a temperature increase from 30 to 60 °C caused a 5% reduction in the pulse velocity. The authors suggested that this reduction is due to the initiation of microcracking in concrete. Moreover, they suggested certain correction factors to pulse velocity measurements due to changes in the temperature.

5.1.3 Water Absorption

Fig. 4.33 through 4.36 show the absorption in the plain and blended cement concrete specimens cast at 20 °C and cured at 20, 35, and 50 °C. While absorption

increased with the curing temperature in the plain and silica fume cement concretes, no significant change in the absorption capacity of blast furnace slag and fly ash cement concretes was observed with the curing temperature. These data indicate that in the hot-weather conditions use of fly ash and blast furnace slag will minimize the deterioration due to elevated temperature curing, provided the concrete is kept humid. After 168 days of curing the lowest absorption was measured in the blast furnace slag specimens and it was the highest in the silica fume cement concrete specimens for curing temperatures of 35 and 50 °C. This shows that at these temperatures the hydration products form a more porous structure in the silica fume cement concrete specimens than in the fly ash and blast furnace slag cement concrete specimens. Another reason for such a behavior may be that of shrinkage. After 168 days of curing, the absorption in the blast furnace slag cement concrete specimens, cured at 35 °C, was 21, 42.5, and 28.3% less compared to plain, silica fume and fly ash cement concrete specimens, respectively. The absorption in the plain, silica fume, and fly ash cement concrete specimens was 19.5, 34.8, and 31.7% more than that in the blast furnace slag cement concrete specimens cured at 50 °C. This indicates the usefulness of blast furnace slag cement concrete specimens in hot and humid environments. In general the compressive strength data indicate that this property in the blast furnace slag cement concrete specimens cast at 20 °C is not affected by the curing temperature. However, the pulse velocity and absorption data indicate that the long-term

performance of plain and silica fume cements may be affected when curing is carried out at elevated temperatures, such as 35 and 50 °C. In these environments, blast furnace slag and fly ash concrete specimens perform better than plain and silica fume cement concrete specimens.

5.2 PROPERTIES OF PLAIN AND BLENDED CEMENT CONCRETES CAST AT 35 °C AND CURED AT 20, 35, AND 50 °C

5.2.1 Compressive Strength

The compressive strength of plain cement concrete specimens cast at 35 °C and cured at 20 and 35 °C (Figure 4.5) continued to increase with age. However, a decrease in the strength was observed in the specimens cured at 50 °C. This indicates that casting and curing plain cement concrete specimens, up to a temperature of 35 °C, may not adversely affect the compressive strength of plain cement concrete. ACI Committee 305 [9] recommends hot weather precautions must be exercised if the temperature exceeds 30 °C. However, these results show that casting and curing at 35 °C is not harmful to the long-term strength development in plain cement concrete specimens.

The compressive strength of blast furnace slag cement concrete specimens cast and cured at 35 °C was more than those cured at 20 and 50 °C (Fig. 4.6). The

higher strength in the specimens cured at 35 °C may be attributed to accelerated hydration of the blast furnace slag. However, these specimens are susceptible to strength retrogression when exposed to 50 °C. This is possibly due to a more rapid increase in the hydration reaction which is probably helpful in the formation of a heterogeneous pore structure.

The compressive strength in the silica fume cement concrete specimens cast at 35 °C and cured at 20 °C was more than those cured at 35 and 50 °C (Fig. 4.7). This indicates that elevated temperature does not accelerate the pozzolanic reaction between cement and silica fume. Another consequence of these results may be that the long-term strength in the concrete specimens cured at elevated temperature, such as 35 °C, may be reduced. On the other hand, elevated temperature curing temperature was observed to be beneficial in the fly ash cement concrete specimens (Fig. 4.8). After 168 days of curing, the compressive strength of concrete specimens cured at 35 °C was more than those cured at 20 and 50 °C. The beneficial effect of fly ash under elevated temperature conditions has been noted by Ravina [23]. According to him, the pozzolanic reaction of fly ash, which is slow under normal exposure conditions is accelerated with increasing exposure temperature.

The data on compressive strength in the plain and blended cement concrete specimens cast at 35 °C and cured at other temperatures indicates the following trend.

1. Curing plain, silica fume and blast furnace slag cement concretes at temperatures of up to 35 °C is not harmful; and
2. Curing fly ash cement concrete specimens at temperature of up to 35 °C has no detrimental effect on the compressive strength.

5.2.2 Pulse Velocity

Figures 4.21 through 4.24 show the pulse velocity in both plain and blended cement concrete specimens cast at 35 °C and cured at 20, 35, and 50 °C. Again, maximum pulse velocity was exhibited in the plain cement concrete specimens cured at 20 °C (Fig. 4.21). Further, a reduction in the pulse velocity was noted in the specimens cured at 35 and 50 °C, after 84 days of curing. In the specimens cured at 20 °C, no reduction in the pulse velocity was noted. A more or less similar trend was observed in the blast furnace slag and fly ash cement concrete specimens (Figs. 4.22 and 4.24). In the silica fume cement concrete specimens, a reduction in the pulse velocity was noted after 84 days of exposure, even in the specimens cured at 20 °C. This indicates that casting at 35 °C is conducive to the development of microcracks in these cement concrete specimens.

5.2.3 Absorption

Figures 4.37 through 4.40 show the absorption in the plain and blended cement concrete specimens cast at 35 °C and cured at 20, 35, and 50 °C. The absorption in the plain and silica fume cement concrete specimens increased with the curing temperature, particularly the later-age absorption. While the increase in the absorption with the curing temperature was not significant, in the plain cement concrete specimens, a tremendous increase was observed in the silica fume cement concrete specimens. This increase was noticeable in the specimens cured at 35 and 50 °C. An increase in the absorption with the curing temperature was also observed in the blast furnace slag and fly ash cement concrete specimens. However, the variation in the absorption due to changing curing temperature was not significant. The lowest absorption was measured in the blast furnace slag cement concrete for all the above curing temperatures, after 3 days of curing. The absorption in the plain, silica fume, and fly ash cement concrete specimens cured at 35 °C was 42, 74.8, 74.5% more than that in the blast furnace slag cement concrete specimens after 168 days of curing. Similarly, the absorption in the blast furnace slag cement concrete specimens cured at 50 °C was 42.6, 70.8, and 75.2%, less than that in the plain, silica fume, and fly ash cement concrete specimens, respectively. This also shows the beneficial role of blast furnace slag cement in producing a durable concrete.

5.3 PROPERTIES OF PLAIN AND BLENDED CEMENT CONCRETES CAST AT 50 °C AND CURED AT 20, 50, AND 65 °C

5.3.1 Compressive Strength

The compressive strength of plain cement concrete specimens cast at 50 °C and cured at 65 °C was more than those cured at 20 and 50 °C, particularly up to 28 days of curing (Fig. 4.9). However, a decrease in the compressive strength was noted after this period. After 168 days of curing, the compressive strength of concrete specimens cured at 65 °C was less than those cured at 50 °C, but slightly more than those cured at 20 °C. The gain in compressive strength, with age, was more significant in the specimens cured at 50 °C than those cured at 20 °C.

The compressive strength of the blast furnace slag cement concrete specimens did not decrease with time (Fig. 4.10). The compressive strength of concrete specimens cast at 50 °C and cured at 20 and 50 °C was more or less similar. However, the compressive strength of concrete specimens cured at 65 °C was more than those cured at 50 and 20 °C. These results indicate that elevated temperature curing and casting is beneficial in the cast of blast furnace slag cements.

The elevated temperature casting affected the long-term compressive strength of silica fume cement concrete specimens (Fig. 4.11). The compressive strength of

these specimens decreased after 84 days of curing. Such a decrease was also observed in the concrete specimens cured at 20 °C. This may be attributed to the formation of micro-cracks, due to elevated temperature casting.

The beneficial effect of curing at 20 °C was also observed in the fly ash cement concrete specimens cast at 50 °C (Fig. 4.12). In summary, the data in Figs. 4.9 through 4.12 indicate that casting at elevated temperature, per se 50 °C, was harmful to the long-term strength development in the silica fume cement concrete specimens only.

5.3.2 Pulse Velocity

Figures 4.25 through 4.28 depict the pulse velocity development in the plain and blended cement concrete specimens cast at 50 °C and cured at 20, 50, and 65 °C. A reduction in the pulse velocity in the plain cement concrete specimens cured at 50 and 65 °C was indicated after 56 days of curing, while it continued to increase in the specimens cured at 20 °C. A more or less similar trend was indicated in the blast furnace slag and fly ash cement concrete specimens. A decrease in the pulse velocity in the silica fume cement concrete specimens was noted for all curing temperatures. This may be attributed to the shrinkage cracks formed in these cements due to elevated temperature casting.

5.3.3 Absorption

Figures 4.41 through 4.44 show the absorption in the plain and blended cement concrete specimens cast at 50 °C and cured at 20, 50, and 65 °C. In these group also the lowest absorption was noted in the blast furnace slag cement concrete specimens, while it was the highest in the silica fume cement concrete specimens. However, the beneficial effect of low temperature curing was observed in both the plain and blended cement concrete specimens. After 168 days of curing, the absorption in the plain, silica fume, and fly ash cement concrete specimens, cured at 50 °C, was 8.8, 19.4, and 14.5% more than that in the blast furnace slag cement concrete specimens. However, the absorption in the blast furnace slag cement concrete specimens, cured at 65 °C, was 10.71, 20.8, and 11.61%, less than that in the plain, silica fume and fly ash cement concrete specimens.

5.4 PROPERTIES OF PLAIN AND BLENDED CEMENT CONCRETES CAST AT 65 °C AND CURED AT 20 AND 65 °C

5.4.1 Compressive Strength

The compressive strength of plain cement concrete specimens cast at 20 °C increased with the period of curing. However, a slight reduction was noticed in the specimens cured at 65 °C. A reduction in the long-term compressive strength of the silica fume cement concrete specimens was also observed in the specimens cast

at 65 °C (Fig. 4.15). However, the long-term compressive strength of blast furnace slag cement concrete specimens (Fig. 4.14) was not affected by the casting temperature.

5.4.2 Pulse Velocity

Figures 4.29 through 4.32 show the pulse velocity in plain and blended cement concrete specimens cast at 65 °C and cured at 20 and 65 °C. A decrease in the long-term pulse velocity after 56 days of curing, was indicated in all the concrete specimens and cured at both the temperatures. Such a trend could be attributed to the effect of elevated temperature casting in the specimens cast at 65 °C and cured at 20 °C, and also in the specimens cast and cured at 65 °C.

5.4.3 Absorption

Figures 4.45 through 4.48 show the absorption in the plain and blended cement concrete specimens cast at 65 °C and cured at 20 and 65 °C. The absorption in these specimens cured at 20 °C was less than those cured at 65 °C. The lowest absorption was measured in the blast furnace slag cement concrete specimens. While it was the highest in the fly ash cement concrete specimens. After 168 days of curing the absorption in the plain, silica fume, and fly ash cement concrete was 26.5, 7.3, and 58.3% more than that in the blast furnace slag cement concrete

specimens, cured at 20 °C. Similarly, the absorption in the blast furnace slag cement concrete specimens, cured at 65 °C, was 1.4, 26.2, and 56% less compared than that in similarly cured plain, silica fume, and fly ash cement concrete specimens, respectively.

5.5 SUMMARY

Table 5.1 shows the effect of casting and curing temperatures on the long-term properties of plain cement concrete specimens cast at 20, 35, 50, and 65 °C and cured at various temperatures. The long-term properties of plain cement concrete specimens cast at 20 °C, were not affected up to a curing temperature of 50 °C. Similarly, the long-term properties of concrete specimens cast at 35 and 50 °C were not affected, provided they were cured at 20 °C. These results contradict the limitations imposed by ACI Committee 305 [9] which states that hot weather precautions must be exercised if the casting temperature is more than 30 °C. The effect of casting and curing temperatures on the long-term properties of blast furnace slag cement concrete specimens is shown in table 5.2. These results indicate that the long-term properties of concrete specimens cast at 20 and 35 °C and cured at 20, 35, and 50 °C were not affected. Moreover in the specimens cast at 50 and 65 °C no harmful effects were noticed, when curing was done

at 20 °C. This indicates that blast furnace slag cement concrete specimens can be beneficially utilized in the hot weather conditions provided they are cured at 20 °C.

The effect of casting and curing temperatures on the long-term properties of silica fume cement concrete specimens were showed in Table 5.3. The long-term properties of the silica fume cement concrete specimens cast and cured at 20 °C were not affected. However, for all other casting and curing temperatures the long-term properties were affected. This indicates that the casting and curing temperatures should be kept low to utilize the technological benefits of silica fume cement. Table 5.4 summarizes the effect of casting and curing temperatures on the long-term properties of fly ash cement concrete specimens. The long-term properties were not affected in the cement concrete specimens cast at 20, 35, and 50 °C, provided curing was carried out at 20 °C. However, at all other casting and curing temperatures the long-term properties were affected. This indicates that these cements can be beneficially utilized up to a casting temperature of 50 °C, for a curing temperature of 20 °C.

Table 5.1: Effect of casting and curing temperatures on the long-term properties of plain cement concrete

PROPERTY	CASTING TEMPERATURE 20 C			CASTING TEMPERATURE 35 C			CASTING TEMPERATURE 50 C			CASTING TEMPERATURE 65 C	
	CURING TEMPERATURES 20 C 35 C 50 C			CURING TEMPERATURES 20 C 35 C 50 C			CURING TEMPERATURES 20 C 50 C 65 C			CURING TEMPERATURES 20 C 65 C	
Comp. Strength	✓	✓	✓	✓	✓	X	✓	✓	X	✓	✓
Pulse Velocity	✓	✓	✓	✓	X	X	✓	X	X	X	X
Absorption	✓	✓	✓	✓	✓	X	✓	X	X	✓	X

✓ : Beneficial
X : Harmful

Table 5.2: Effect of casting and curing temperatures on the long-term properties of blast furnace slag cement concrete

PROPERTY	CASTING TEMPERATURE				CASTING TEMPERATURE				CASTING TEMPERATURE			
	20 C				35 C				50 C			
	CURING TEMPERATURES				CURING TEMPERATURES				CURING TEMPERATURES			
	20 C	35 C	50 C		20 C	35 C	50 C		20 C	50 C	65 C	
Comp. Strength	✓	✓	✓		✓	✓	✓		✓	✓	✓	
Pulse Velocity	✓	✓	✓		✓	✓	✓		✓	X	✓	
Absorption	✓	✓	✓		✓	✓	✓		✓	✓	✓	

✓ : Beneficial
X : Harmful

Table 5.3: Effect of casting and curing temperatures on the long-term properties of silica fume cement concrete

PROPERTY	CASTING TEMPERATURE				CASTING TEMPERATURE				CASTING TEMPERATURE			
	20 C				35 C				50 C			
	CURING TEMPERATURES				CURING TEMPERATURES				CURING TEMPERATURES			
	20 C	35 C	50 C		20 C	35 C	50 C		20 C	35 C	50 C	
Comp. Strength	✓	✓	✓		✓	✓	X		X	X	X	
Pulse Velocity	✓	X	X		X	X	X		X	X	X	
Absorption	✓	X	X		X	X	X		X	X	X	

✓ : Beneficial
X : Harmful

Table 5.4: Effect of casting and curing temperatures on the long-term properties of fly ash cement concrete

PROPERTY	CASTING TEMPERATURE				CASTING TEMPERATURE				CASTING TEMPERATURE			
	20 C				35 C				50 C			
	CURING TEMPERATURES				CURING TEMPERATURES				CURING TEMPERATURES			
	20 C	35 C	50 C	50 C	20 C	35 C	50 C	50 C	20 C	50 C	65 C	65 C
Comp. Strength	✓	X	X	X	✓	X	X	X	✓	X	X	X
Pulse Velocity	✓	X	X	X	✓	X	X	X	✓	X	X	X
Absorption	✓	✓	X	X	✓	X	X	X	✓	X	X	X

✓ : Beneficial
X : Harmful

CHAPTER 6

CONCLUSIONS

1. The compressive strength of both plain and blended cement concrete specimens increased with the period of curing.
2. The long-term properties of plain cement concrete specimens cast up to 50 °C were not affected provided they were cured at 20 °C. However, they were affected when the curing temperatures were 35 and 50 °C.
3. In the plain cement concrete specimens cast and cured at 35 °C, the long-term properties were affected. However, the properties of the blast furnace slag cement concrete were not affected for casting temperatures of up to 50 °C. This indicates the usefulness of blast furnace slag cements under hot-weather conditions.
4. Blast furnace slag cements can be beneficially utilized up to a casting temperature 65 °C, provided curing is done at 20 °C.

5. The long-term compressive strength, pulse velocity, and absorption of silica fume cement concrete specimens were not affected when the casting and curing temperature was 20 °C. However, when they were cured at 35 °C and 50 °C the long-term properties were affected.
6. The long-term properties of fly ash cement concrete specimens were not affected for a casting temperature of up to 50 °C, provided curing was done at 20 °C. This indicates that the long-term properties of fly ash cement concrete are controlled by both the casting and curing temperatures.
7. The cumulative pore volume increased with the casting temperature in both plain and blended cement concrete specimens, except in the fly ash cement concrete specimens cast at 50 °C in which a decrease was observed.
8. Elevated temperature casting results in a more porous structure which may affect the concrete durability as indicated by the pulse velocity and absorption data.

9. In the plain cement concrete specimens cast and cured at 20 °C, the transition zone was more preferentially oriented, indicating that lower temperature casting results in a stronger transition zone. However, at higher temperatures the transition zone was less preferential.

10. At higher casting temperatures, the transition zone in the fly ash cement concrete specimens was more preferentially oriented, which may be attributed to the acceleration in the pozzolanic reaction. Therefore, the use of fly ash at elevated temperature casting may be beneficial, provided it is cured at 20 °C.

REFERENCES

1. Rasheeduzzafar, Dakhil, F. H., and Al-Gahtani, A. S., "Corrosion of Reinforcement in Concrete Structures in the Middle East", *Concrete International*, Vol. 7, No. 9, 1985, pp. 48-55.
2. Rasheeduzzafar, Dakhil, F. H., and Al-Gahtani, A. S., "The Deterioration of Concrete Structures in the Environment of the Middle East", *ACI Journal Proceedings*, Vol. 81, No. 1, January-February 1984, pp. 13-20.
3. Maslehuddin, M., Saricimen, H., Al-Mana, A. I., and Shameem, M., "Performance of Concrete in a High Chloride-Sulfate Environment", *ACI Special Publication*, SP-22, 1990, American Concrete Institute, Detroit, pp. 469-494.
4. Hsu, J.J.C., "Mathematical Analysis of Shrinkage in a Model of Hardened Concrete", *ACI Journal, Proceedings*, Vol. 60, No. 3, March 1963, pp. 371-390.
5. Slate, F. O., and Matheus, R. E., "Volume change upon Setting and Curing of Cement Paste and Concrete from Time zero to Seven days", *ACI Journal Proceedings*, Vol. 64, No. 1, January 1967, pp. 34-39.
6. Jaegerman, C. H., Ravina, D., and Pundak, B., "Accelerated Curing of Concrete by Solar Radiation", *Proc. Int. Rilem Symp. on Concrete and Reinforced Concrete in Hot Countries*, Haifa, August 1971, Vol. II pp. 339-362.
7. Ish-Shalon, M., and Bentur, A., "Some observation on the effect of Initial Temperature on the Hydration and Strength of Portland Cement with different Aluminate Contents", *Proc. Int. Rilem Symp. on Concrete and Reinforced Concrete in Hot Countries*, B.R.S., Haifa, Israel, Vol. II, 1971, pp. 259-273.
8. Shalon, R., and Raphael, M., "Corrosion of Reinforcing Steel in Hot Countries", *RILEM Bulletin*, No. 24, September 1964, pp. 29-45.
9. American Concrete Institute, Hot weather concreting, "ACI Committee 305 Report" *ACI Materials Journal*, July-August 1991, pp. 417-436.
10. Shalon, R., "Concrete and Reinforced Concrete in Hot Countries", *Report on Behavior of Concrete in Hot Climate, Materials and Structures*, No. 62, March-April 1978, pp. 127-131.

11. Waris, M. A., "Effect of Plastic Shrinkage Cracking in Hot Climate", *M.S. Thesis, KFUPM*, May 1996.
12. Bentur, A., and Goldman, A., "Curing Effects on Strength and Physical Properties of High Strength Silica Fume Concretes" *Journal of Materials in Civil Engineering*, Vol. 1, No. 1, February, 1989, pp. 46-58.
13. Novokshchenov, V., "Cracking in Hot Countries", *Concrete International*, August 1986, pp. 27-33.
14. Klieger, P., "Effect of Mixing and Curing Temperature on Concrete Strength", *ACI Journal Proceedings*, Vol. 54, No. 12, June 1958.
15. Mehta, P. K., *Concrete: Structure, Properties and Materials*, Prentice Hall, Inc., New Jersey, 1986, pp. 37.
16. Shalon, R., and Ravina, D., "Studies in Concreting in Hot countries", *Proc. Int. RILEM Symp. on Concrete and Reinforced concrete in Hot Countries*, B.R.S., Haifa, Israel, Vol. I, 1960.
17. Ravina, D., "Retempering of Prolonged-Mixed Concrete with Admixtures in Hot Weather", *ACI Journal*, June 1975, pp. 291-295.
18. Tsui, L., "An investigation on Time-Strength relationship of Concrete in HongKong", *Proc. Int. RILEM Symp. on Concrete and Reinforced Concrete in Hot Countries*, B.R.S., Haifa, Vol. II, 1979, pp. 297-307.
19. Ridgley, T., "An Investigation in to manufacture of High-Strength Concrete in a Tropical climate", *Proc. Institute of Civil Engineers, London*, Vol. 13, 1959, pp. 23-24.
20. Court, C. L., "An investigation in to Manufacture of High Strength Concrete in a Tropical Climate", *Proc. Institute of Civil Engineers, London*, Vol. 15, 1960, pp. 170-181.
21. Hermite, L., "Introductory Lecture", *Proc. Int. Symp. on Concrete and Reinforced Concrete in Hot Countries*, Haifa, Israel, Vol. 1, 1971.
22. Verbeck, G. J., and Helmuth, R. H., "Structures and Physical Properties of Cement Paste", *Proc., fifth Int. Symp. on the Chemistry of Cement*, Tokyo, Vol. III, 1968, pp. 1-32.

23. Ravina, D., "Fly Ash Concrete Under Hot Weather Conditions", ACI Special Publication, SP-39, American Concrete Institute, Detroit, pp. 172-183.
24. Ray, I., Gupta, A. P., and Biswas, M., "The effect of Latex and Superplasticiser on Portland Cement Mortar in the Hardened State" *Cement and Concrete Composites*, Vol. 17, 1995, pp. 9-21.
25. Haque, M. N., "Some Concretes Need 7-Days Initial Curing", *Concrete International*, February 1990, pp. 42-47.
26. Haque, M. N., and Kayyali, O. A., "Strength and Porosity of Hardened Cement Fly Ash Pastes in a Hot Environment", *ACI Materials Journal*, March-April 1989, pp. 128-134.
27. Lapinas, R. A., "Hot Concrete for Achievement of High Early Strength" *ACI Special Publications SP 39-7*, American Concrete Institute, Detroit, pp. 109-138.
28. Zivkovic, S. D., "The effect of Increased Temperature on Fresh and Hardened Concrete", *Proc., Third Intr. Conference held by RILEM*, Committee 94-CHC on Concrete in Hot Climates, pp. 3-12.
29. Wainwright, P. J., Cabrera, G. J., and Al-Amri, A. M., "Performance Properties of Mortars Cured in Hot Dry Environments", *Ibid.*, pp. 115-127.
30. Powers, T. C., "A Discussion of Cement Hydration in Relation to the Curing of Concrete", *Proceedings, Highway Research Board*, Vol. 27, 1947, pp. 178-188.
31. Rasheeduzzafar, Al-Gahtani, A. S., and Al-Saadoun, S. S., "Influence of Construction Practices on Concrete Durability", *ACI Materials Journal*, 1989, pp. 566-575.
32. Page, C. L., Short, N. R., and El-Tarras, A., "Diffusion of Chloride Ions in Hardened Cement Pastes", *Cement and Concrete Research*, Vol. 11, No. 3, 1981, pp. 295, 406.
33. Smolczyk, H. G., "Slag Structure and Identification of Slags", *Proceedings, 7th International Congress on the Chemistry of Cement*, Edition, Septima, Paris, Vol. I, 1980, 111-1/3-111-1/17.

34. Brit, J. C., "Curing Concrete - An Appraisal of Attitudes, Practices and Knowledge", *CIRIA Report No. 43*, Construction Industry Research and Information Associations, London, 1973, pp. 36.
35. Gowripalan, N., Cabrera, J. G., Cusens, A. R., and Wainwright, P. J., "Effect of Curing on Durability", *Concrete International*, 1990, pp. 47-54.
36. Wainwright, P. J., Cabrera, J. G., and Gowripalan, N., "Assessment of the Efficiency of Chemical Membranes to Cure Concrete", *Protection of Concrete*, Dhir, and Green Editors, E. & F.N. Spon, London, 1990, pp. 907-920.
37. Taryal, M. S., Chowdhury, M. K., and Matala, S., "The Effect of Practical Curing Methods used in Saudi Arabia on Compressive Strength of Plain Concrete", *Cement and Concrete Research*, Vol. 16, No. 5, 1986, pp. 633-645.
38. Al-Ani, S. H., Mokdad, A. K., and Al-Zaiwary "The effect of Curing Period and Curing Delay on Concrete in Hot weather", *Materials and Structures*, No. 21, 1988, pp. 205-212
39. Bergstrom, S. G., "Curing Temperature, Age and Strength of Concrete", *Swedish Cement and Concrete Research Institute*, Stockholm, pp. 61-66.
40. Nurse, R. W., "Steam Curing of Concrete", *Magazine of Concrete Research*, Vol. 1, No. 2, June 1949, pp. 79-88.
41. Saul, A.G.A., "Principles Underlying the Steam Curing of Concrete at Atmospheric Pressure", *Magazine of Concrete Research*, Vol. 2, No. 6, March 1951, pp. 127-140.
42. Marzouk, H., and Hussein, A., "Effect of Curing Age on High Strength Concrete at Low Temperatures", *Journal of Materials in Civil Engineering*, August 1995, pp. 161-167.
43. Saroka, I., Jaegermann, H., and Bentur, A., "Short-term Steam Curing and Later age Strength of Concrete", *Materials and Structures*, Vol. II, No. 62, pp. 93-96.
44. Kjellsen, K. O., "Physical and Mathematical Modelling of Hydration and Hardening of Portland Cement Concrete as a Function of Time and Curing Temperature", *The Norwegian Institute of Technology*, Division of Building Materials.

45. Skalny, J., and Odler, I., "Pore Structure of Hydrated Calcium Silicates" *Journal of Colloid and Interface Science*, Vol. 40, 1972, pp. 199-205.
46. Berger, R. L., and McGregor, J. D., "Effect of Temperature and Water-Solid Ratio on growth of $\text{Ca}(\text{OH})_2$ Crystals formed during Hydration of Ca_3SiO_5 ", *Journal of American Ceramic Society*, Vol. 56, 1973, pp. 73-79.
47. Odler, I., "Hydration of Tri-Calcium Silicate at Elevated Temperatures", *Journal of Applied Chemistry and Biotechnology*, Vol. 23, 1973, pp. 661-667.
48. Alunno-Rosetti, V., Chiocchio, G., and Collepari, M., "Low Pressure Steam Hydration of Tri-Calcium Silicate" *Cement and Concrete Research* Vol. 4, 1974, pp. 279-288.
49. Bentur, A., and Berger, R. L., "Chemical Composition of C-S-H gel Formed in the Hydration of Calcium Silicate Pastes", *Journal of American Ceramic Society*, Vol. 62, 1979, pp. 117-120.
50. Bentur, A., Berger, R. L., Kung, J. H., Milestone, N.B., and Young, J. F., "Structural Properties of Calcium Silicate Paste, :II: Effect of Curing Temperature", *Journal of American Ceramic Society*, Vol. 62, 1979, pp. 362-366.
51. Boyer, J. P., and Berger, R. L., "Influence of Temperature Increases During the Induction Period of C_3S Hydration on the Microstructure and Strength of C_3S Mortars", *Journal of American Ceramic Society*, Vol. 63, 1980, pp. 675.
52. Radjy, F., and Richards, C. W., "Effect of Curing and Heat Treatment History on the Dynamic Mechanical Response and the Pore Structure of Hardened Cement Paste", *Cement and Concrete Research*, Vol. 3, 1973, pp. 7-21.
53. Sellevold, E. J., "Mercury Porosimetry of Hardened Cement paste Cured or Stored at 97 °C", *Cement and Concrete Research*, Vol. 4, No. 3, May-June 1974, pp. 399-404.
54. Goto, S., and Roy, D. M., "The Effect of W/C Ratio and Curing Temperature on the Permeability of Hardened Cement Paste", *Cement and Concrete Research*, Vol. 11, No. 4, July-August 1981, pp. 575-579.
55. Odler, I., Abdul-Maula, S., and Zhongya, L., "Effect of Hydration Temperature on Cement Paste Structure", *Material Research Society Symposium, Proceedings*, Vol. 85, 1987, pp. 139-144.

56. Cabrera, J. G., and Claisse, P. A., "The Effect of Curing Conditions on the Properties of Silica Fume Cement Concrete" *International Conference on Blended Cements in Construction*, Sheffield, U.K, 1991, pp. 293-301.
57. Cao, Y., and Detwiler R. J., "BackScattered Electron Imaging of Cement pastes Cured at Elevated Temperatures", *Cement and Concrete Research*, Vol. 25, No. 3. pp. 627-638.
58. Austin, S. A., and Robins, P. J., "Performance of Slag Concrete in Hot Climates", *Proc., Third Intr. Conference held by RILEM, Committee 94-CHC on Concrete in Hot Climates*, pp. 129-139.
59. Wang, J., and Black, A., "Performance Evaluation of Curing Membranes", *Ibid.*, pp. 199-205.
60. Patel, H. H., Bland, C. H., and Poole, A. B., "The Micro Structure of Concrete Cured at Elevated Temperatures", *Cement and Concrete Research*, Vol. 25, No. 3, 1995, pp. 485-490.
61. Roy, D. M., and Parker, K. M., "Micro Structures and Properties of Granulated Slag-Portland Cement Blended at Normal and Elevated Temperatures", *Fly Ash, Silica Fume, Slag, and other Mineral By-Products in Concrete*, M. Malhotra, Ed., SP-79, American Concrete Institute, Detroit, 1983, pp. 397-414.
62. Marsh, Brian K., Day, Robert L., and Bournier, D. J., "Pore Structure Characteristics Affecting the Permeability of Cement Paste containing Fly Ash", *Cement and Concrete Research*, Vol. 15, No. 6, Nov-1985, pp. 1027-1038.
63. Villadsen, J., "High Temperatures in Fly Ash Hardened Cement Pastes Pore Structures", *Diploma Thesis*, Technical University of Denmark, Department of Civil Engineering, July 1989 (in Danish).
64. Ozyildirim, C., "Laboratory Investigation of Low-Permeability Concrete Containing Slag and Silica Fume", *ACI Materials Journal*, Vol. 91, No. 2, March-April 1994. pp. 197-202.
65. Ozyildirim, C., and Halstead, W. J., "Improved Concrete Quality with Combination of Fly Ash and Silica Fume", *ACI Materials Journal*, Vol. 91, No. 6, November-December 1994, pp. 587-594.

66. Bisailon, A., Rivest, M., and Malhotra, V. M., "Performance of High Volume Fly Ash Concrete in Large Experimental Monoliths" *ACI Materials Journal*, Vol. 91, No. 2, March-April 1994, pp. 178-187
67. Sybertz, F., and Wiens, U., "Effect of Fly Ash Fineness on Hydration Characteristics and Strength Development", *International Conference on Blended Cements in Construction*, Sheffield, U.K, 1991, pp. 152-165.
68. Marsh, B. K., "Temperature Rise in Thin Concrete Sections Containing Fly Ash" *Ibid.*, pp. 207-220
69. Nakamura, N., Sakai, M., and Swamy, R. N., "Effect of Slag Fineness on the Engineering Properties of High Strength Concrete" *Ibid.*, pp. 302-316.
70. Meland, I., "Carbonation in Hardened Fly Ash Cements", *Ibid.*, pp. 329-335.
71. Justnes, H., and Havdahl, J., "The effect of Curing Temperature on the Micro Structure of Cementitious Paste for Light LWA Concrete", *Ibid.*, pp. 138-151.
72. Owens, P. L., "Effect of Temperature Rise and Fall on the Strength and Permeability of Concrete made with and without Fly Ash", *Temperature Effects on Concrete*, ASTM STP 858, T.R Naik, Ed., American Society for Testing and Materials, Philadelphia, 1985, pp. 134-149.
73. Powers, T. C., Copeland, L. E., and Mann H. M., "Capillary Continuity or Discontinuity in Cement Pastes", *Journal of the Portland Cement Association*, Research and Development Laboratories, No. 2, May 1959, pp. 38-48.
74. Ramezaniapour, A. A., and Malhotra, V. M., "Effect of Curing on the Compressive Strength, Resistance to Chloride-Ion Penetration & Porosity of Concretes Incorporating Slag, Fly Ash or Silica Fume", *Cement and Concrete Composites*, Vol. 17, 1995, pp. 125-133
75. Campbell, G. M., and Detwiler, R. J., "Development of Mix Designs for Strength and Durability of Steam-Cured Concrete", *Concrete International*, Vol. 15, No. 7, July 1993, pp. 37-39.
76. Saroka, I., and Peer, E., "Influence of Cement Composition on the Compressive Strength of Concrete Cast and Initially Cured at High Temperatures", *Proc. Int. RILEM Symp. on Concrete and Reinforced Concrete in Hot Countries*, B.R.S., Haifa, Vol. I, 1971, pp. 241-258.

77. Kanda, T., Sakuramoto, F., and Suzuki, K., "Compressive Strength of Silica Fume Concrete at Higher Temperature" *ACI Special Publication SP 132-59*, American Concrete Institute, Detroit, pp. 1089-1093.
78. Vandewalle, L., and Mortelmans, F., "The Effect of Curing on the Strength Development of Mortar Containing High Volumes of Fly ash" *ACI Special Publication SP 132-4*, American Concrete Institute, Detroit, 1992 pp. 53-63
79. Wimpenny, D., and Ellis, C., "The Effect of GGBS on the Temperature and Strength Development in Concrete Elements under Low Ambient Temperatures" *International Conference on Blended Cements in Construction*, Sheffield, U.K, 1991, pp. 222-235.
80. Tanaka, S., Inone, K., Shimoyama, Y., and Tomita, R., "Methods of Estimating Heat of Hydration & Temperature Rise in Blast Furnace Slag Blended Cement" *ACI Materials Journal*, July-August 1995, pp. 429-436.
81. Detwiler, R. J., Fapohunda, C. A., and Natale, J., "Use of Supplementary Cementing Materials to Increase the Resistance to Chloride Ion Penetration of Concretes Cured at Elevated Temperatures", *ACI Materials Journal*, Vol. 91, No. 1, January-February 1994, pp. 63-66.
82. Malhotra, V. M., "Testing Hardened Concrete: Nondestructive Methods", *Published jointly by Iowa State University Press & American Concrete Institute*, 1976, pp. 71-102.
83. Mehta, P. K., and Manmohan, D., "Pore Size Distribution and Permeability of Hardened Cement Pastes", *Proceedings, 7th International Congress on the Chemistry of Cement*, Paris, 1980, Vol. II, pp. V II 1- V II 5.
84. Knut, O. K., Rachel, J. D., Gjorv, O. E., "Pore Structure of Plain Cement Pastes Hydrated at Different Temperatures", *Cement and Concrete Research*, Vol. 20, pp. 927-933.
85. Mangat, P. S., and El-Khatib, J. M., "Influence of Curing on the Pore Structure and Porosity of Blended Cement Concretes", *ACI SP-132*, Detroit, pp. 813-833.
86. Reinhardt, H. W., and Gaber, K., "From Pore Size Distribution to an Equivalent Pore Size of Cement Mortar", *Materials and Structures*, No. 23, 1990, pp. 3-15.
87. Goldman, A., and Bentur, A., "Effects of pozzolanic and non-reactive microfillers on the transition zone in high strength concretes", *Interfaces in*

Cementitious Composites, Proceedings of International Conference held by RILEM, pp. 53-61.

88. Idorn, G. M., "Hydration of Portland Cement Paste at High Temperature under Atmospheric Pressure", *International Symposium on Cement*, Tokyo, 1968.
89. Kasai, Y. Hiraga., T. Yokoyama, K., "Initial Strength of Concrete at Varied Curing Temperature", *18th General Meeting of JCEA*, Tokyo, 1964, pp. 123-128.
90. Klieger, P., "Effect of Mixing and Curing Temperature on Concrete Strength", *ACI Journal Proceedings*, Vol. 22, 1951, pp. 417-432.
91. Price, W. H., "Factors Influencing Concrete Strength", *ACI Journal Proceedings*, Vol. 22, 1951, pp. 417-432.
92. Brunauer, S., and Kantro, D. L., "The Hydration of Tri Calcium Silicate and Dicalcium Silicate from 5 °C to 50 °C", *Chemistry of Cements*, Taylor, H.F. W., Ed., Vol. 1, Academic Press, London, 1964, pp. 287-309.
93. Jones, R., and Facaoaru, I., "Recommendations for Testing Concrete by the Ultrasonic Pulse Method", *Materials and Structure*, Vol. 2, No. 10, July-Aug. 1969.

CURRICULUM VITAE

Name MOHAMMED SHARFUDDIN AHMED

Permanent Address : H.No 12-1-604/A/63
Syed Ali Guda
PO: Humanyun Nagar
Hyderabad: 500028
India

Date of birth : October 1970

Bachelors Degree : Osmania University, 1991